STRUCTURAL ANALYSIS OF A WAVE ENERGY DEVICE

School of Science & Engineering

Civil Engineering Discipline

Student: Shuijin Li

Programme: China 3+1+1

Supervisor: Dr. Hayatdavoodi

March 2017

Contents

List of Figures V

List of Tables X

Abstract XI

Acknowledgements XII

Declaration XIII

1. Introduction ..... - 1 -

1.1. Background ..... - 1 -

1.2. Renewable energy ..... - 4 -

1.3. Wave Energy ..... - 7 -

1.4. A Novel Wave Energy Device ..... - 7 -

1.5. Thesis Structure ..... - 8 -

2. Literature Review ..... - 9 -

2.1. Wave Energy Converters ..... - 9 -

2.1.1. Type of WEC ..... - 9 -

2.1.2. Typical Locations ..... - 10 -

2.1.3. Challenges with Traditional WECs ..... - 10 -

2.1.4. The Advantages of the Proposed Novel Wave Energy Device ..... - 11 -

2.2. Wave Conditions around the UK ..... - 11 -

2.3. Method ..... - 13 -

3. The Wave Energy Device ..... - 14 -

3.1. Introduction ..... - 14 -

3.2. Modeling ..... - 14 -

4. Wave Condition and Load ..... - 17 -
4.1. Coordinate system ..... - 17 -
4.2. Wave Environment ..... - 17 -
4.3. Wave Loads ..... - 18 -
4.3.1. Morison's Equation ..... - 18 -
4.3.2. The GN Equations ..... - 20 -
4.3.2.1. Introduction ..... - 20 -
4.3.2.2. Calculation ..... - 21 -
5. Structural Analysis ..... - 24 -
5.1. Mechanics of Deformable Bodies ..... - 24 -
5.1.1. Concept of Stress ..... - 24 -
5.1.1.1. Stress Definition ..... - 24 -
5.1.1.2. Components of Stress ..... - 24 -
5.1.1.3. Strain Defined ..... - 25 -
5.1.1.4. Normal Stress ..... - 25 -
5.1.1.5. Shearing Stress ..... - 26 -
5.1.1.6. Stress-Strain Diagram ..... - 27 -
5.1.1.7. Principal Stress ..... - 28 -
5.1.1.8. Von Mises Theory ..... - 28 -
5.2. Finite Element Method ..... - 29 -
5.2.1. Numerical Methods ..... - 29 -
5.2.2. Basic Steps in the Finite Element Method ..... - 29 -
5.3. Preliminary Test ..... - 30 -
5.3.1. Process ..... - 31 -

5.3.2. Theoretical Method ..... - 31 -
5.4. Formal Analysis ..... - 33 -
5.4.1. The Analysis Flowchart ..... - 33 -
5.4.2. Theoretical Methods ..... - 34 -
5.4.3. Analysis ..... - 34 -
6. Results ..... - 35 -
6.1. Wave conditions ..... - 35 -
6.2. Results of Wave Loads ..... - 35 -
6.2.1. Wave Loads on the Cylindrical Components ..... - 35 -
6.2.1.1. Data of Forces on Cylinders at Condition 1 ..... - 37 -
6.2.1.2. Data of Forces on Cylinder at Condition 2 ..... - 46 -
6.2.2. Wave Loads on the Disc ..... - 55 -
6.2.2.1. Differential Pressure on the Disc at Condition 1 ..... - 57 -
6.2.2.2. Differential Pressure on the Disc at Condition 2 ..... - 60 -
7. Analysis and Discussion ..... - 62 -
7.1. Condition 1 ..... - 62 -
7.2. Condition 2 ..... - 66 -
7.3. Discussion ..... - 69 -
8. Conclusion ..... - 71 -
9. Bibliography ..... - 72 -
10. Appendices ..... - 76 -
10.1. Process in Running the GN Equation Program ..... - 76 -
10.2. Preliminary Computational Steps ..... - 77 -
10.2.1. Import 3D Model into ANSYS Workbench ..... - 77 -

10.2.2. Mesh Generation ..... - 79 -
10.2.3. Loads Input ..... - 82 -
10.2.4. Give Supports ..... - 86 -
10.2.5. Analysis ..... - 87 -
10.3. MATLAB Code ..... - 88 -
10.3.1. The Time of the Wave Movement ..... - 88 -
10.3.2. Horizontal Cylinder ..... - 89 -
10.3.3. Inclined Cylinder ..... - 91 -
10.3.4. Vertical Cylinder ..... - 92 -

List of Figures

Figure 1-1 World Energy Demand in Different Periods (1993, 2011. 2020) (Courtesy of World Energy Resources 2013 Survey)····· - 1 -

Figure 1-2 Energy Consumption to 2050, based on Spreadsheet Data (Courtesy of http://www.2052.info)····· - 2 -

Figure 1-3 Energy Reserves (Courtesy of https://www.ecotricity.co.uk/)····· - 3 -

Figure 1-4 Global Fossil Carbon Emission by Fuel Type, 1800–2007. (Courtesy of https://en.wikipedia.org/wiki/Fossil_fuel)····· - 3 -

Figure 2-1 Mean significant wave height for January-December 2010. (Courtesy of Venugopal and Nemalidinne, 2015)····· - 12 -

Figure 2-2 Maximum Wave Power for January-December 2010 (Courtesy of Venugopal and Nemalidinne, 2015)····· - 12 -

Figure 2-3 Mean Wave Power for January-December 2010 (Courtesy of Venugopal and Nemalidinne, 2015)····· - 13 -

Figure 2-4 Maximum Significant Wave Height for January-December 2010. (Courtesy of Venugopal and Nemalidinne, 2015)····· - 13 -

Figure 3-1 Schematic Diagram of the WEC····· - 14 -

Figure 3-2 3D Diagram of WEC····· - 15 -

Figure 3-3 2D Diagram of WEC····· - 16 -

Figure 4-1 Right-handed Coordinates····· - 17 -

Figure 4-2 Schematic Diagram of the Wave Environment ····· - 18 -

Figure 4-3 Inertial, Drag and the Total Forces on a Vertical Cylinder Calculated by Morison's Equation ····· - 20 -

Figure 4-4 Dimensionless Horizontal Force (H=4m, S=3m, T=15s)···· - 22 -

Figure 4-5 Dimensionless Vertical Force (H=4m, S=3m, T=15s)····· - 22 -

Figure 4-6 Differential Pressure in the Time of a Wave Crest (H=4m, S=3m, T=15s, t=873.98s)····· - 23 -

Figure 5-1 Three-dimensional state of stress (courtesy of Ugural 1991) ··· - 24 -
Figure 5-2 Deformation of a prismatic bar ····· - 25 -
Figure 5-3 Idealised stress in a straight bar with uniform cross-section (Courtesy of https://en.wikipedia.org/wiki/Stress_(mechanics)) ····· - 25 -
Figure 5-4 A Force F on a Bar (Courtesy of https://lms.ctl.cyut.edu.tw/sys/read_attach.php?id=2312780) ····· - 26 -
Figure 5-5 Analysis of the Separated Section (Courtesy of https://lms.ctl.cyut.edu.tw/sys/read_attach.php?id=2312780) ····· - 26 -
Figure 5-6 Stress-Strain Plot for Ductile Materials (courtesy of http://www.sciencebuddies.org/science-fair-projects/project_ideas) ····· - 27 -
Figure 5-7 Principal Stress (Courtesy of http://baike.baidu.com/view/1583998.htm) ····· - 28 -
Figure 5-8 Preliminary Test Flowchart ····· - 31 -
Figure 5-9 Wave Loads on a Submerged Disc (Simplified Mode) (Drawing by Shuijin LI) ····· - 33 -
Figure 5-10 Formal Analysis Flowchart as Followed in This Thesis ····· - 33 -
Figure 6-1 Cylinder Label ····· - 36 -
Figure 6-2 Sectional Forces on Horizontal Cylinder ····· - 38 -
Figure 6-3 Sectional Forces on Vertical Cylinder ····· - 38 -
Figure 6-4 Sectional Forces on Inclined Cylinder ····· - 39 -
Figure 6-5 Sectional Forces on Horizontal Cylinder ····· - 40 -
Figure 6-6 Sectional Forces on Vertical Cylinder ····· - 40 -
Figure 6-7 Sectional Forces on Inclined Cylinder ····· - 41 -
Figure 6-8 Sectional Forces on Horizontal Cylinder ····· - 42 -
Figure 6-9 Sectional Forces on Vertical Cylinder ····· - 42 -
Figure 6-10 Sectional Forces on Inclined Cylinder ····· - 43 -
Figure 6-11 Sectional Forces on Horizontal Cylinder ····· - 44 -

Figure 6-12 Sectional Forces on Vertical Cylinder ····· - 44 -
Figure 6-13 Sectional Forces on Inclined Cylinder ····· - 45 -
Figure 6-14 Sectional Forces on Horizontal Cylinder ····· - 47 -
Figure 6-15 Sectional Forces on Vertical Cylinder ····· - 47 -
Figure 6-16 Sectional Forces on Inclined Cylinder ····· - 48 -
Figure 6-17 Sectional Forces on Horizontal Cylinder ····· - 49 -
Figure 6-18 Sectional Forces on Vertical Cylinder ····· - 49 -
Figure 6-19 Sectional Forces on Inclined Cylinder ····· - 50 -
Figure 6-20 Sectional Forces on Horizontal Cylinder ····· - 51 -
Figure 6-21 Sectional Forces on Vertical Cylinder ····· - 51 -
Figure 6-22 Sectional Forces on Vertical Cylinder ····· - 52 -
Figure 6-23 Sectional Forces on Horizontal Cylinder ····· - 53 -
Figure 6-24 Sectional Forces on Vertical Cylinder ····· - 53 -
Figure 6-25 Sectional Forces on Inclined Cylinder ····· - 54 -
Figure 6-26 Dimensionless Sectional Vertical Force (Time Horizon from 0 to 1000) ····· - 55 -
Figure 6-27 Dimensionless Sectional Vertical Force (Time Horizon from 860 to 920) ····· - 56 -
Figure 6-28 Differential Pressure in the Time of Wave Crest (H=4m, S=3m, T=15s, t=873.98s) ····· - 57 -
Figure 6-29 Differential Pressure in the Time of Wave Trough (H=4m, S=3m, T=15s, t=883.31s) ····· - 57 -
Figure 6-30 Schematic diagram of x in the disc (x in this table is measured from the leading edge of this disc) ····· - 58 -
Figure 7-1 Deformation in true scale ····· - 62 -
Figure 7-2 Von-Mises Stress in the WEC at Condition 1 (H=4m, S=3m, T=15s, t=883.98s) ····· - 63 -
Figure 7-3 The Distribution of Deformation on the WEC‘s Disc (H=4m,

S=3m, T=15s, t=873.98s)····· - 63 -
Figure 7-4 Maximum deformation of different materials ····· - 64 -
Figure 7-5 Maximum deformation of different materials in Condition 1 with different test cases sequences ····· - 65 -
Figure 7-6 Deformation in true scale····· - 66 -
Figure 7-7 Von-Mises Stress in the WEC at Condition 2 (H=4m, S=3m, T=15s, t=883.98s)····· - 66 -
Figure 7-8 The Distribution of Deformation on the WEC‘s Disc (H=4m, S=3m, T=15s, t=883.98s)····· - 67 -
Figure 7-9 Maximum deformation of different materials ····· - 68 -
Figure 10-1 Cinput.INP file····· - 76 -
Figure 10-2 The interface of GNSP.exe····· - 76 -
Figure 10-3 Create a Section of Analysis····· - 77 -
Figure 10-4 Select Import External Geometry File...····· - 78 -
Figure 10-5 Open File····· - 78 -
Figure 10-6 Import file ····· - 78 -
Figure 10-7 Select "Generate"····· - 79 -
Figure 10-8 Select “Unfreeze”····· - 79 -
Figure 10-9 Select "Generate"····· - 79 -
Figure 10-10 Select "Model" ····· - 80 -
Figure 10-11 Insert mesh method····· - 80 -
Figure 10-12 Select model····· - 81 -
Figure 10-14 Select detailed method····· - 81 -
Figure 10-14 Select Free Mesh Type ····· - 81 -
Figure 10-16 Select Relevance Center ····· - 82 -
Figure 10-16 Select Span Angle Center····· - 82 -
Figure 10-17 Generate mesh ····· - 82 -
Figure 10-18 Select Loads type····· - 83 -

Figure 10-19 Select the pressure surface ····· - 83 -
Figure 10-20 Alter Coordinate System ····· - 84 -
Figure 10-21 Change the coordinate origin ····· - 84 -
Figure 10-23 Change the form of inputting Magnitude ····· - 84 -
Figure 10-23 Change Independent Variable ····· - 84 -
Figure 10-24 Input data ····· - 85 -
Figure 10-25 Change Analysis Settings ····· - 85 -
Figure 10-26 Select Supports ····· - 86 -
Figure 10-27 Select all cylindrical surfaces ····· - 86 -
Figure 10-28 Select the form of deformation ····· - 87 -
Figure 10-29 Select the form of Strain ····· - 87 -
Figure 10-30 Select the form of Stress ····· - 87 -
Figure 10-31 Select "Solve" to analyse results ····· - 88 -

List of Tables

Table 1-1 Key Indicators for 1993, 2011 and 2020 (Courtesy of World Energy Council 2013) ..... - 5 -

Table 5-1 Properties of Different Materials ..... - 34 -

Table 6-1 Environmental Conditions considered in This Study ..... - 35 -

Table 6-2 Sectional Forces on Horizontal Cylinder ..... - 38 -

Table 6-3 Sectional Forces on Horizontal Cylinder ..... - 40 -

Table 6-4 Sectional Forces on Horizontal Cylinder ..... - 42 -

Table 6-5 Sectional Forces on Horizontal Cylinder ..... - 44 -

Table 6-6 Sectional Forces on Horizontal Cylinder ..... - 47 -

Table 6-7 Sectional Forces on Horizontal Cylinder ..... - 49 -

Table 6-8 Sectional Forces on Horizontal Cylinder ..... - 51 -

Table 6-9 Sectional Forces on Horizontal Cylinder ..... - 53 -

Table 6-10 Differential pressure on the disc in condition 1 ..... - 58 -

Table 6-11 Differential pressure on the disc in condition 2 (x in this table is measured from the leading edge of this disc) ..... - 60 -

Abstract

The ocean is a trove of energy treasure. In recent years, the development of marine renewable energy is getting hotter. More and more equipment will work undersea. This project is devoted to studying the structural analysis of a novel wave energy device. The wave energy converter consists of a submerged, vertically oscillating disc attached to a direct-drive power take-off system. The concrete method for this project is to establish a 3D model of the WEC in AutoCAD, calculate the wave load of WEC by using Morison's Equation and The GN Equations and analyse the structure response in ANSYS Workbench. The results obtained in this project include the deformation of WEC of different materials, including stainless steel, concrete, aluminium alloy, titanium alloy, under extreme environmental conditions. For each of the materials, 24 extreme wave conditions are tested, resulting in a total of 96 test cases. Finally, according to Von Mises Theory, the durability of the device is assessed for all cases considered here.

Shuijin

Acknowledgements

I would like to express my deepest gratitude first and foremost to Dr Masoud Hayatdavoodi, my supervisor, who helped me so much during the process of writing this thesis and guided my project during the past several months. In the preparations of this thesis, he has spent much time helping me modify each draft and provide me with inspiring advice. In the last few months, every of my growing footprints has Professor's credit.

Secondly, I would like to express my whole-hearted gratitude to my family for supporting me to study overseas. Thank them for sharing my worries, frustrations and happiness, and giving me hope and confidence.

Thirdly, I would like to devote my great acknowledgement to Hohai University and University of Dundee, both of which provide the funds for the China 3+1+1 Programme students.

Finally, I would like to thank those who have helped me in the past few months, whether they are friends or strangers in reality or the internet.

Declaration

I hereby declare that the work contained in this document is my own work, and that has not been presented in a previous application for a higher degree.

Signed: 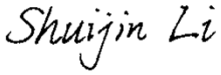

1. Introduction

1.1. Background

With the development of society, energy consumption is growing rapidly. From drilling wood for the fire to generate electricity from solar, the way that people exploit energy is changed dramatically over time. To drive this society operating normally, energy consumption is increasing rapidly. From Figure 1-1, although energy consumption is increasing, fossil still the main approach to get energy. A 2013 survey acclaimed that the main fossil fuels (include coal, oil, and natural) can last for decades (World Energy Resources 2013 Survey 2013, 7-8).

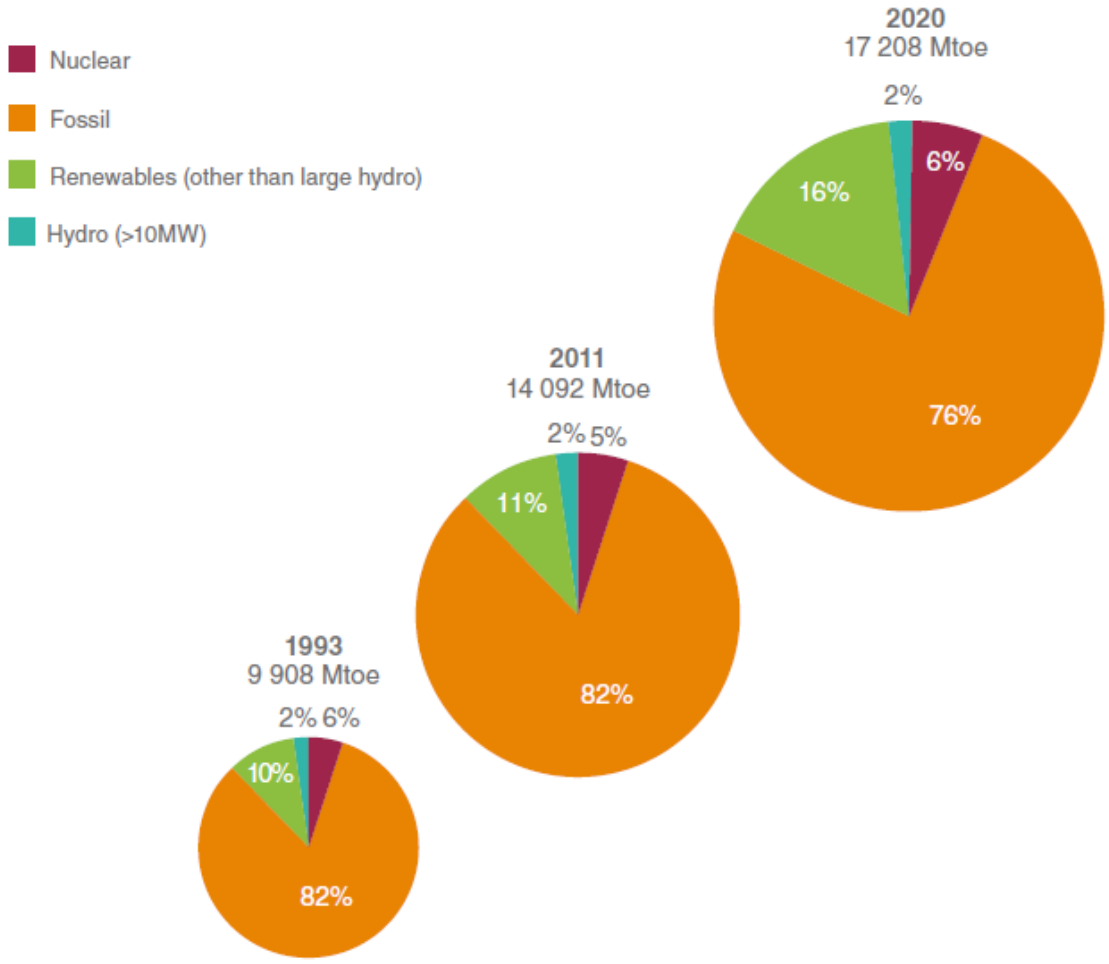

Figure 1-1 World Energy Demand in Different Periods (1993, 2011. 2020) (Courtesy of World Energy Resources 2013 Survey)

Nowadays, developing countries have a higher level of energy consumption than developed countries. Fuelwood is playing a primary role in developing countries, 3 billion people use solid fuels for heating and cooking but not used in commercial (World Energy Council, Global Energy Assessment). Energy growth is driven by population and economic growth. Transparently, world energy consumption increased steadily in the past few decades and will increase exponentially in the future.

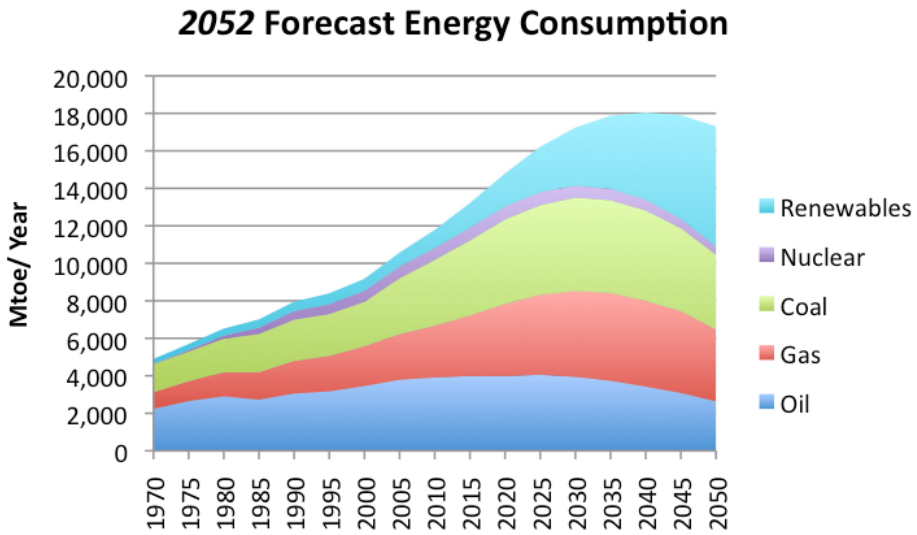

Figure 1-2 Energy Consumption to 2050, based on Spreadsheet Data (Courtesy of http://www.2052.info)

Figure 1-2 shows energy consumption to 2025. We can see that the total demand will peak at 18,000 Mtoe then decrease from 2040, and the percentage of renewables will increase dramatically over time. Figure 1-3 shows energy reserves in the world, which illustrates conventional energy will consume entirely in 2088. The energy consumption is growing rapidly; the fossil reserves are so limited. One day, fossil fuels can no longer support global energy consumption. So, to fill the energy demand blank, it is the high time that we should turn our attention to exploit renewable energy. On the other hand, the damage of using conventional sources has emerged gradually, which has driven the research and development (R&D) of the renewable energy technologies. Although any energy technologies have some environmental impact, the influence of the environment

of the renewable energy technologies is less than that of the fossil fuel technologies (Pelc and Fujita 2002, 471-479).

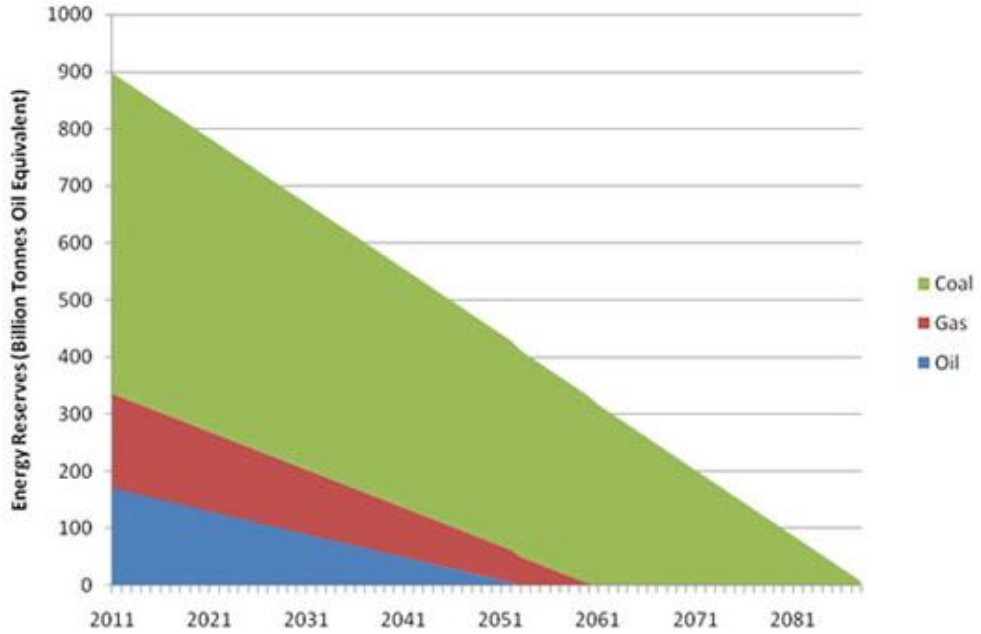

Figure 1-3 Energy Reserves (Courtesy of https://www.ecotricity.co.uk/)

Conventional sources have many remarkable issues, although it still the primary energy today (GEA 2012). Fossil fuel, which is so limited, will be consumed in the near future. P. E. Hodgson (2008) insisted that the world oil, the main source of conventional sources, is excepted to peak in ten years and then fall. If a more efficient and promising renewable energy technology could not be developed, we will face an energy crisis soon. Fossil fuel has another problem is the serious pollution of the environment. Environmental Protection Agency's survey in 2012 shows that more than 90% of greenhouse gas emissions come from the combustion of fossil fuels in U.S.A

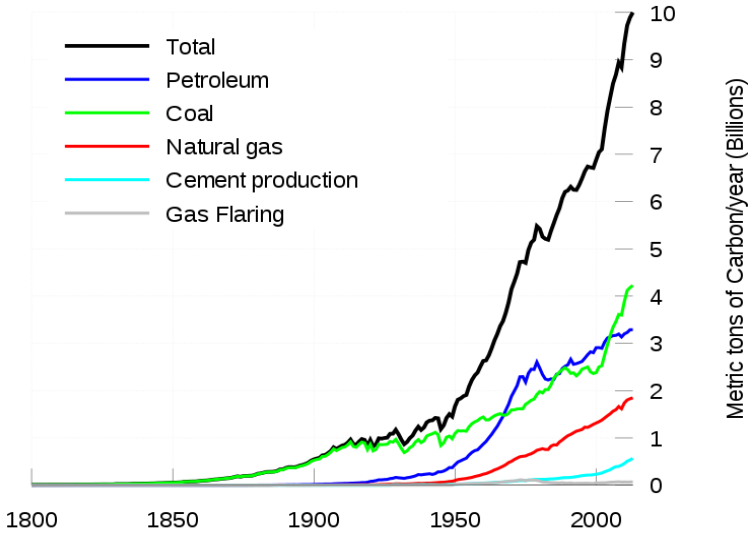

Figure 1-4 Global Fossil Carbon Emission by Fuel Type, 1800–2007. (Courtesy of https://en.wikipedia.org/wiki/Fossil_fuel)

(EPA 2012). Some other air pollution also made by combustion of fossil fuels, such as nitrogen oxides, sulphur dioxide, volatile organic compounds and heavy metals (Wikipedia 2016). Figure 1-4 shows global fossil emission by fuel type between 1800 to 2007. The total carbon emission in 2007 was about 10 times than in 1950, which shows it increased rapidly from 1950. To avoid the impact of the environment caused by air pollutions, energy companies need to pay more. A 2015 report, studied 20 of the largest oil, gas and coal producing fossil fuel companies, illustrated that these companies had large hidden economic cost to society while the profit is enormous (Hope, Gilding and Alvarez 2016) (University of Cambridge Judge Business School 2016). The report demonstrated that, for all companies and all years, the economic cost to society of CO_2 emissions was greater than their after-tax profit.

Global Energy Assessment (GEA, 2012) predicted that a share of renewable energy (biomass, hydro, wind, solar, and geothermal) will increase sharply over a half of the global energy supply. Using renewable energy technologies will be the primary approach in the future. But, nowadays, there still some difficulties to renewable energy technologies. The remarkable one is the price. Renewable energy technologies would derive a benefit in a long-term, because of the renewable energy – solar, wind, ocean waves, etc. – are unrestricted and boundless. So, in a short-term, renewable energy technologies couldn't profit as much as conventional energy technologies. For example, wind power cost 30cents/kWh in the 1980s, it was not feasible to be commercial in that period. But the price of wind power dropped to 5 cents/kWh in 1999, which made it more competitive to fossil fuels (Herzog 1999). From this, we can see renewable energy will be the cheaper and more efficient energy in the future.

1.2. Renewable energy

There are many kinds of renewable energy, such as Hydro, Bioenergy, Waste to Energy, Solar Energy, Geothermal Energy, Wind Energy, Marine Energy

(World Energy Council 2013). See Table 1-1 for details.

Table 1-1 Key Indicators for 1993, 2011 and 2020 (Courtesy of World Energy Council 2013)

Source: 1993, 2020 figures from Energy for Tomorrow's World (WEC, 1995). 2011 figures from World Energy Resources (WEC, 2013). Other renewables 2020 figure from World Energy Scenarios report (WEC, 2013)

	1993	2011	2020	% Growth 1993–2011
Population, billion	5.5	7	8.1	27%
GDP				
Trillion USD	25	70	65	180%
TPES Mtoe	9 532	14 092	17 208	48%
Coal Mt	4 474	7 520	10 108	68%
Oil Mt	3 179	3 973	4 594	25%
Natural Gas bcm	2 176	3 518	4 049	62%
Nuclear TWh	2 106	2 386	3 761	13%
Hydro Power TWh	2 286	2 767	3 826	21%
Biomass Mtoe	1 036	1 277	1 323	23%
Other renewables* TWh	44	515	1 999	n/a
Electricity Production/year				
Total TWh	12 607	22 202	23 000	76%
Per capita MWh	2	3	3	52%
CO_2 emissions/year				
Total CO_2 Gt	21	30	42	44%
Per capita tonne CO_2	4	4	n/a	11%
Energy intensity koe, 2005 USD	0.24	0.19	n/a	-21%

* Includes figures for all renewables, except Hydro

(1) Hydropower – exploiting the energy of moving water of power - represents a large part of the world's energy, which has been developed in more than 100 countries all over the world, providing about 15% of the world's electricity (World Energy Council 2013).

(2) Biomass can make a significant contribution to the supply of the future energy needs in a sustainable way, which is currently the largest global contributor to renewable energy and has great potential in the

development of heat, electricity and fuel production. Bioenergy is mainly produced from local wood resources. Traditionally, biomass is used for cooking and heating (World Energy Council 2013).

(3) Waste-to-Energy technologies are made up of any energy waste treatment processes that generate electricity, heat, or transport energy from a source of waste (World Energy Council 2013).

(4) Solar energy is a rich and eternal energy on Earth, but how to use it more efficiently still need time to develop. Solar energy is available to use it for its direct and indirect forms of energy (wind, biomass, hydro, ocean, etc.) (World Energy Council 2013).

(5) Geothermal energy comes from the earth's natural heat, mainly due to produce from the decay of uranium, thorium and potassium natural radioisotope (World Energy Council 2013).

(6) The Wind has many applications, including electricity generation. A survey (World Energy Council 2013) illustrated that world wind energy reserves have doubled every 3.5 years since 1990. We've made a progress on exploit wind energy (World Energy Council 2013).

(7) Marine energy has three separate sections, Tidal Energy, Wave Energy and Ocean Thermal Energy Conversion (OTEC) (World Energy Council 2010). Technology developers in these areas are constrained by a shortage of capital and, especially, by investors are often reluctant to commit to a large amount of capital required to demonstrate commercial viability (World Energy Council 2013).

The ocean is a treasure house. It has a huge potential for us to exploit renewable energy from waves. There are four main renewable energy resources from the ocean, ocean thermal energy conversion (OTEC), wave energy, tidal, and wind energy (Pelc and Fujita 2002). Wave energy is considered to be one of the feasible energy technologies, which is because the wave energy is enormous and

it is highly available than other renewable energy. In addition, at a given site, wave power can be available up to 90% of the time, which is more available than solar and the wind that is available just 20%-30% of the time (Pelc and Fujita 2002). In this thesis, we focus on wave energy.

1.3. Wave Energy

Wave energy, which is produced by wind action, is an indirect form of solar energy. Because of the wonderful wave destructive effects, the energy from the ocean waves is the most remarkable form of ocean energy (Falcão 2010).

Although the wave energy technology is relatively new to fossil fuel technologies, and currently has not economically competition with more mature technologies such as wind energy, the interest from governments and industries is increasing steadily. An important feature of sea waves is their high energy density, which is the highest one among renewable energy sources. Over the past 25 years, wave energy technology had undergone a cycle of enthusiasm, disappointment and reconsideration. But the continued development and efforts in technology are constantly changing the performance of wave energy technology and make today's wave energy technology is closer to commercial development than in the past. Different solutions have been proven that is suitable for a large number of operations under different conditions in different parts of the world. Other equipment is also in the final stages of R&D, and have a prospect of success. However, in order to steadily better the performance of wave energy technology and to build competitiveness in the global energy market, more extensive research and development in wave energy technology are needed at the basic and application level (Clément, et al. 2002).

1.4. A Novel Wave Energy Device

The wave energy converter (WEC hereafter) is comprised of a horizontal disc connected to direct-drive a generator within a column. The bottom of the

device is fixed on the seabed. The platform will oscillate vertically with the wave motion, making the generator generate electricity. The WEC will be used to exploit marine renewable energy.

1.5. Thesis Structure

This project is aiming at the structural analysis of a WEC. Before analysing the structure of the WEC, we will determine the wave conditions discussed in chapter 4. After that, we will calculate the wave loads on the device. The wave loads will be calculated by Morison's Equation and The GN Equations given in chapter 4.3. Then we can analyse the structural integrity of the WEC. To analysis, we will create a 3D model of the WEC by using of AutoCAD discussed in chapter 3. Then the 3D model will be imported into ANSYS Workbench. After that, an integrated mesh will be creating in the 3D model. Then, a complete set of wave loads, which will be calculated in chapter 4, will be loaded to act on the WEC. Then we will compare with the capacity of the material properties and assess the integrity of the structure under the wave loads to check whether it is strong enough or not.

2. Literature Review

2.1. Wave Energy Converters

Wave is generated by wind passing over the surface of the ocean. Wave energy is the transportation of energy by wind waves. Wave energy is considered one of the most dependable renewable technologies, because of its vast energy reserves and availability. However, wave energy technology is not mature compared with other renewable energy technologies. Many wave energy converters (WECs) have been investigated, but most of them are still at the R&D stage, with just a tiny part of devices having been tested at large scale, implemented in the oceans (Drew, Plummer and Sahinkaya 2009).

There are more than 1000 concepts about wave energy conversion technologies, which have been monopolistic in Japan, North America, and Europe (Callaghan and Boud 2006). Here, we will review some of the popular devices.

2.1.1. Type of WEC

Despite there are numerous kinds of concepts and patents of WECs which can be classified into three main types suggested by B. Draw, A. R. Plummer and M. N. Sahinkaya (A review of wave energy converter technology. 2009, 889).

(1) Attenuator

Attenuators lie parallel to the predominant wave direction and float in the ocean. Pelamis is a classic example to the attenuator. Pelamis Wave Energy Convertor (PWEC) is a technology that utilises the movement of ocean surface waves to create electricity, operating in water depths greater than 50m. PWEC is a floating device composed of some cylindrical hollow steel segments connected to each other by two degree-of-freedom hinged joints (Pelamis Wave Energy Converter 2016).

(2) Point absorber

A point absorber is a floating structure at/near the water surface or

submerged in the water, which absorbs energy from all directions over the sea through oscillating up and down with waves (EMEC 2016 and López, et al. 2013). An example is Ocean Power Technology's PowerBuoy, which can be connected to the electrical grid using cables, generates power using a hydroelectric turbine (Ocean Power Technologies 2016).

(3) Terminator

Terminator is similar to Attenuator in shape. But, Terminator is perpendicular to the predominant wave direction. One example is the WavePlane converter (WavePlane Production 2016), WavePlane converts waves directly into a fast and smooth rotation without any moving parts.

2.1.2. Typical Locations

There are three main kinds of locations of WECs, Shoreline Devices, Nearshore Devices and Offshore Devices suggested by Drew, Plummer and Sahinkaya.

Shoreline devices are close to the utility work and easy to maintain. But wave in shoreline is too weak, so shoreline device cannot get much energy.

Nearshore devices attach to the seabed in shallow water. Wave in shallow water also has a limitation for devices to harvest energy.

Offshore devices are in deep water, which can harvest amounts of wave energy. But in deep water, devices are not easy to maintain.

2.1.3. Challenges with Traditional WECs

The WECs have some typical challenges which should be considerable to solve in all kinds of converters (Drew, Plummer and Sahinkaya 2009).

(1) Converting the slow, random, high-force oscillating motion into functional motion to generate electricity.

(2) Wave direction is highly mutable in offshore locations. Most of the devices, however, are only efficient in a certain direction.

(3) The devices are under the impact of extreme wave conditions that occur

near the surface.

(4) How to decrease the highly corrosive environment of devices in the sea.

2.1.4. The Advantages of the Proposed Novel Wave Energy Device

As shown in Chapter 1.4 and Chapter 3, we can know the structures of the novel WEC. Because of its structures, it can overcome the challenge mentioned in Chapter 2.1.3.

Since the WEC is fully submerged, it is protected from the impact of extreme wave conditions. In fact, the extreme wave condition is an advantage to this device. Simultaneously, the WEC can convert the waves that generated by extreme wave motion into energy safely. Secondly, the WEC can be efficient in all directions on account of that the WEC generates energy through the waves drive the disc moving vertically. Finally, the WEC will use the corrosion resistant materials to work under seawater to overcome the corrosive environment in the sea. We shall discuss the proposed WEC in Chapter 3.

2.2. Wave Conditions around the UK

Venugopal and Nemalidinne (2015) used a buoy to make a large scale spectral wave model to show the wave condition around the UK, in particular for Scottish waters. From Figure 2-1 to Figure 2-4, we can see that in the northern waters of UK has better wave conditions than other places around the UK. In the northern waters of UK, whether the mean significant wave height, the maximum significant height, the mean wave power, or the maximum significant wave power are good for supporting wave energy technology. So, we can site our WEC in the northern waters of UK, such as near the Durness (a northern city in Scotland), waters around Mainland.

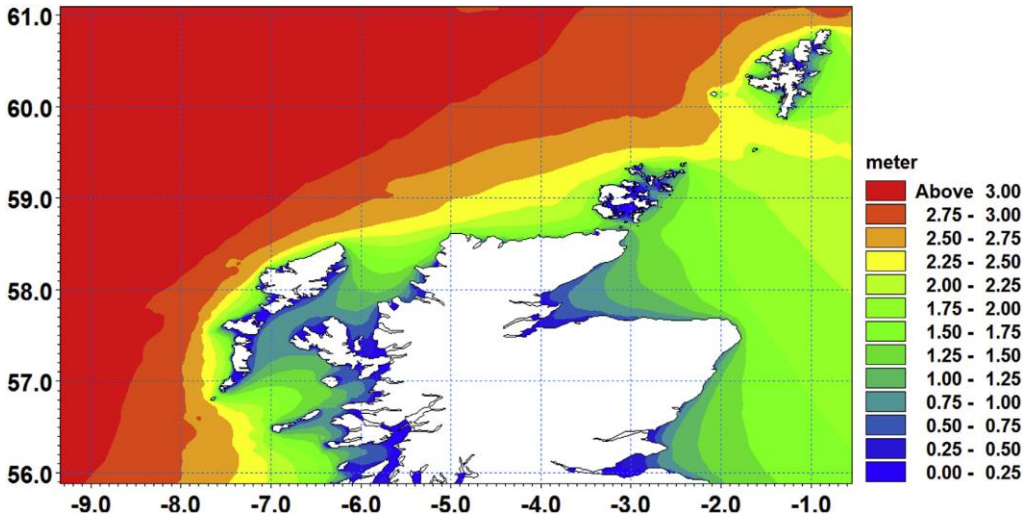

Figure 2-1 Mean significant wave height for January-December 2010. (Courtesy of Venugopal and Nemalidinne, 2015)

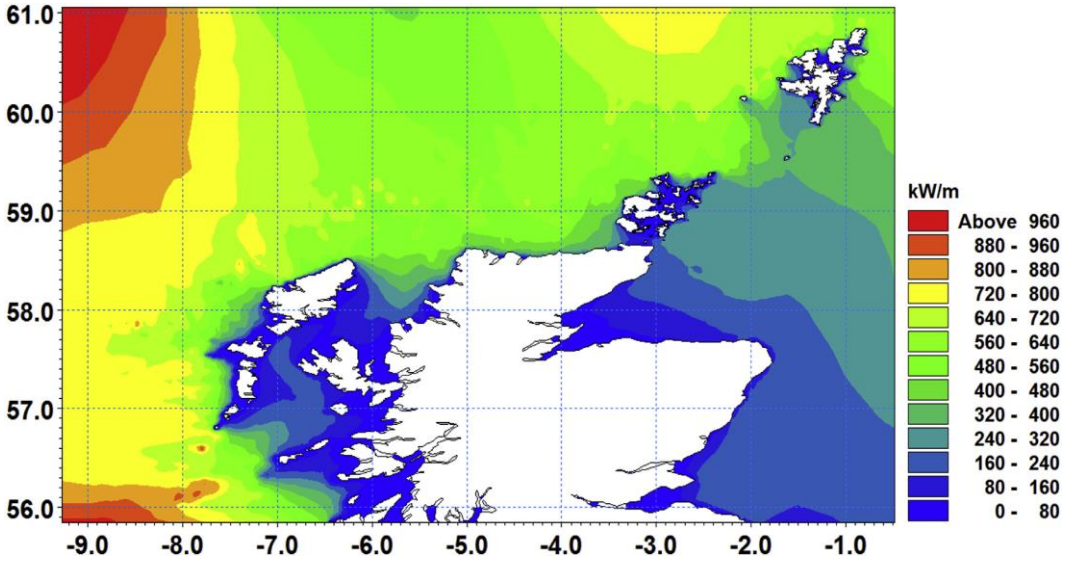

Figure 2-2 Maximum Wave Power for January-December 2010 (Courtesy of Venugopal and Nemalidinne, 2015)

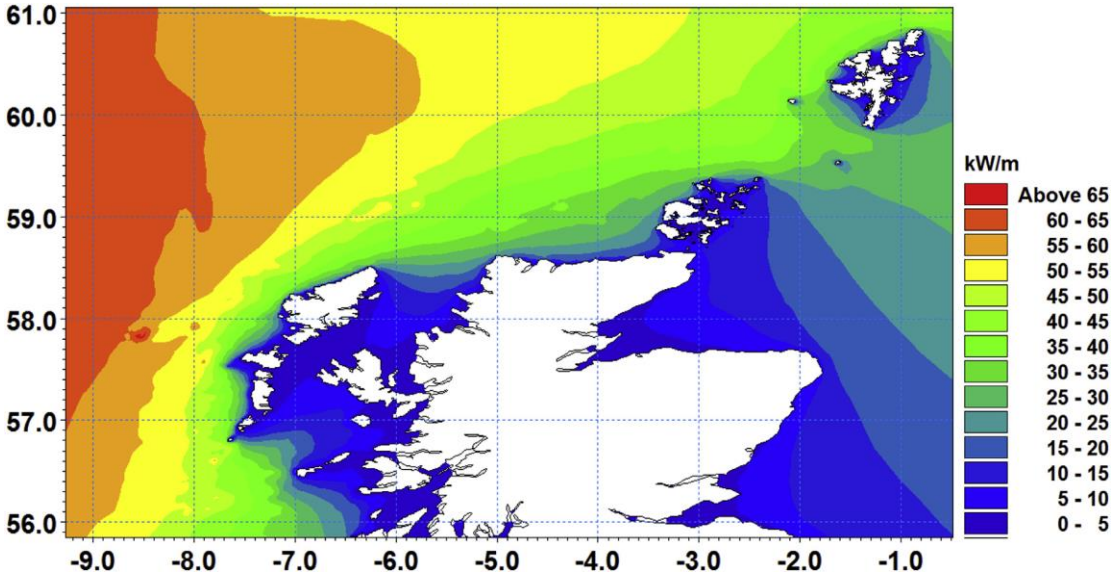

Figure 2-3 Mean Wave Power for January-December 2010 (Courtesy of Venugopal and Nemalidinne, 2015)

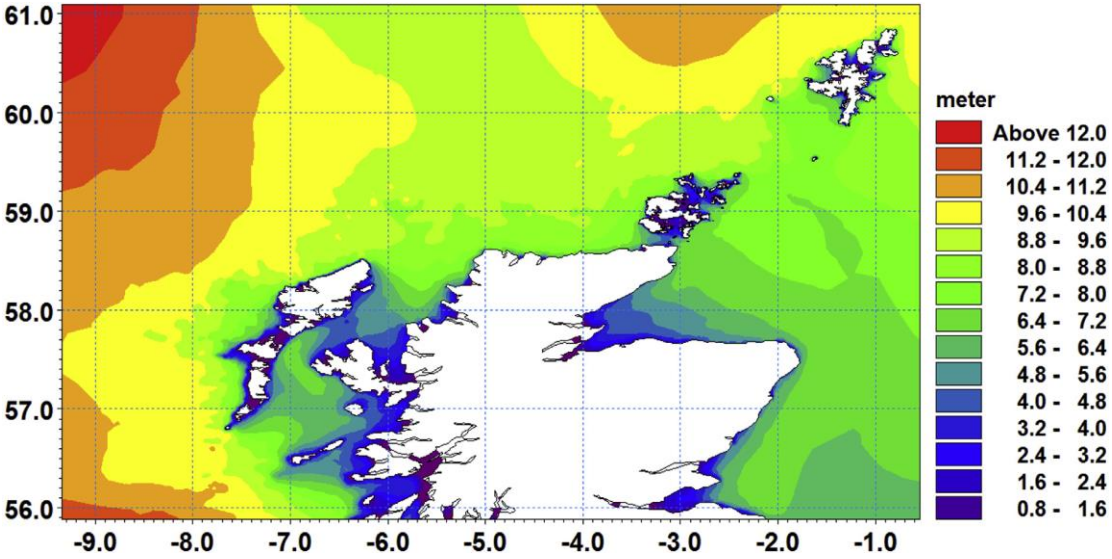

Figure 2-4 Maximum Significant Wave Height for January-December 2010. (Courtesy of Venugopal and Nemalidinne, 2015)

2.3. Method

We use Morison's Equation (Morison, et al. 1950) and the GN Equation (Green and Naghdi 1976) to calculate the pressure around WEC (See Chapter 4.3.1 and 4.3.2 for details)

In this project, we programme Morison's Equation in MATLAB to calculate the pressure around the cylinders under different wave conditions. In addition, there are 12 different wave conditions to be tested, and each wave condition is divided into 2 cases by the time of wave crest or trough movement. So the time of the wave crest or trough movement to the top centre of WEC needs to be calculated. See Chapter 10.3 for a specific code.

Furthermore, we use the GN Equation to calculate the differential pressure on the disc. By running a program, we can get the pressure differential on the disc easily. See Chapter 10.1 for the running process.

3. The Wave Energy Device

3.1. Introduction

According to Chapter 1.4 and Chapter 2.2, we already know that the WEC is located in the shallow sea of northern Scotland which has an environment for supporting wave energy technology.

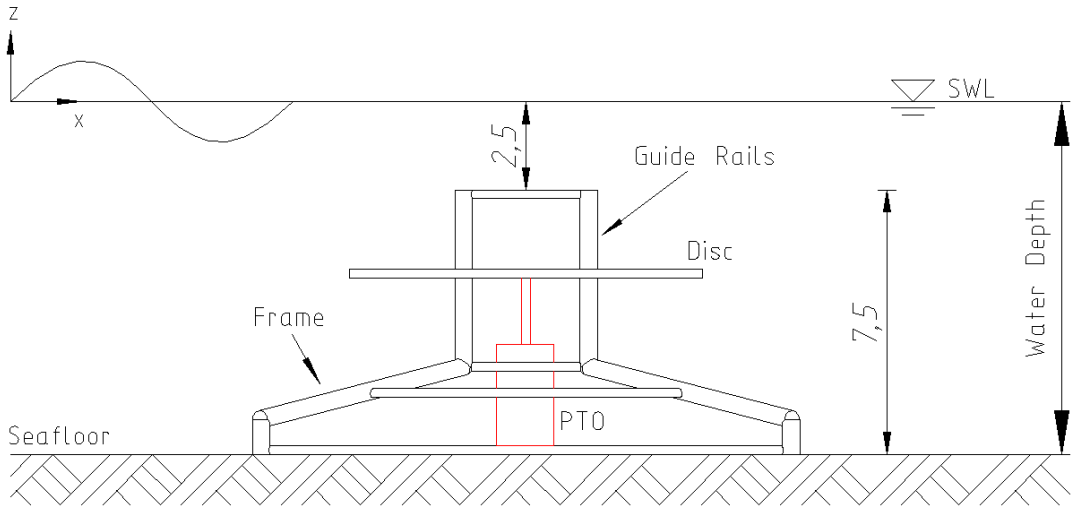

Figure 3-1 Schematic Diagram of the WEC

See Figure 3-1, the WEC is made up of a disc with a diameter of 10m and a number of cylindrical rods of 0.25m and 0.5m in diameter. The disc is a platform connected to a generator which is a direct drive power take-off (PTO) system for energy extraction, this part is located in the centre of the WEC. Other columns are distributed in the vicinity as support frames. The platform will move up and down with the movement of waves, thus driving power generation equipment. For this project only analyses the structural of the WEC, only the disc and columns structures are retained in the analysis. A detailed figure for the WEC will be shown in Chapter 3.2.

3.2. Modeling

Before we perform a detailed calculation, we need to know what the model looks like, so that we can calculate the corresponding position data later.

Modelling is carried in AutoCAD (a computer-aided design and drafting

software developed and marketed by *Autodesk*). Because the model is not complicated, so using the function of AutoCAD is enough. In this part, Dr Hayatdavoodi gave a draft of the equipment, then Shuijin Li completed the modelling in AutoCAD. The following figures (Figure 3-2 and Figure 3-3) are the three-dimensional and the two-dimensional maps of the WEC, respectively.

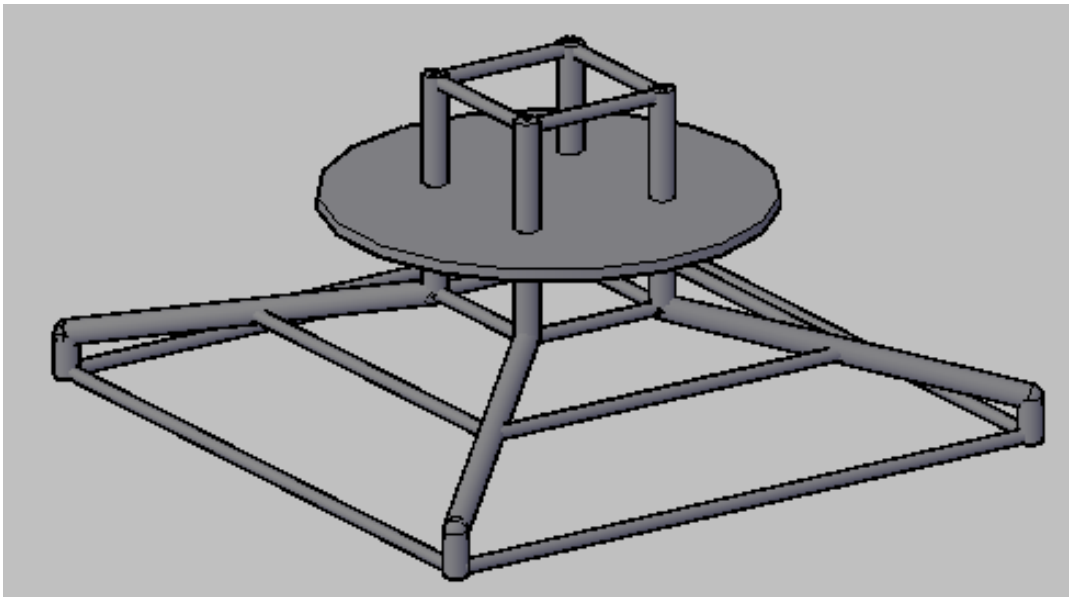

Figure 3-2 3D Diagram of WEC

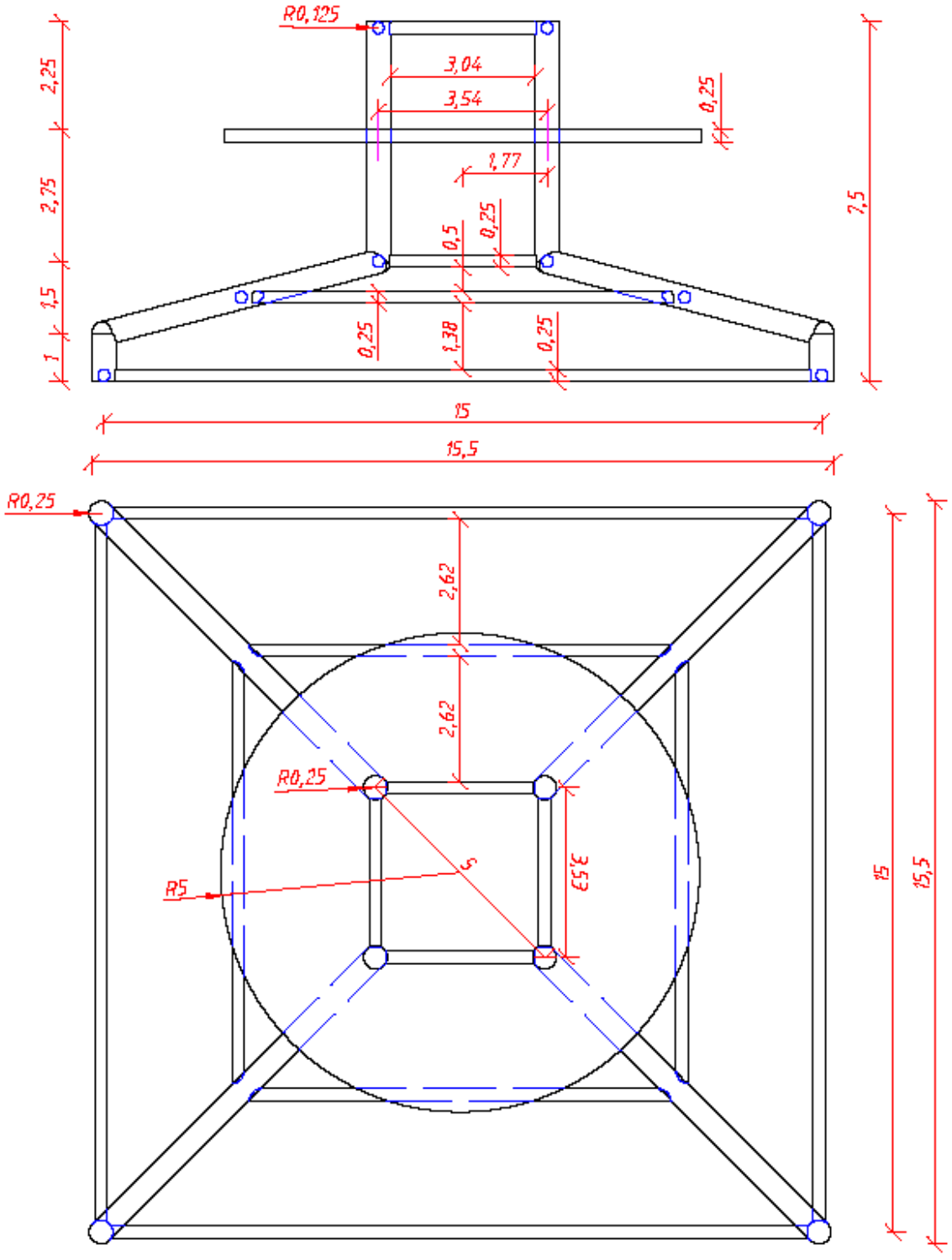

Figure 3-3 2D Diagram of WEC

4. Wave Condition and Load

4.1. Coordinate system

In this thesis, the coordinate system is a Cartesian coordinate system which is an orthogonal coordinate system.

The three-dimensional Cartesian coordinate system here is a right-hand system. For right-handed coordinates, X axis points to the right, Z axis points upward against the direction of gravitational acceleration and Y axis points into the paper.

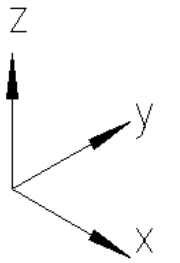

Figure 4-1 Right-handed Coordinates

4.2. Wave Environment

The WEC is located in a shallow water, let's premeditate a simple water environment that the water is two-dimensions, inviscid, incompressible and homogeneous. We assume that:

- the waves are regular waves;
- wave height H=3m or 4m;
- wave period T=10s or 15s;
- water depth h=10m;
- WEC is on the seabed;
- the temperature of sea water is 4°C;
- the density of sea water is ρ, ρ = $1.025 \times 10^3 \mathrm{kg}/m^3$.

Apart from this, we will calculate the disc that submerged in 3m, 5m, and 7m under the still water level and we'll calculate different situations when the crest and trough of the wave at the top centre of the WEC, respectively.

Figure 4-2 illustrates a schematic diagram of the wave environment:

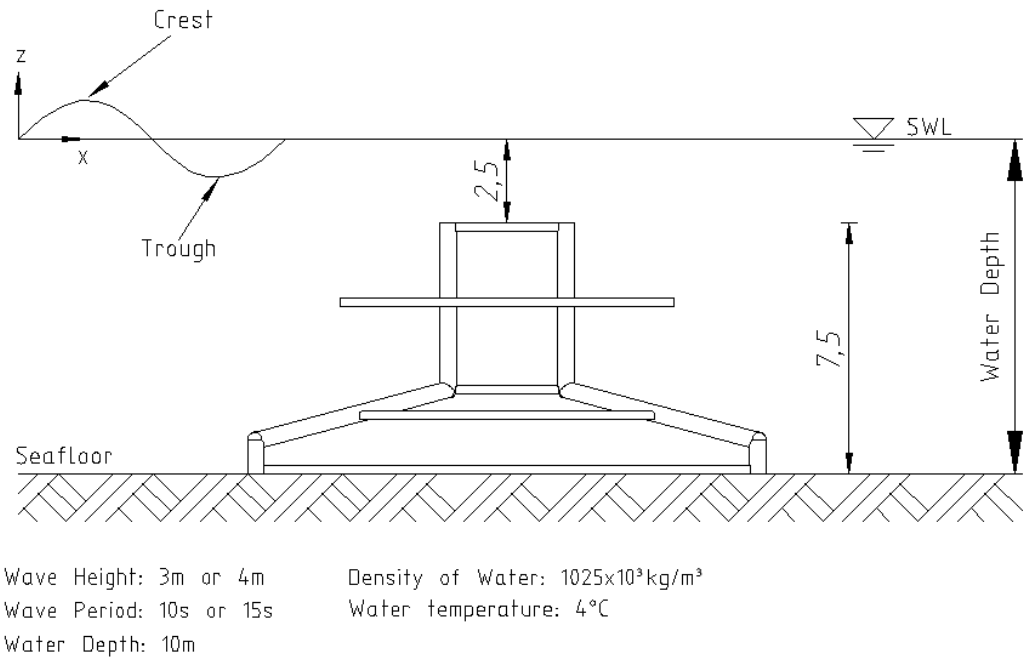

Figure 4-2 Schematic Diagram of the Wave Environment

4.3. Wave Loads

4.3.1. Morison's Equation

Due to the development of the sea in the 1940s, engineers needed to calculate the force on the cylinder submerged in seawater. Morison, et al. (1950) established a theory on how to calculate the force wielded by unbroken surface waves on a cylindrical component. This theory applies to single piles. It is necessary to be modified if multiple piles are driven, such as one within the influence of the other, or where a plurality of piles are connected by submerged support (Morison, et al. 1950).

The force is comprised of 2 components, drag force and virtual mass force. The drag force is proportionated to the square of the velocity which may be epitomised by a drag coefficient having substantially the same value as for steady flow. Virtual mass force is proportionated to the horizontal component of the acceleration force exerted on the mass of water displaced by the pile (Morison, et al. 1950).

Morison's Equation (Morison, et al. 1950) is developed from the equations

for waves of small amplitude, which is used to calculate the horizontal wave force F acting at any height z of a cylinder structure. Two empirical hydrodynamic coefficients (Inertia coefficient and drag coefficient) are contained in the Morison's Equation, which is determined from the data that from experiments. In an oscillatory flow with flow velocity $\mathrm{u} = \mathrm{u}(\mathrm{x}, \mathrm{y}, \mathrm{z}, \mathrm{t})$, the Morison's Equation gives the aligned force parallel to the flow direction:

$$dF = dF_I + dF_D \quad (1)$$

Where

- F_I is the inertia force, $dF_I = C_M \rho \frac{\pi D^2}{4} \frac{du}{dt}$;
- F_D is the drag force. $dF_D = C_D \rho \frac{D}{2} u|u|$;
- ρ is the density of fluid, ρ = 1.025 × 10^3kg/m^3 in seawater;
- u is the velocity of the flow, $\mathrm{u} = \mathrm{u}(\mathrm{x}, \mathrm{y}, \mathrm{z}, \mathrm{t})$;
- $\frac{du}{dt}$ is the flow acceleration, i.e. the time derivative of the flow velocity;
- C_D is the drag coefficient, which is a dimensionless quanlity in fluid mechanics that is used to characterise the resistance of an object in a fluid. The drag ccoefficient is related to the shape of the object and its surface properties. Here we assume that $C_D = 1.2$;
- C_M is the inertia coefficient, $C_M = 1 + C_a$ and C_a is the added mass coefficient. The dimensionless added mass coefficient is the added mass by the mass of the displaced fluid, which means divided by the fluid density times the volume of the vody. Here we assume that $C_M = 2$;
- D is the diameter of the cylinder structure.

Morison's Equation is an empirical equation gained from the equation of small amplitude wave. The first assumption is that the flow acceleration is uniform at the location of the body (Patel and Witz 2013). Secondly, it is assumed that the inertial and drag force is valid for a minute and enormous Keulegan–Carpenter numbers. Nevertheless, in this intermediary method, drag force and inertia are

both making remarkable contributions from experiments (Sarpkaya 2010).

As an example, here we show the inertia, drag and the total wave force on a vertical cylinder calculated by Morison's Equation, which is shown in Figure 4-3. The wave condition here is H=4m, h=10m, T=15m. The cylinder length is 1m, the diameter of the cylinder is 0.5m.

As seen in Figure 4-3, the drag force has a large amplitude as time goes by, which means it is dominant in the total force on a vertical cylinder.

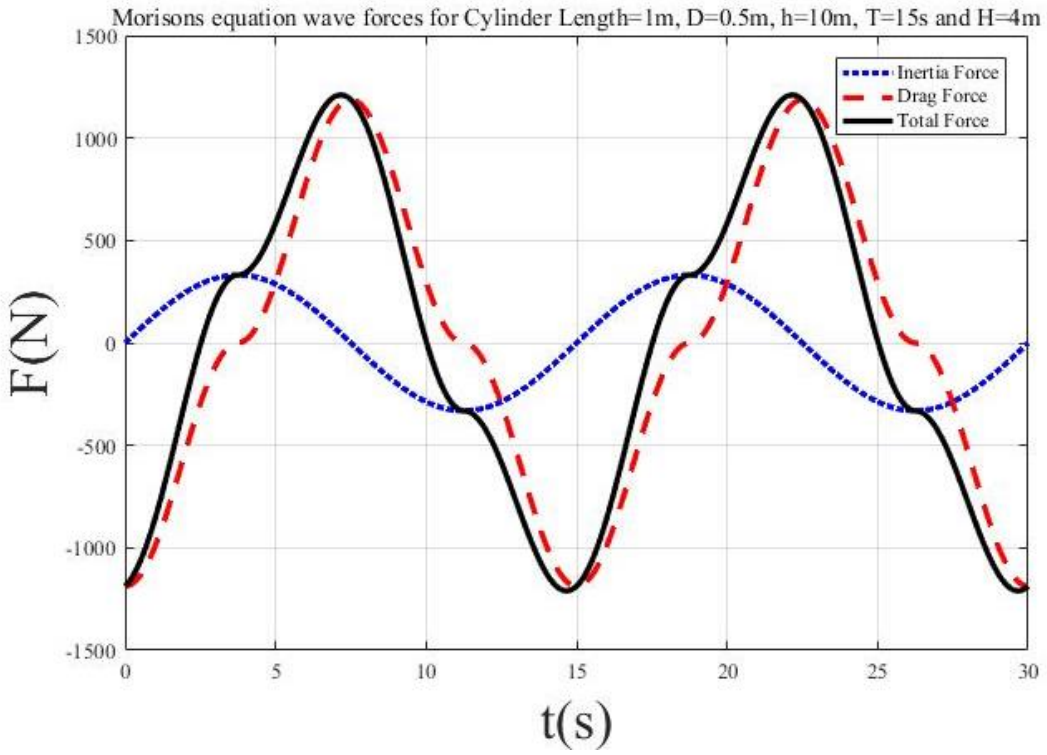

Figure 4-3 Inertial, Drag and the Total Forces on a Vertical Cylinder Calculated by Morison's Equation

4.3.2. The GN Equations

4.3.2.1. Introduction

In recent years, the development of the ocean became more and more prevalent, offshore facilities are gradually transferred from the coast to the ocean. Every so often, in order to avoid the effects of extreme climate events (such as a hurricane), some installations are completely submerged in seawater. Taking this situation into account, it is demanding to develop the accurate theoretical approach to calculate the wave-induced forces and overturning moments

(Hayatdavoodi and Ertekin 2015).

Green and Naghdi (1976) constructed a theory on directed fluid sheets which is named the Green-Naghdi theory of water waves (GN hereafter), which considers a three-dimensional fluid named the fluid sheet and counts on the top and bottom surfaces that are unremitting and smooth. Usually, the theory assumes the fluid is incompressibility. After that, the GN theory was developed more comprehensive by Naghdi and Rubin (1981), Naghdi and Vongsarnpigoon (1986), Xia, Ertekin and Kim (2008), and Ertekin and Xia (2014).

4.3.2.2. Calculation

In this project, we will calculate wave loads above and below a submerged horizontal plate, developed by Hayatdavoodi and Ertekin (2015).

We consider the two-dimensional motion of a homogeneous, incompressible and inviscid fluid sheet. Additionally, cnoidal waves are propagating over a two-dimensional, stationary, horizontal, submerged thin plate. We assume the seafloor is stationary and horizontal here. The specific calculation is referred to Hayatdavoodi and Ertekin, Wave forces on a submerged horizontal plate-Part I: Theory and modelling (2015) and Hayatdavoodi and Ertekin, Wave forces on a submerged horizontal plate–Part II: Solitary and cnoidal waves (2015).

As an example, Figure 4-4 and Figure 4-5 show the dimensionless horizontal force and the dimensionless vertical force on the disc by using the GN Equations. The wave condition here is the same as in Figure 4-3. Among Figure 4-4 and Figure 4-5 and the remaining sections, the dimensionless horizontal force, vertical force and time are calculated as (Hayatdavoodi and Ertekin 2015):

$$\overline{F_H} = \frac{F_H}{\rho g a h L_p} \tag{2}$$

$$\overline{F_V} = \frac{F_V}{\rho g h^2 L_p} \tag{3}$$

$$\bar{t} = t\sqrt{\frac{g}{h}} \tag{4}$$

Where:

- $\overline{F_H}$ is dimensionless horizontal force, $\overline{F_V}$ is dimensionless vertical force;
- F_H is horizontal force, F_V is vertical force
- a is the disc thickness;
- L_p is the diameter of the disc;
- And the above vectors are defined by the preamble.

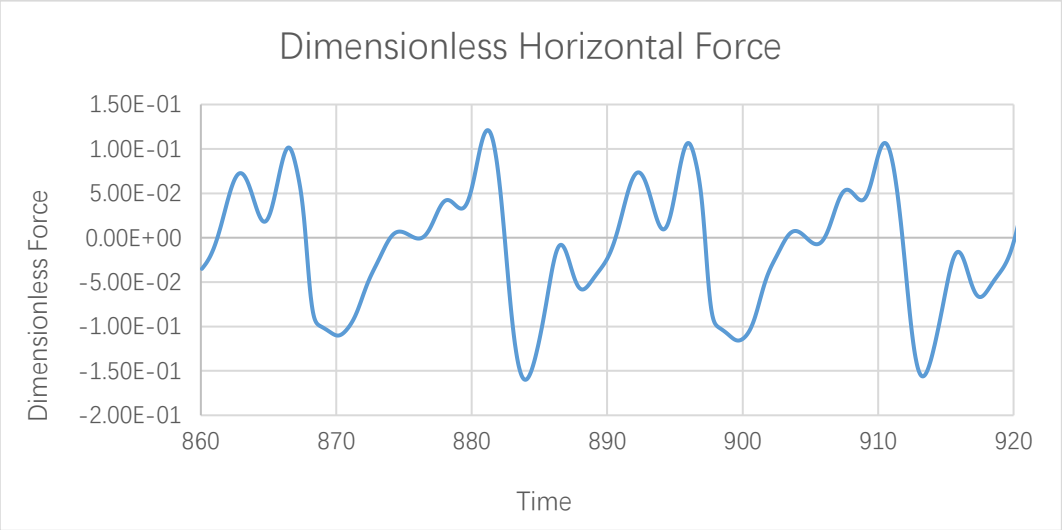

Figure 4-4 Dimensionless Horizontal Force (H=4m, S=3m, T=15s)

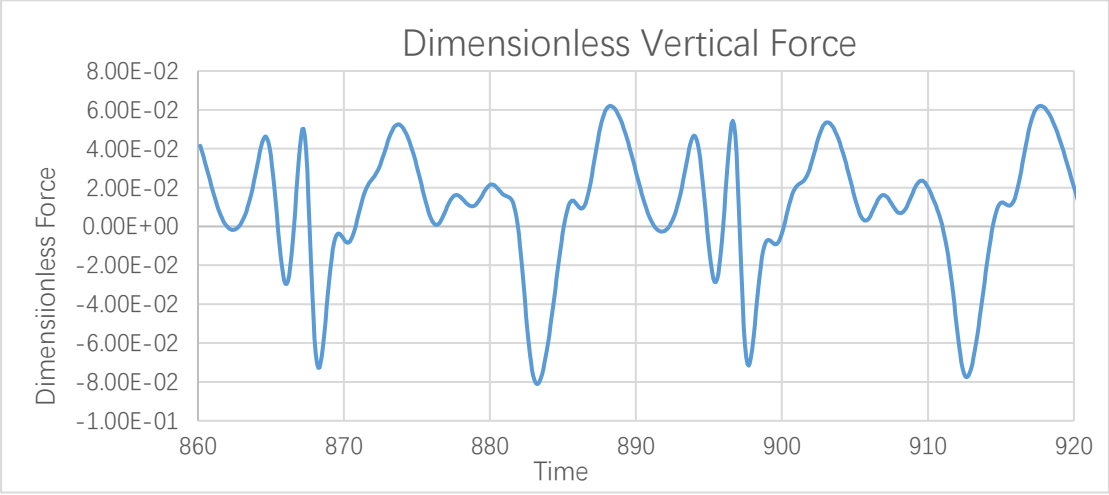

Figure 4-5 Dimensionless Vertical Force (H=4m, S=3m, T=15s)

And Figure 4-6 shows the differential pressure in a wave crest time (t=873.98s) in Figure 4-5. The net pressure is calculated as (Hayatdavoodi and Ertekin 2015):

$$\bar{P} = \frac{\mathrm{P}}{\rho g h} \tag{5}$$

Where:

- $\bar{P}$ is the dimensionless pressure;
- P is the pressure.

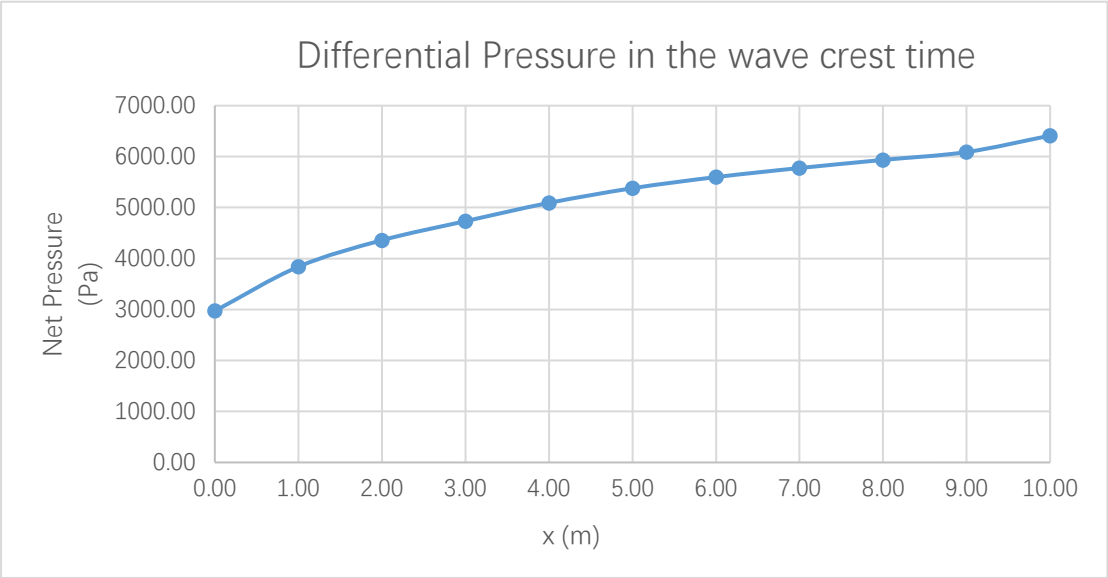

Figure 4-6 Differential Pressure in the Time of a Wave Crest (H=4m, S=3m, T=15s, t=873.98s)

5. Structural Analysis

5.1. Mechanics of Deformable Bodies

5.1.1. Concept of Stress

5.1.1.1. Stress Definition

When an object is deformed by external factors (Such as force, humidity, temperature field changes, etc.), internal forces are generated in various parts of the object. The internal force per unit area is called stress. Stress is a vector, the component along the normal direction of the section is called the normal stress (σ), and the component along the tangential direction is called the shear stress (τ).

5.1.1.2. Components of Stress

Mechanics of Materials (Ugural 1991) supports approaches to inspect whether the material of a structure under loads is strong enough. Some mechanical symbol will be explained here.

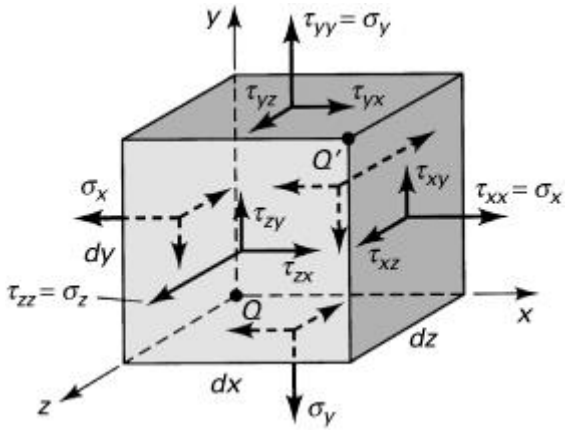

Figure 5-1 Three-dimensional state of stress (courtesy of Ugural 1991)

The general case of a three-dimensional state of stress is shown in Figure 5-1, σ is normal stress, τ is shearing stress.

5.1.1.3. Strain Defined

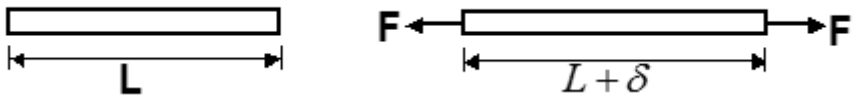

Figure 5-2 Deformation of a prismatic bar

In Figure 5-2, after application of a force F, the length of the bar increases an amount δ (delta). Defining the normal strain ε (epsilon) is the unit change in length (A positive sign elongation, a negative sign to contraction):

$$\varepsilon = \frac{\delta}{L} \tag{6}$$

5.1.1.4. Normal Stress

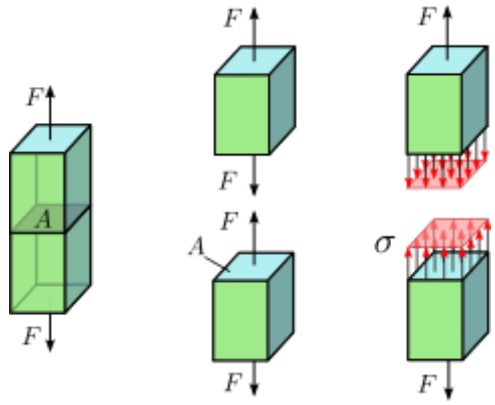

Figure 5-3 Idealised stress in a straight bar with uniform cross-section (Courtesy of https://en.wikipedia.org/wiki/Stress_(mechanics))

Figure 5-3 shows a simple idealised stress pattern (Wikipedia 2017). A straight bar with a uniform material and a cross-section apply tension by an opposing force F along its axis. If the system is in balance and does not change over time, and the weight of the rod is negligible, the top must be pulled on the bottom with the same force F through each lateral portion of the rod. Therefore, the stress across the bar across any horizontal surface can be described by the number

$$\sigma = \frac{F}{A} \tag{7}$$

, where A is the area of the cross-section.

When the rod is stretched as shown in Figure 5-3, the stress produced is a *uniaxial tensile* stress; If the direction of the force is reversed in Figure 5-3, the bar

is compressed and the force received by the bar is a *uniaxial compressive* stress.

5.1.1.5. Shearing Stress

Consider the effect of force F on the bar in Figure 5-4. If the support is rigid and F is large enough, the material of the rod will be deformed and damaged along the plane formed by AB and CD. Let us analyse the intermediate unsupported section, as shown in Figure 5-5. The shear force acting on each section must be V = F / 2, otherwise, the section can not be balanced.

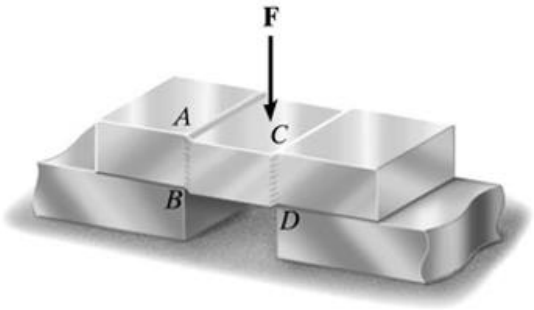

Figure 5-4 A Force F on a Bar (Courtesy of https://lms.ctl.cyut.edu.tw/sys/read_attach.php?id=2312780)

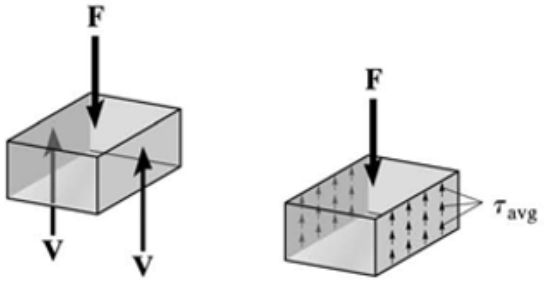

Figure 5-5 Analysis of the Separated Section (Courtesy of https://lms.ctl.cyut.edu.tw/sys/read_attach.php?id=2312780)

Therefore, the average shearing force can be expressed as:

$$\tau_{avg} = \frac{V}{A} \qquad (8)$$

, where:

- τ_{avg} is the average shearing stress at the cross-section. Assume that the points on this section are the same.
- V is the shearing forces that obtain from the equilibrium equation in the internal system.
- A is the cross-sectional area.

5.1.1.6. Stress-Strain Diagram

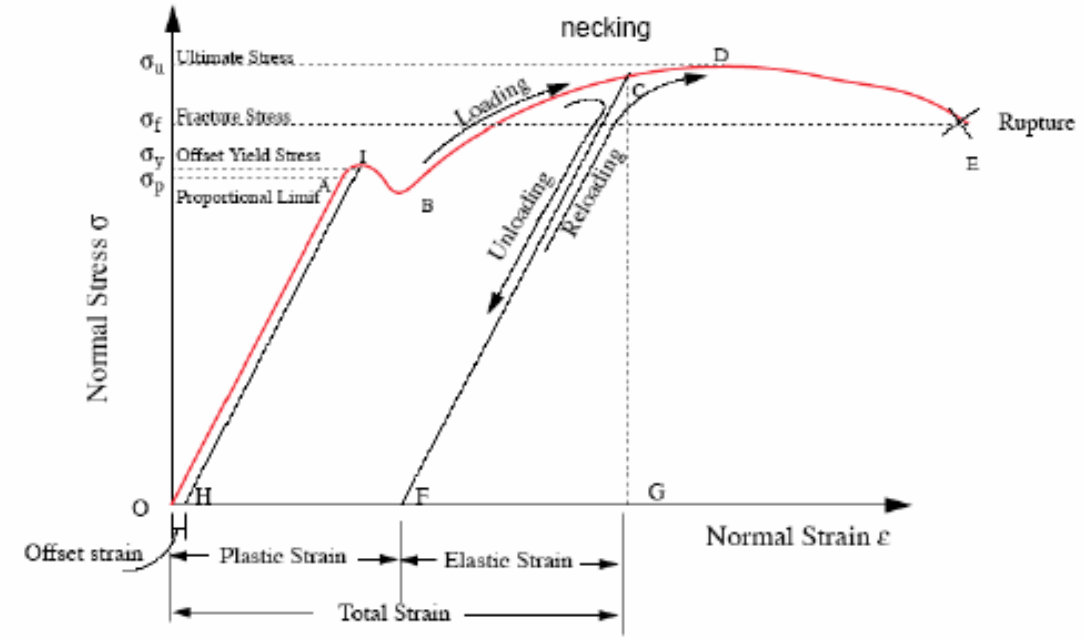

Figure 5-6 Stress-Strain Plot for Ductile Materials (courtesy of http://www.sciencebuddies.org/science-fair-projects/project_ideas)

Figure 5-6 shows stress-strain diagrams. The linear variation of stress-strain ends at the proportional limit. When the load on the bar is increased beyond the proportional limit, a stress level is reached at which the material continues to stretch without an increase in applied stress. σ_{yp} is the yeild-point stress determined from a tensile test (Mechanics of Materials 1991) . According to Hooke's law, for the straight-line portion of Figure 5-6, the stress is directly proportional to the strain:

$$\sigma = E\varepsilon \tag{9}$$

where:

- E is the modulus of elasticity, E lies between 200 and 210 GPa.

5.1.1.7. Principal Stress

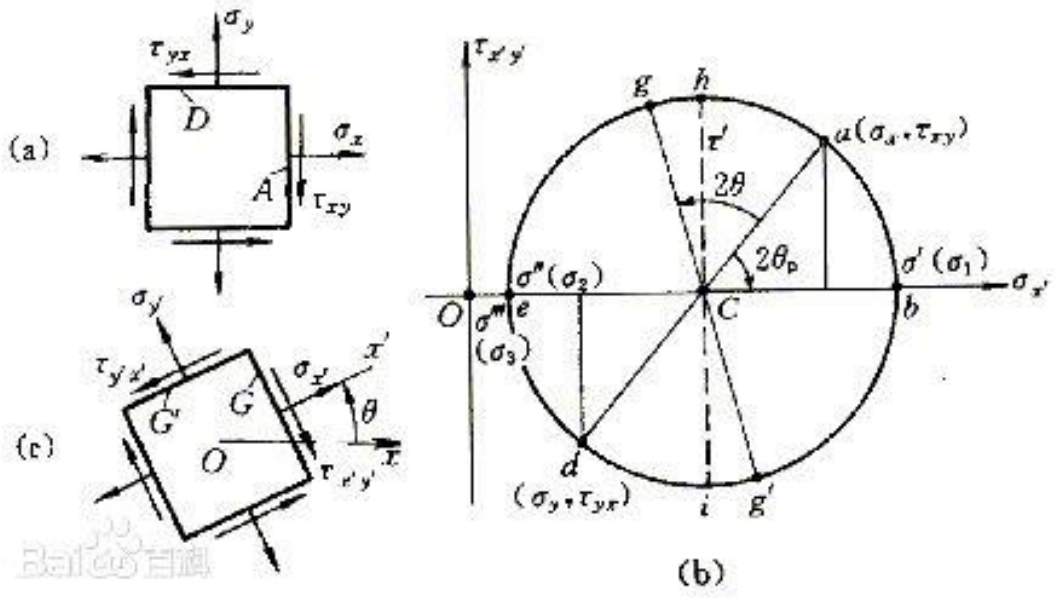

Figure 5-7 Principal Stress (Courtesy of http://baike.baidu.com/view/1583998.htm)

The principal stress is the normal stress when the shearing stress is zero on the microelement area with the normal vector n = (n1, n2, n3) at a certain point in the object. In this case, the direction of n is called the principal direction of stress at this point. The normal stress on a certain element area is taken as a value in the principal direction of stress when the normal vector n of the area changes. For a stress tensor σ_{ij} (i, j = 1, 2, 3), there are usually three principal stresses, which satisfy the equation ($\|\sigma_{ij} - \sigma\delta_{ij}\| = 0$). The solution of this cubic equation is the principal stress σ_i (i = 1,2,3). For a given stress tensor, the principal stress is invariant under coordinate transformation. (Baidupedia 2017)

5.1.1.8. Von Mises Theory

In the development which follows, we consider an element subjected to triaxial principal stressed where $\sigma_1 > \sigma_2 > \sigma_3$.

Von Mises Theory states that yielding occurs when the root mean square of the difference between the principal stresses for a three-dimensional state of stress reaches the same value in a tensile test (Mechanics of Materials 1991, 237). Thus at the beginning of yielding,

$$(\sigma_1-\sigma_2)^2+(\sigma_2-\sigma_3)^2+(\sigma_3-\sigma_1)^2=2{\sigma_{yp}}^2 \quad (10)$$

The Von Mises theory agrees best with the test data for ductile materials and is in common use in design. In order to test the WEC if its structural strength is strong enough, we use von Mises Theory to check it out.

5.2. Finite Element Method

5.2.1. Numerical Methods

There are many engineering problems we can not get accurate results. To obtain accurate results, may involve the problems about solving the complex boundary and initial conditions. In order to solve such problems, we turn to numerical approximation. Relative to the direct solution, the numerical approximation method approximate exact solution at detached points, called nodes. So the first step of numerical approximation is discretization, which separates the object into a number of small subregions and nodes. (Saeed 1999)

There are two commonplace methods in numerical methods: (1) *finite difference methods* and (2) *finite element methods*. The finite difference methods are easy to understand, which has been used in some simple questions, but they are too difficult to apply to problems with complex geometries or complex boundary conditions. In contrast, the finite element methods are easier than the finite difference methods to solve complex engineering problems in using a computer. The finite element method uses *integral formulations* rather than difference equations to create a system of algebraic equations. In addition, the finite element method is assumed that the approximate continuous function represents the solution of each element. The individual solution is then combined to produce a complete solution by connecting, allowing continuity at the interelement boundaries. (Finite Element Analysis: Theory and Application with ANSYS 1999)

5.2.2. Basic Steps in the Finite Element Method

Any finite element analysis involves the following basic steps (Saeed 1999):

(1) Preprocess Phase

a. Construct and discretize the solution sphere in the finite element. i.e. segment the problem into nodes and elements;

b. A shape function is assumed to epitomise the physical behaviour of an element;

c. Develop equations for elements;

d. Accumulate the elements to hand over the whole problem. Then build the global stiffness matrix;

e. Apply boundary conditions, initial conditions and loading.

(2) Solution Phase

f. Obtain nodal results while solving series of linear or nonlinear algebraic equations.

(3) Postprocessing Phase

g. Get other important information. At this phase, you could add other principles, such as stresses, heat, fluxes, etc.

In the usual course of events, there are 3 ways to ripen finite element problems: (1) *Direct Formulation*, (2) *The Minimum Total Potential Energy Formulation*, and (3) *Weighted Residual Formulations*. No matter how we generate the finite element model, the basic steps in any finite element analysis should be consistent with the same stages described in this chapter.

5.3. Preliminary Test

Before the formal analysis, a preliminary test will be conducted to practice with the steps which would be taken in the formal analysis.

In the preliminary test, a simple example will be tested. A disc is submerged in seawater and suffered water pressure from wave motion. Due to this is a preliminary that aims at getting familiar with all steps, we just need a set of wave

loads data to be practised. The wave loads here is calculated by linear wave equation (Airy 1841).

5.3.1. Process

In this part, every step is compiled by a process which is shown in Figure 5-8, which is a preliminary test that uses ANSYS Workbench to test a disc. As shown in Figure 5-8, a 3D model of the disc will be created in AutoCAD, then it'll be imported into ANSYS Workbench and endowed mesh. On the other hand, wave loads will be calculated in MATLAB with lines of code. After recording the data of wave loads, the data will be imported into ANSYS Workbench as the real pressure above the disc. Nextly, ANSYS Workbench will analyse and output results. Then we can collect the data and analyse them.

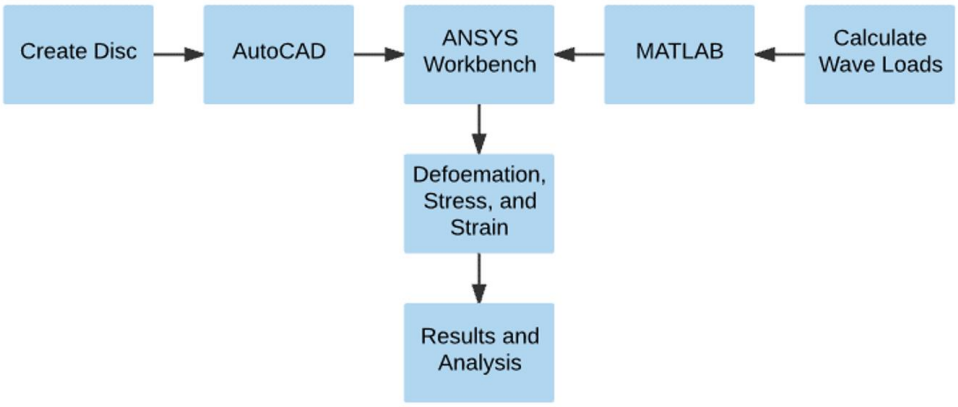

Figure 5-8 Preliminary Test Flowchart

Have to say is that this is a preliminary testing process, the process of the formal test will be a little different from the preliminary test. See Chapter 5.4 for more details of the formal test.

5.3.2. Theoretical Method

In the preliminary test, the linear wave equation (Airy 1841) will be used to calculate the loads above a disc.

When a structure at the surface of the sea, it will suffer a pulsed or wavelike load. In another situation, when a structure submerges undersea, it will be subjected to hydrostatic pressure from water and hydrodynamic pressure from

wave motion.

A progressive wave associated with a pressure field, which contains two terms, the hydrostatic pressure and the dynamic pressure (Airy 1841):

$$P(x,t) = -\rho g z + \frac{1}{2}\rho g H \frac{\cosh(ks)}{\cosh(kd)}\cos(kx - \omega t) \qquad (11)$$

Where

- ρ is the density of water, $\rho = 1.025 \times 10^3 \mathrm{kg}/m^3$ in seawater;
- g is the standard acceleration due to gravity, $\mathrm{g} = 9.80665\ \mathrm{m/s^2}$;
- z is the axis of vertical direction, origin at still water level (SWL). z is less than 0 below the water surface;
- x is the axis of horizontal direction;
- H is wave height – the difference in elevation between crest and trough;
- k is the angular wave number in radian per meter, which is related to the wave length λ as $\mathrm{k} = \frac{2\pi}{\lambda}$;
- d is water depth;
- s = d + z;
- ω is the angular frequency in radian per second, related to the period T and frequency f by $\omega = \frac{2\pi}{T} = 2\pi f$;
- t is time.

Submerged structures would suffer pressure from waves motion when waves travel on the sea. Figure 5-9 shows a simplified mode of wave loads on a submerged disc.

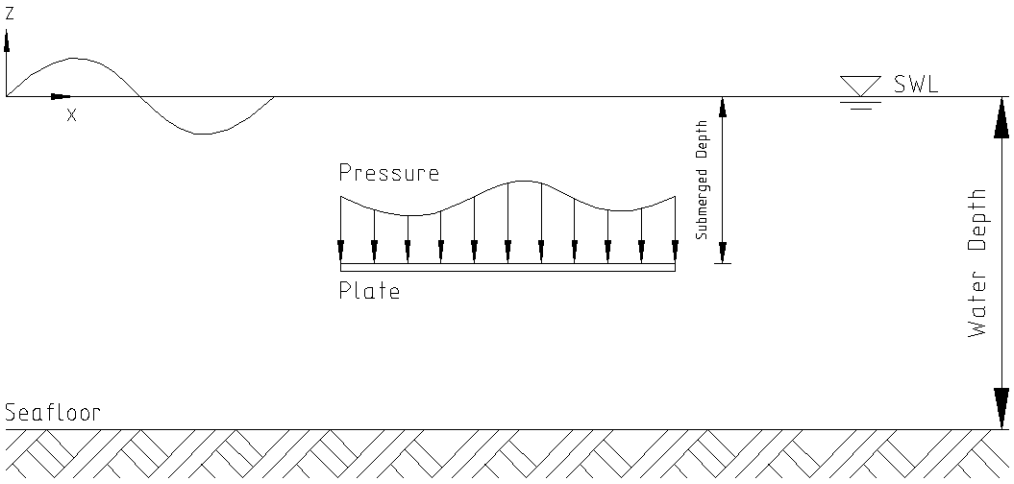

Figure 5-9 Wave Loads on a Submerged Disc (Simplified Mode)

5.4. Formal Analysis

In this project, formal analysis is to analyse the structural performance of WEC in the sea, which means the model of the WEC, the wave conditions will be imported into ANSYS Workbench. Then we'll collect the results data to analyse whether the structures are good or not. The detail process is shown below.

5.4.1. The Analysis Flowchart

The process of formal computation is followed by the process of analysis (as shown in Figure 5-10 Formal Analysis Flowchart as Followed in This Thesis).

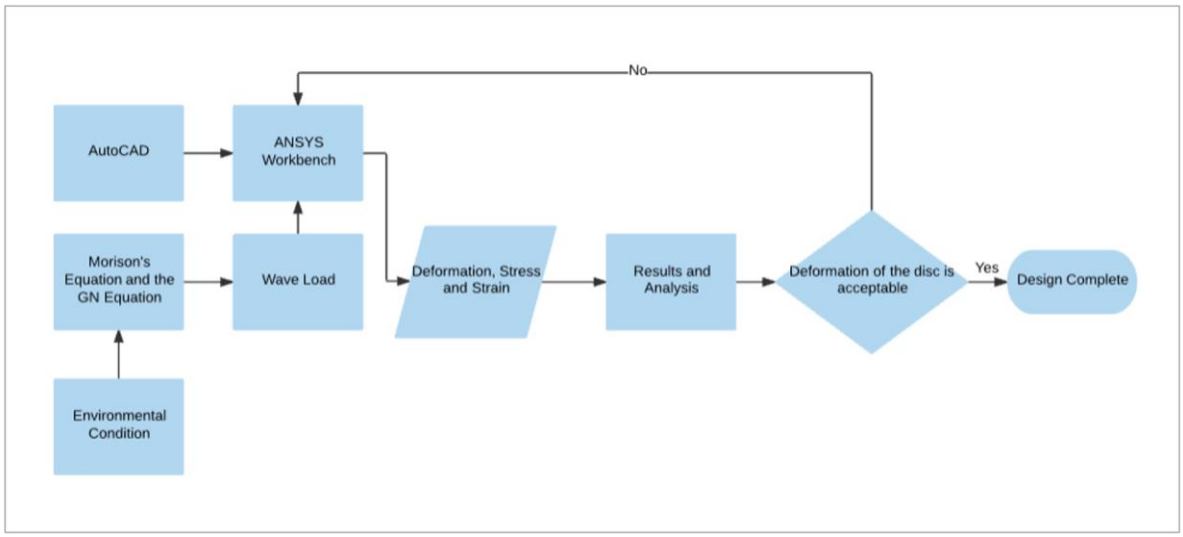

Figure 5-10 Formal Analysis Flowchart as Followed in This Thesis

Firstly, a 3D model of WEC will be created in AutoCAD (see Chapter 3.2 for details). On the other hand, according to an environmental condition, in using of

Morison's Equation and The GN Equations to obtain wave loads (see Chapter 4 for details). Secondly, we import the 3D model into ANSYS Workbench and give it mesh. Then add wave loads into ANSYS Workbench to analyse and record data, such as deformation in this model. Nextly, we'll collect the data and analyse them. If the deformation of the disc is acceptable, we think the results are good enough, which means the design is complete. If not, we'll turn to the step of importing data into ANSYS Workbench, like showing in Figure 5-10, to re-analyse it until the results are satisfying.

5.4.2. Theoretical Methods

The theoretical methods in the analysis will use the Morison's Equation and The GN Equations, we've discussed these before and will not be repeated here. See Chapter 2.3 for more details about Morison's Equation and The GN Equations.

5.4.3. Analysis

In the formal analysis, the steps are similar to those in the Preliminary Test and are not repeated here. Four different materials which are stainless steel, concrete, aluminium alloy, and titanium alloy respectively will be tested in this section. The detailed properties of these materials are shown in Table 5-1:

Properties of Different Materials				
	Concrete	Aluminium Alloy	Titanium Alloy	Stainless Steel
Density (mg/m³)	2300	2770	4620	7750
Young's Modulus (Pa)	3.00E+10	7.10E+10	9.60E+10	1.93E+11
Poisson's Ratio	0.18	0.33	0.36	0.31
Tensile Yield Strength (Pa)	0	2.80E+08	9.30E+08	2.07E+08
Compressive Yield Strength (Pa)	0	2.80E+08	9.30E+08	2.07E+08
Tensile Ultimate Strength (Pa)	5.00E+06	3.10E+08	1.07E+09	5.86E+08
Compressive Ultimate Strength (Pa)	4.10E+07	0	0	0

Table 5-1 Properties of Different Materials

6. Results

6.1. Wave conditions

There are 12 different environmental conditions in the analysis, which is shown in Table 6-1 below.

Need to mention is that every test case of environmental conditions has to be tested in 2 cases (one in the crest of a wave at the top centre of the WEC, another one in the trough of the wave at the top centre of the WEC). So every material should be tested in 24 different environmental conditions in the analysis section. See Chapter 6.1 for the detailed analysis data.

Table 6-1 Environmental Conditions considered in This Study

Test Case	1	2	3	4	5	6	7	8	9	10	11	12
H	3	3	4	4	3	3	4	4	3	3	4	4
S	3	3	3	3	5	5	5	5	7	7	7	7
T	10	15	10	15	10	15	10	15	10	15	10	15

Note that H is wave height, S is submergence depth of disc defined as the depth from the SWL to the disc top, T is wave period.

Condition 1 tests when the crest of a wave at the top centre of the WEC. Condition 2 tests when the trough of the wave at the top centre of the WEC. For each of the wave conditions, given in Table 6-1, these two conditions are considered, i.e. Total of 24 cases. To use the code *The Time of the Wave Movement* (see Chapter 10.3.1 for details) in MATLAB, we can know the time of the wave crest or trough movement to the top centre of WEC (The time in Condition 1 is t_1 hereafter, in Condition 2 is t_2 hereafter). After running code, we can know when wave peirod T=10s, $t_1 = 8.0935\mathrm{s}$, $t_2 = 3.0935\mathrm{s}$. When wave period T=15s, $t_1 = 11.8206\mathrm{s}$, $t_2 = 4.3206\mathrm{s}$.

6.2. Results of Wave Loads

6.2.1. Wave Loads on the Cylindrical Components

Since wave loads on different elements are considered dissimilarly, in order

to illustrate pressure data on every cylinder conveniently, we label every cylinder as shown in Figure 6-1. And the forces distributions of the columns H5/H6/H7/H8/H9/H10/H11/H12 are constant (Because the wave propagates along the X axis, the pressure is equal in the Y axis), so the data are given directly.

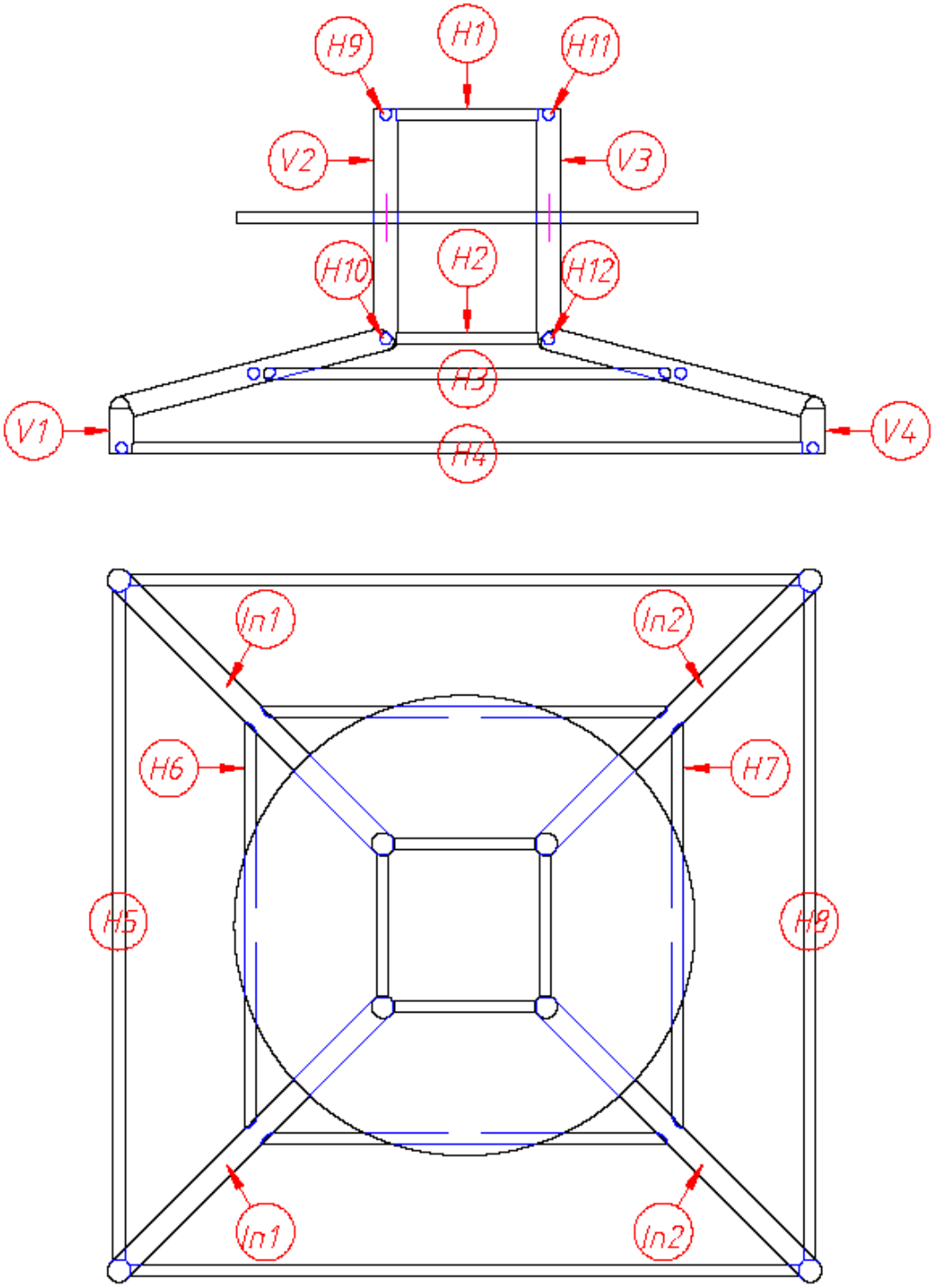

Figure 6-1 Cylinder Label

6.2.1.1. Data of Forces on Cylinders at Condition 1

There are 3 kinds of cylinders (Horizontal, vertical, and inclined) and 4 different environmental condition cases at condition 1 of the forces on the cylinders, respectively.

Due to sectional forces is related to the velocity of flow $\mathbf{u}$ (according to Morison's Equation), and $\mathbf{u} = \mathbf{u}(\mathbf{x}, \mathbf{y}, \mathbf{z}, \mathbf{t})$ which means $\mathbf{u}$ will change with the variation of $\mathbf{x}, \mathbf{y}, \mathbf{z}$ and $\mathbf{t}$. In this project, we analyse the static situation, so t is constant, which means $\mathbf{u}$ is changed with the change of $\mathbf{x}, \mathbf{y}, \mathbf{z}$. Hence, due to the differences of locations and the change of $\mathbf{x}, \mathbf{y}, \mathbf{z}$ with different types cylinders, the sectional forces on the different types of cylinders are different. So, we illustrate the distribution of sectional forces separately by the different types of cylinders.

Figure 6-2 to Figure 6-13 and Table 6-2 to

Column	H5	H6	H7	H8
Sectional Forces (N/m)	107301.31	85674.10	42107.77	3127.92
Column	H9	H10	H11	H12
Sectional Forces (N/m)	80448.83	77111.11	69817.06	67314.06

Table 6-5 show the wave loads on these cylinders calculated by Morison's Equation. We note that the code of Morison's Equation is given in Chapter Appendices 10.3.

Need to note here is that in Figure 6-2, Figure 6-5, Figure 6-8 and Figure 6-11 the sectional forces on the H2, H3 and H4 are overlapped. This is because although z is changing between H2, H3 and H4, z makes a negligible impact on the velocity of the fluid and sectional forces, that is, under the depth of H2, the change of x is the dominant element to impact the change of sectional forces. So the plotting of the data of H2, H3 and H4 are overlapped.

a) H=3m, T=10s

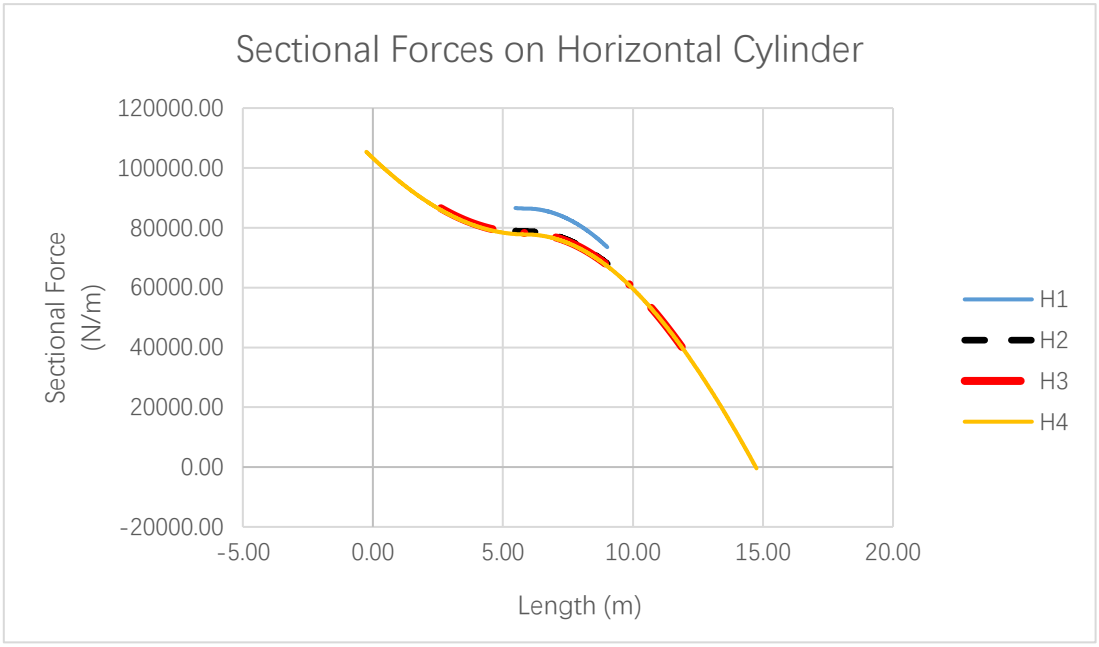

Figure 6-2 Sectional Forces on Horizontal Cylinder

Column	H5	H6	H7	H8
Sectional Forces (N/m)	105369.76	86507.99	40080.33	-435.63
Column	H9	H10	H11	H12
Sectional Forces (N/m)	86578.03	78863.23	73471.49	67848.15

Table 6-2 Sectional Forces on Horizontal Cylinder

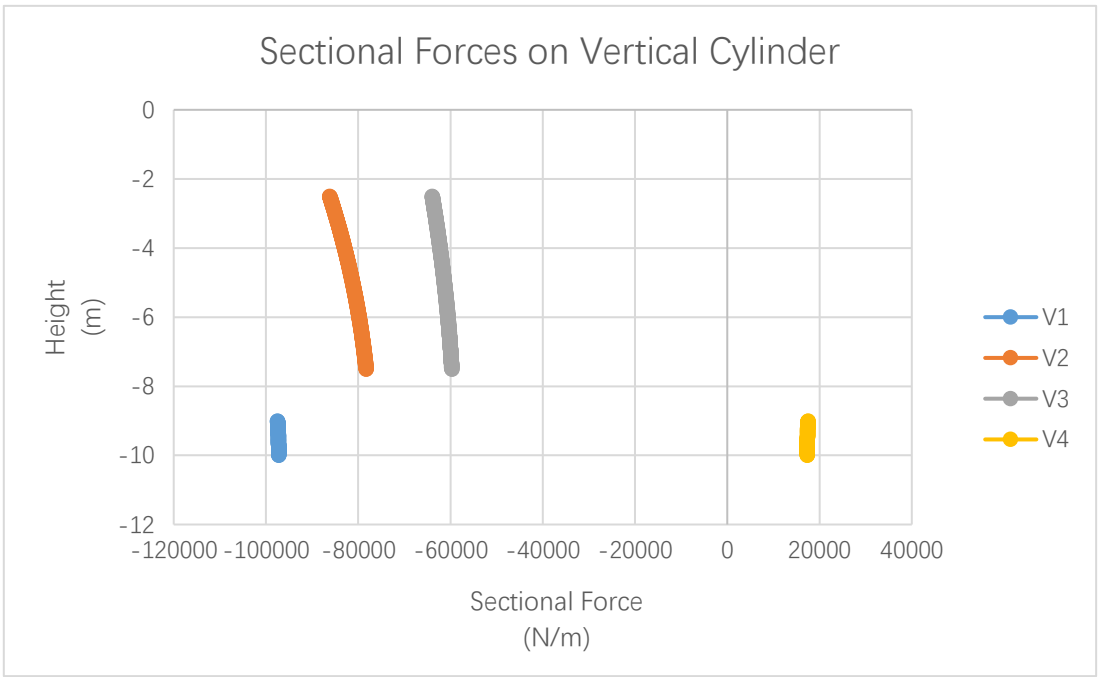

Figure 6-3 Sectional Forces on Vertical Cylinder

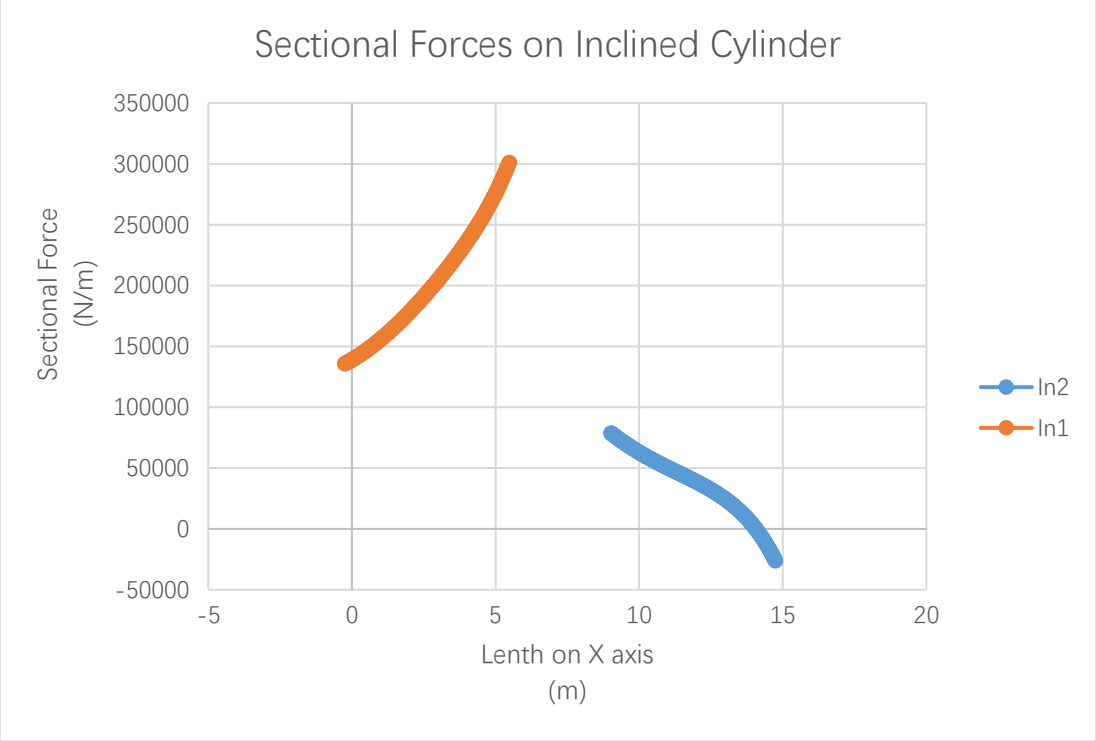

Figure 6-4 Sectional Forces on Inclined Cylinder

b) H=3m, T=15s

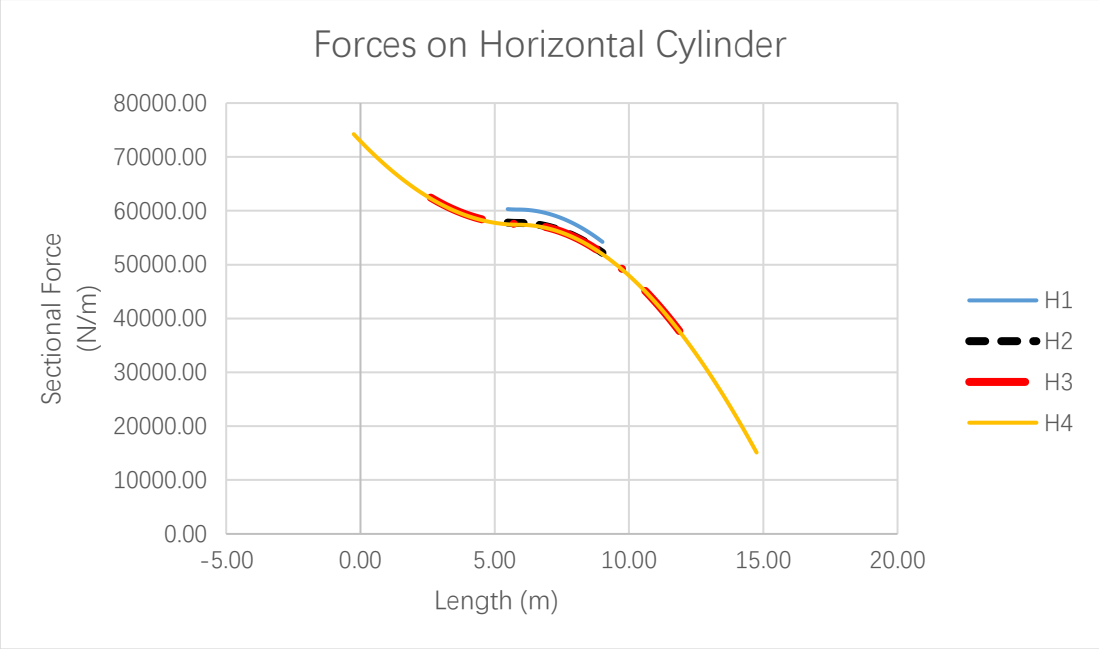

Figure 6-5 Sectional Forces on Horizontal Cylinder

Column	H5	H6	H7	H8
Sectional Forces (N/m)	74230.88	62447.39	37616.36	15114.26
Column	H9	H10	H11	H12
Sectional Forces (N/m)	60307.25	57806.35	54196.48	52170.50

Table 6-3 Sectional Forces on Horizontal Cylinder

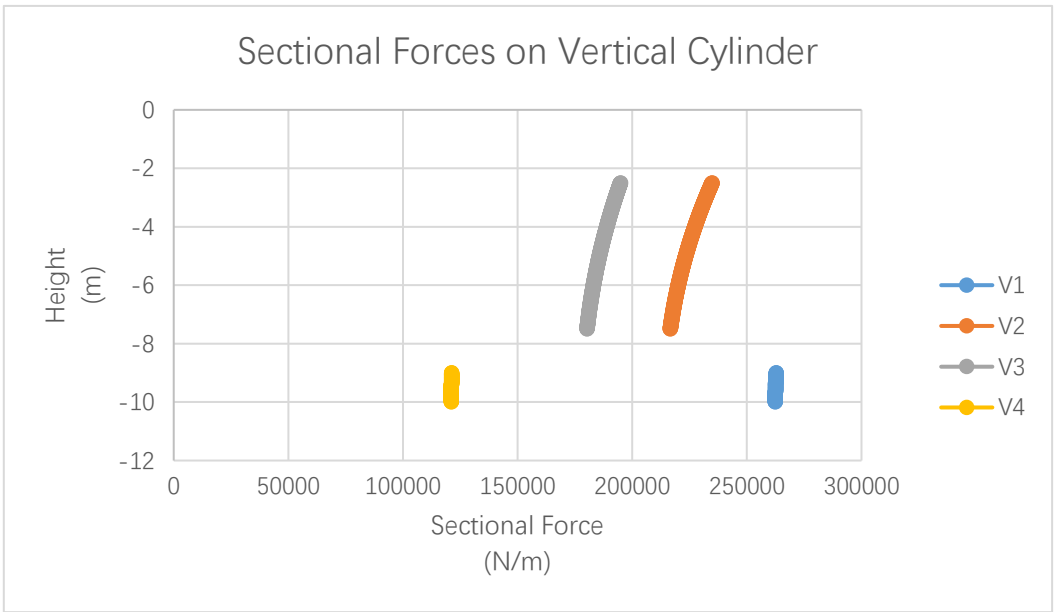

Figure 6-6 Sectional Forces on Vertical Cylinder

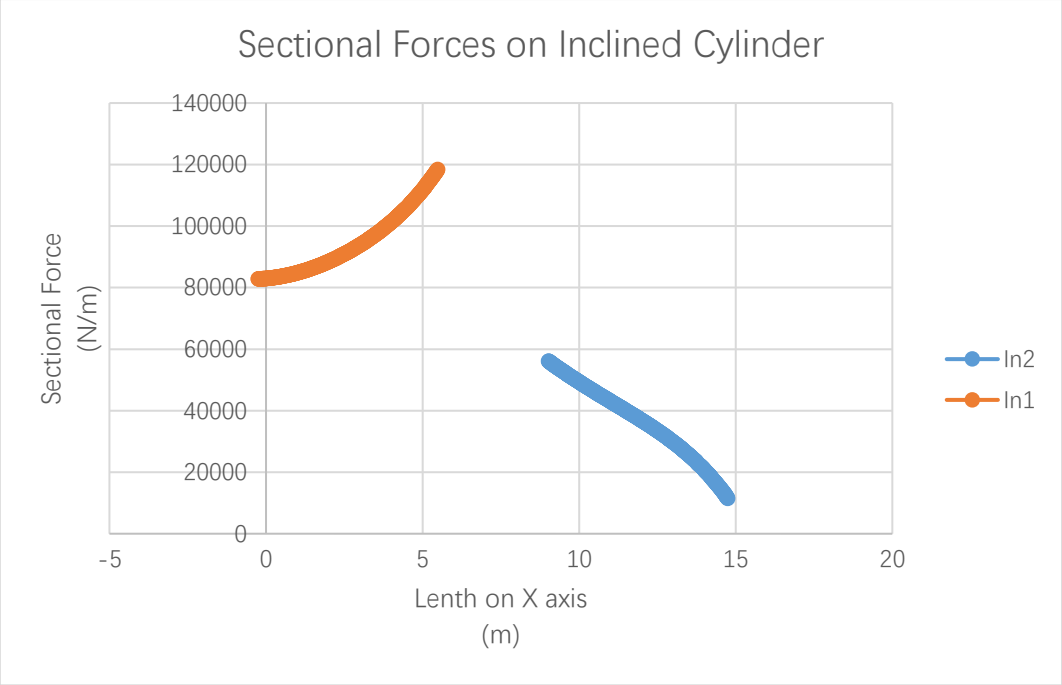

Figure 6-7 Sectional Forces on Inclined Cylinder

c) H=4m, T=10s

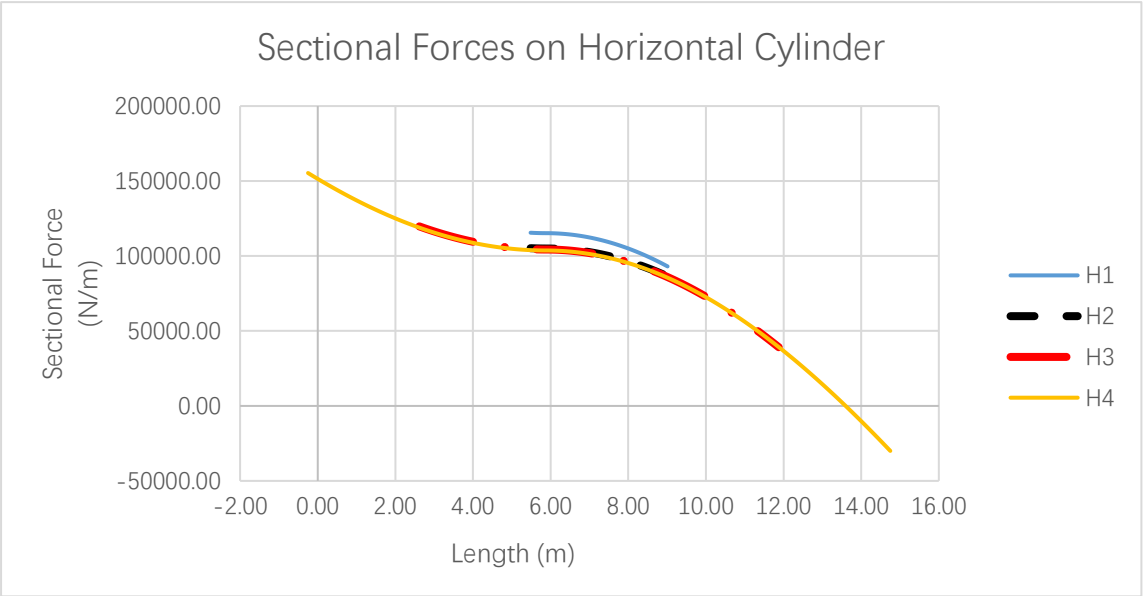

Figure 6-8 Sectional Forces on Horizontal Cylinder

Column	H5	H6	H7	H8
Sectional Forces (N/m)	155342.94	119761.48	38974.57	-30004.19
Column	H9	H10	H11	H12
Sectional Forces (N/m)	115517.99	105217.89	92964.59	86316.20

Table 6-4 Sectional Forces on Horizontal Cylinder

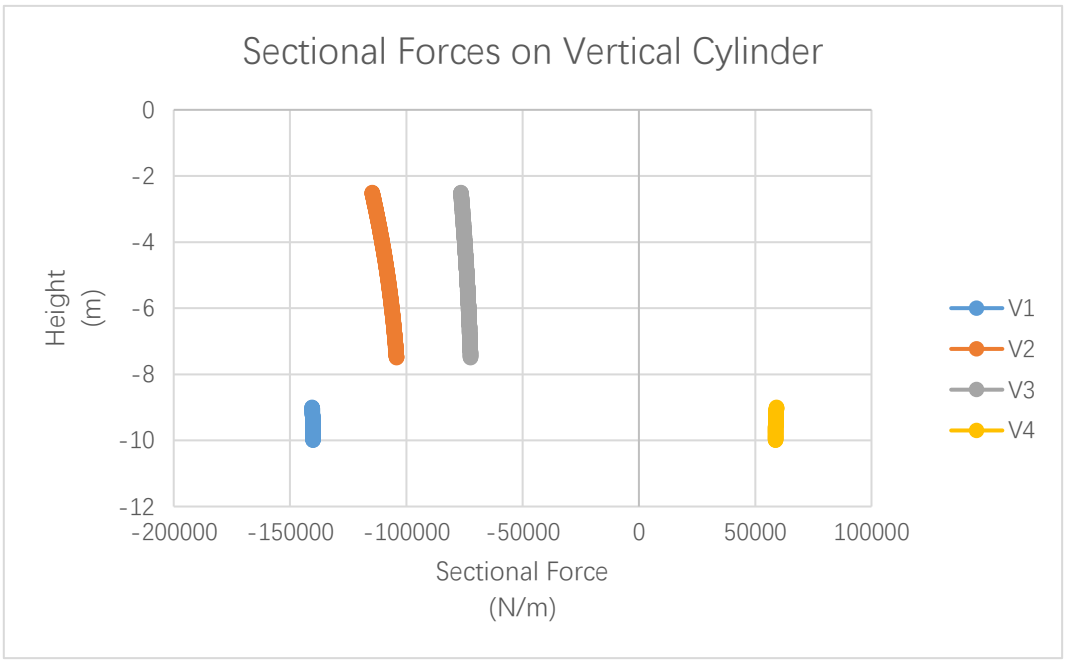

Figure 6-9 Sectional Forces on Vertical Cylinder

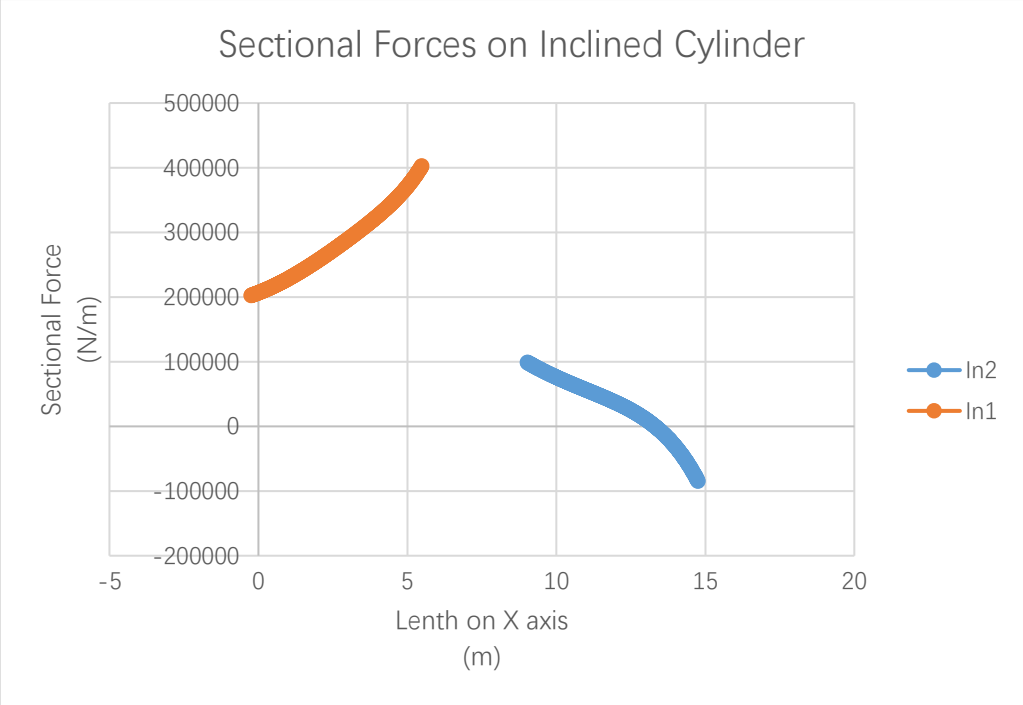

Figure 6-10 Sectional Forces on Inclined Cylinder

d) H=4m, T=15s

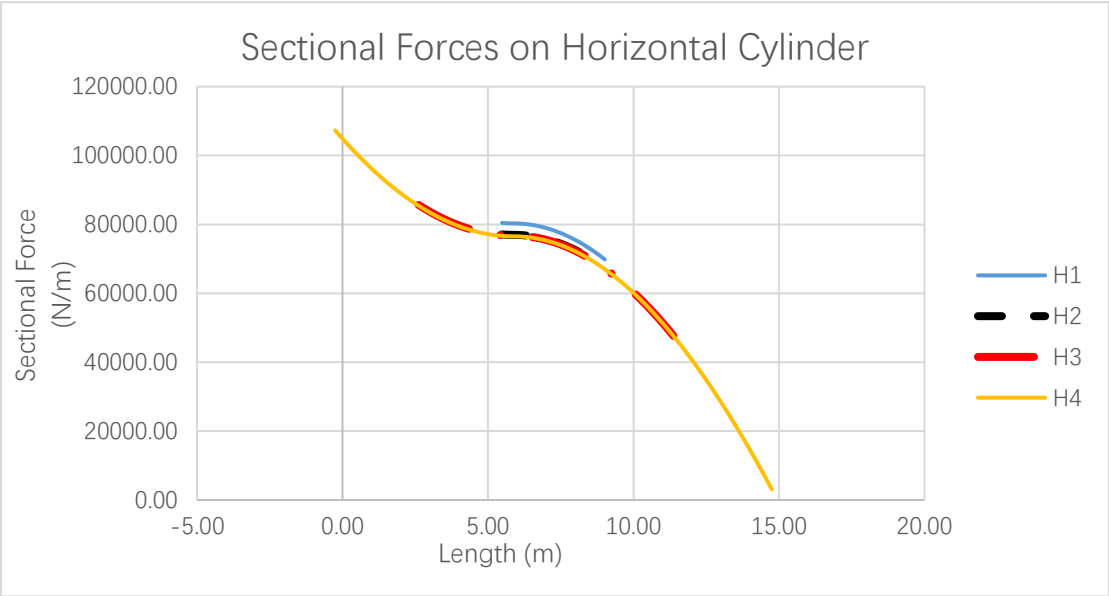

Figure 6-11 Sectional Forces on Horizontal Cylinder

Column	H5	H6	H7	H8
Sectional Forces (N/m)	107301.31	85674.10	42107.77	3127.92
Column	H9	H10	H11	H12
Sectional Forces (N/m)	80448.83	77111.11	69817.06	67314.06

Table 6-5 Sectional Forces on Horizontal Cylinder

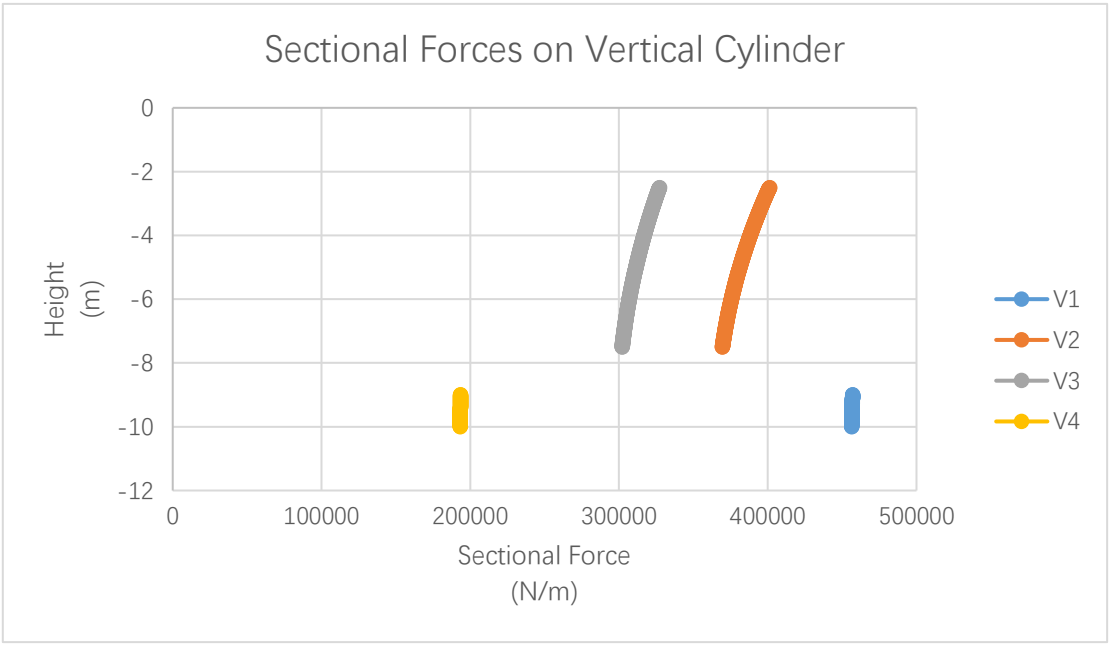

Figure 6-12 Sectional Forces on Vertical Cylinder

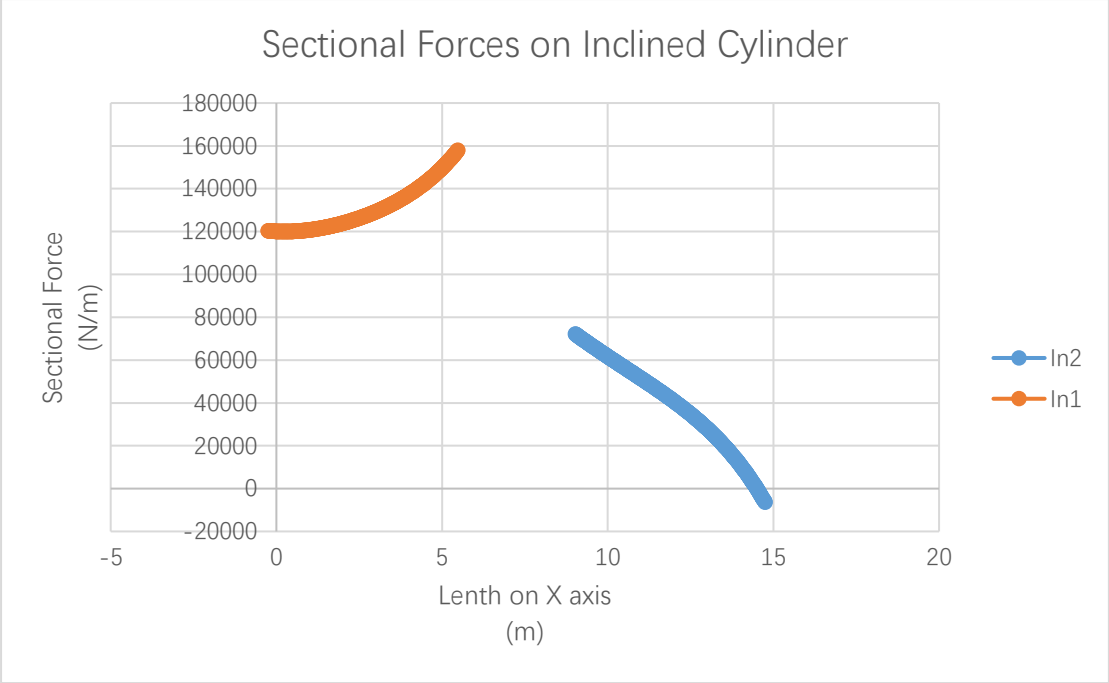

Figure 6-13 Sectional Forces on Inclined Cylinder

6.2.1.2. Data of Forces on Cylinder at Condition 2

Also, like in Chapter 6.2.1.1, there are 3 kinds of cylinders (Horizontal, vertical, and inclined) and 4 different environmental condition cases at condition 2 of the forces on the cylinders, which is given below, respectively. Additionally, the interpretation of why the distribution of sectional forces is given separately is discussed in Chapter 6.2.1.1.

Figure 6-14 to Figure 6-25 and Table 6-6 to Table 6-9 illustrate the wave loads on these cylinders calculated by Morison's Equation. We note that the code of Morison's Equation is given in Chapter Appendices 10.3.

Also, like in Chapter 6.2.1.1, in Figure 6-14, Figure 6-17, Figure 6-20 and Figure 6-23 the sectional forces on the H2, H3 and H4 are overlapped. This is because although z is changing between H2, H3 and H4, z contributes negligible impact to the velocity of the fluid and sectional forces, that is, under the depth of H2, the change of x is the dominant element to impact the change of sectional forces. So the plotting of the data of H2, H3 and H4 are overlapped.

a) H=3m, T=10s

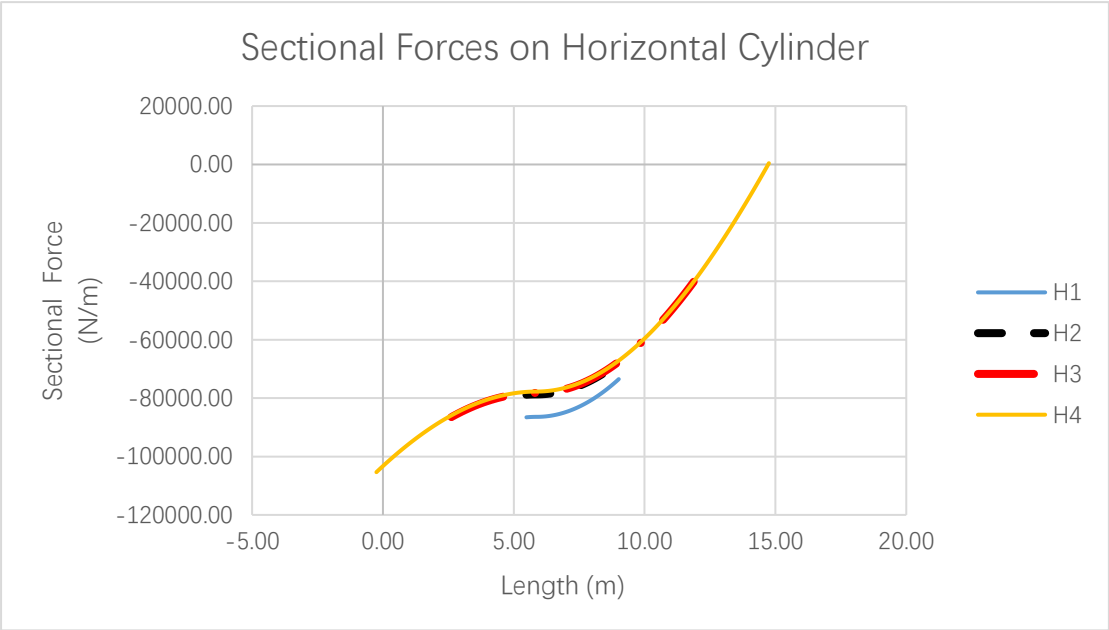

Figure 6-14 Sectional Forces on Horizontal Cylinder

Column	H5	H6	H7	H8
Sectional Forces (N/m)	-105369.76	-86507.99	-40080.33	435.63
Column	H9	H10	H11	H12
Sectional Forces (N/m)	-86578.03	-78863.23	-73471.49	-67848.15

Table 6-6 Sectional Forces on Horizontal Cylinder

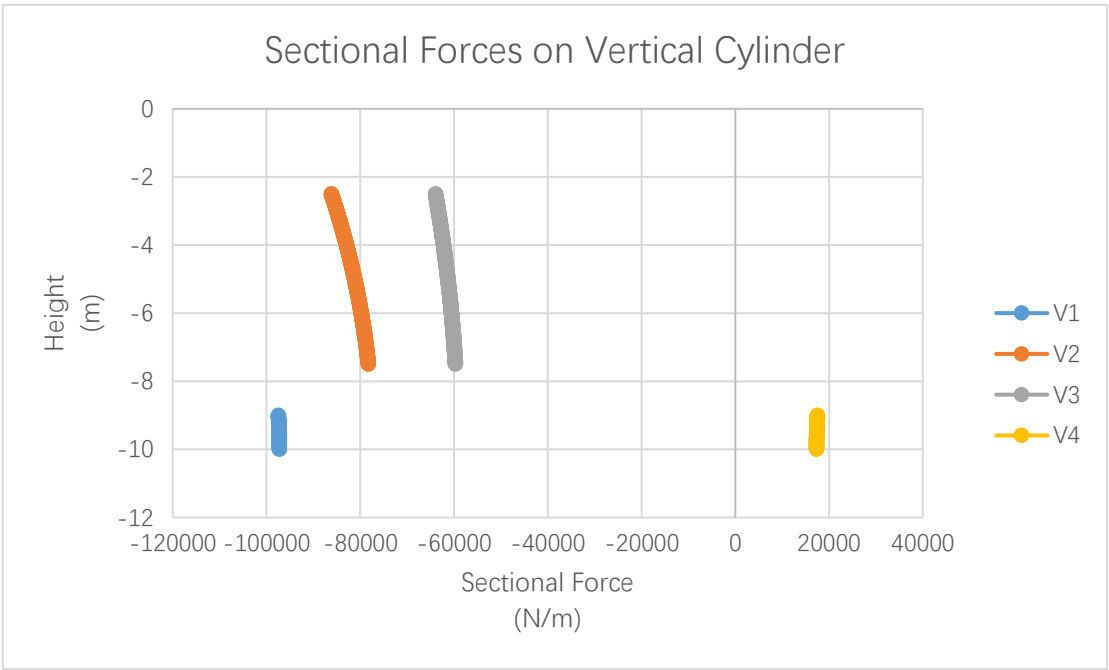

Figure 6-15 Sectional Forces on Vertical Cylinder

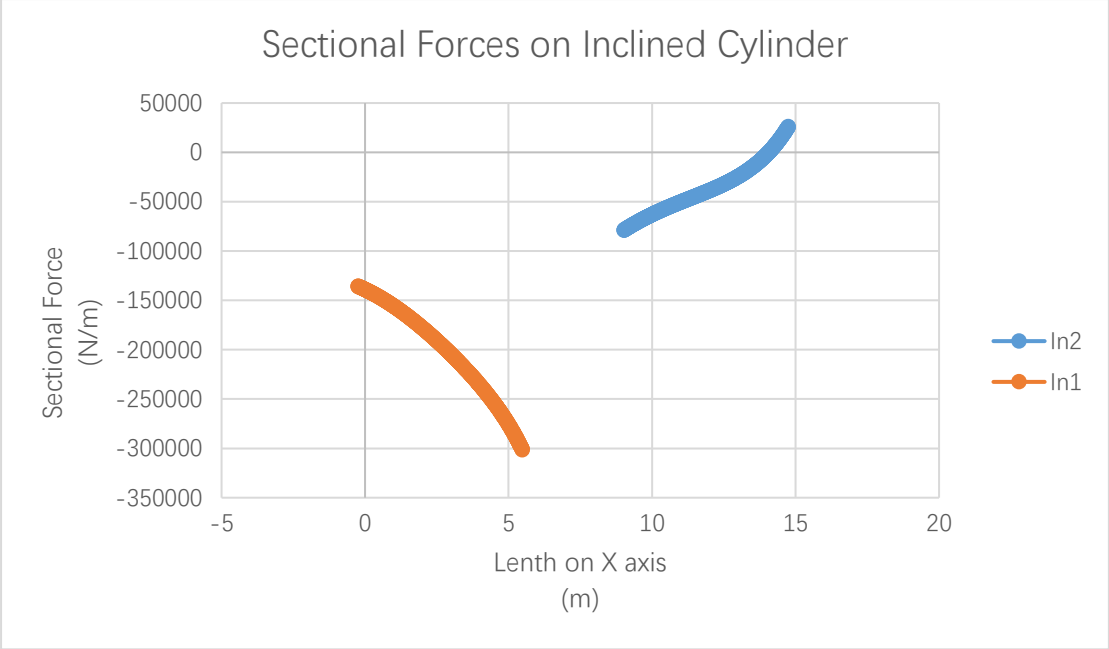

Figure 6-16 Sectional Forces on Inclined Cylinder

b) H=3m, T=15s

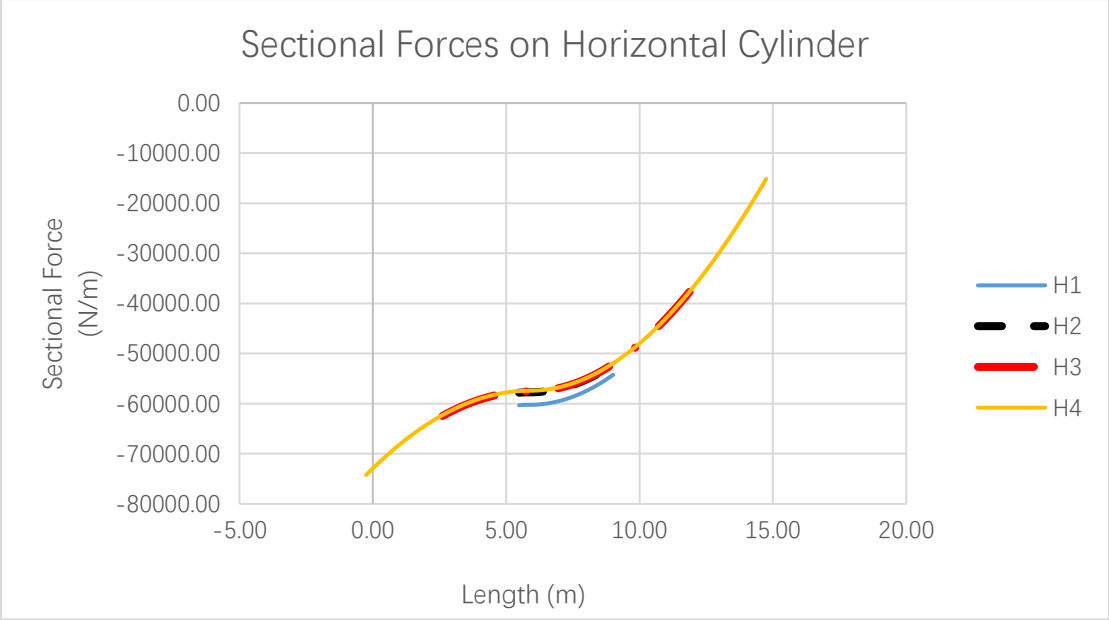

Figure 6-17 Sectional Forces on Horizontal Cylinder

Column	H5	H6	H7	H8
Sectional Forces (N/m)	-74230.88	-62447.39	-37616.36	-15114.26
Column	H9	H10	H11	H12
Sectional Forces (N/m)	-60307.25	-57806.35	-54196.48	-52170.50

Table 6-7 Sectional Forces on Horizontal Cylinder

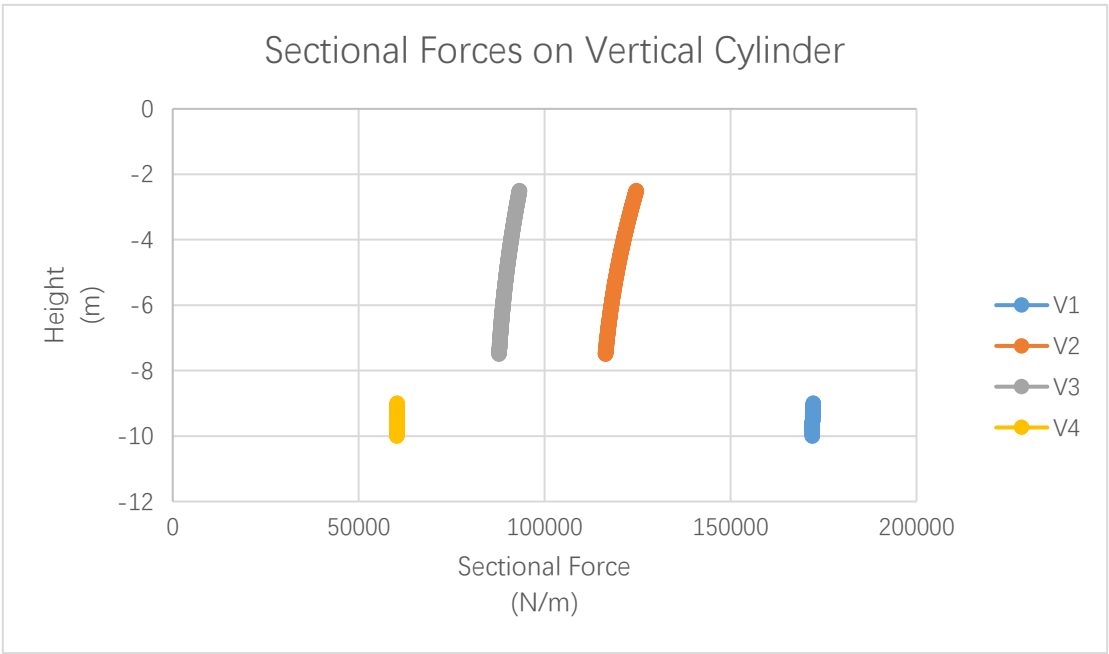

Figure 6-18 Sectional Forces on Vertical Cylinder

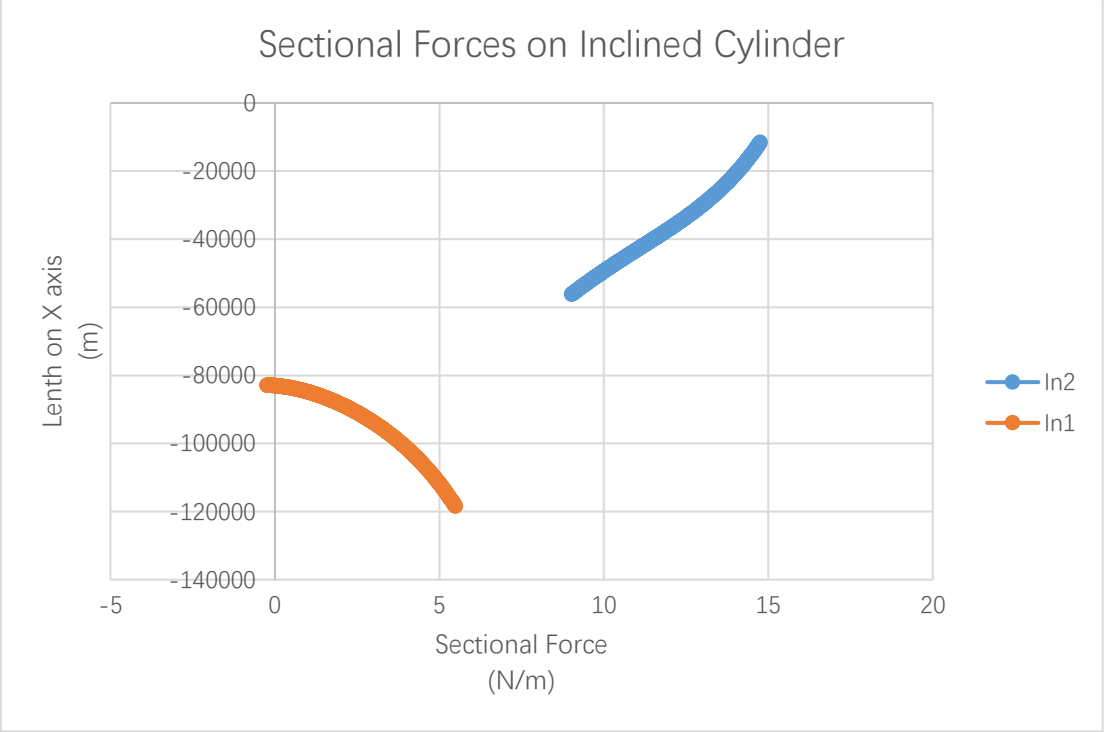

Figure 6-19 Sectional Forces on Inclined Cylinder

c) H=4m, T=10s

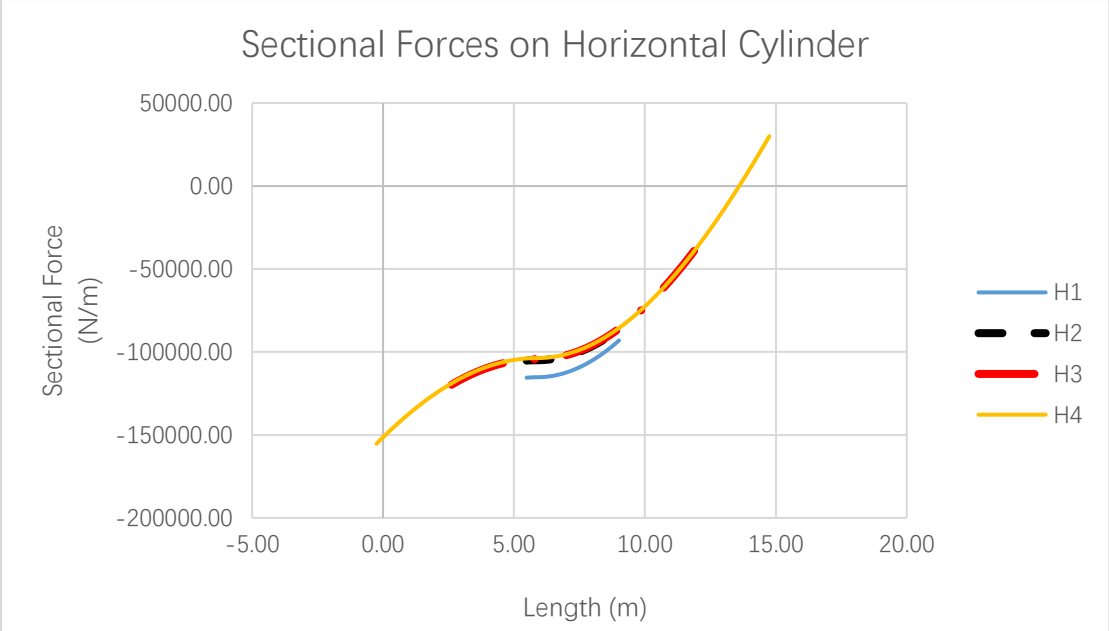

Figure 6-20 Sectional Forces on Horizontal Cylinder

Column	H5	H6	H7	H8
Sectional Forces (N/m)	-155342.94	-119761.48	-38974.57	30004.19
Column	H9	H10	H11	H12
Sectional Forces (N/m)	-115517.99	-105217.89	-92964.59	-86316.20

Table 6-8 Sectional Forces on Horizontal Cylinder

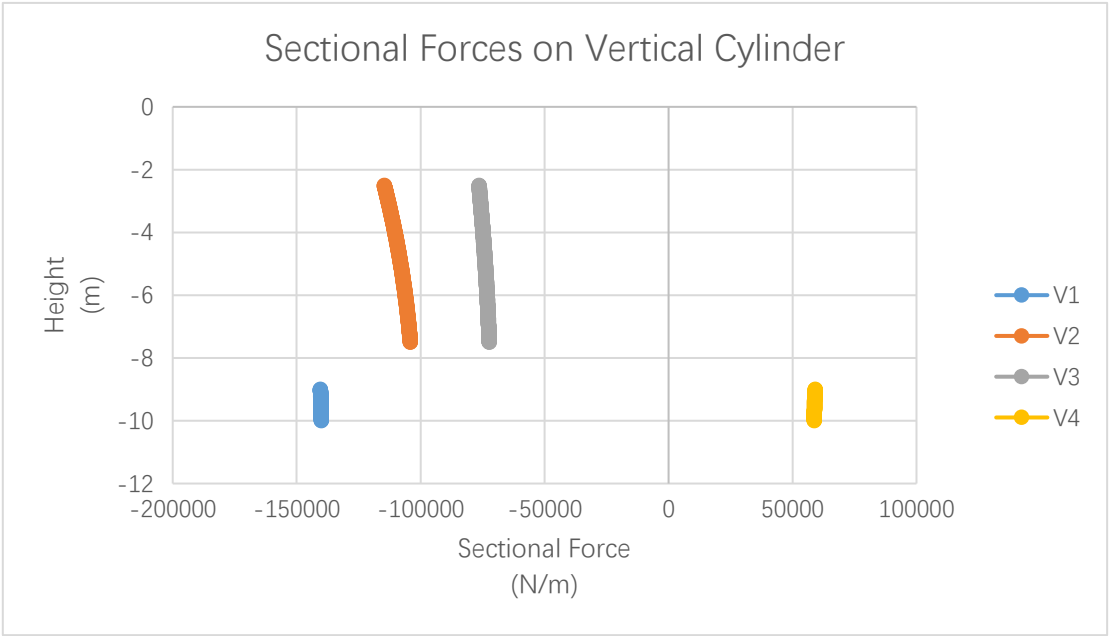

Figure 6-21 Sectional Forces on Vertical Cylinder

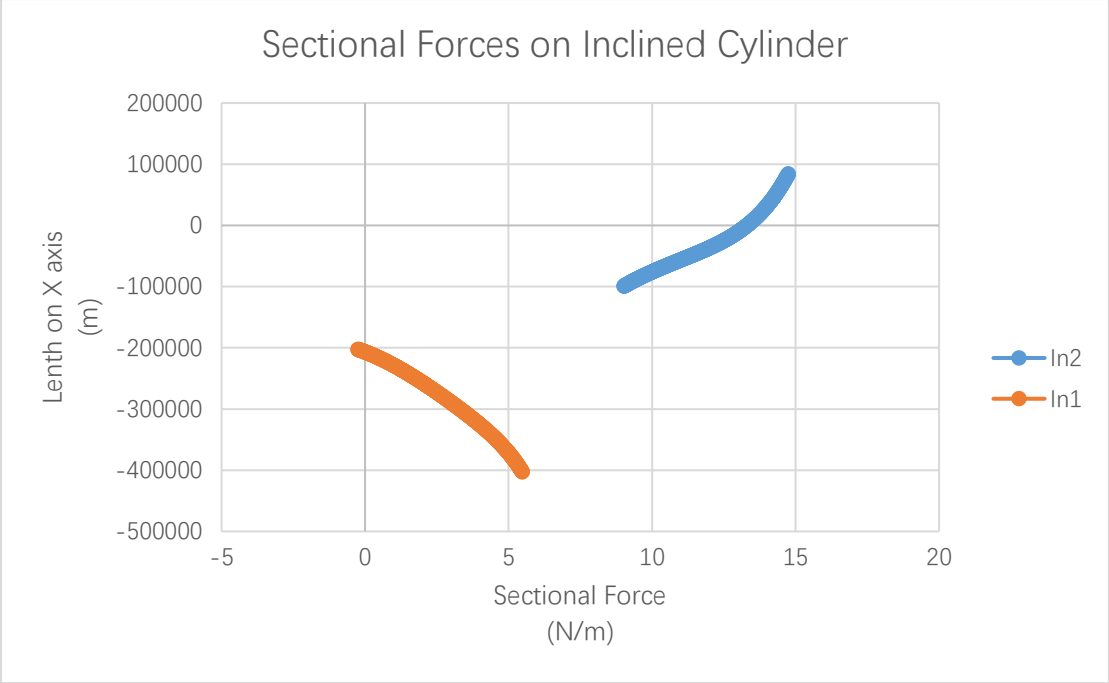

Figure 6-22 Sectional Forces on Vertical Cylinder

d) H=4m, T=15s

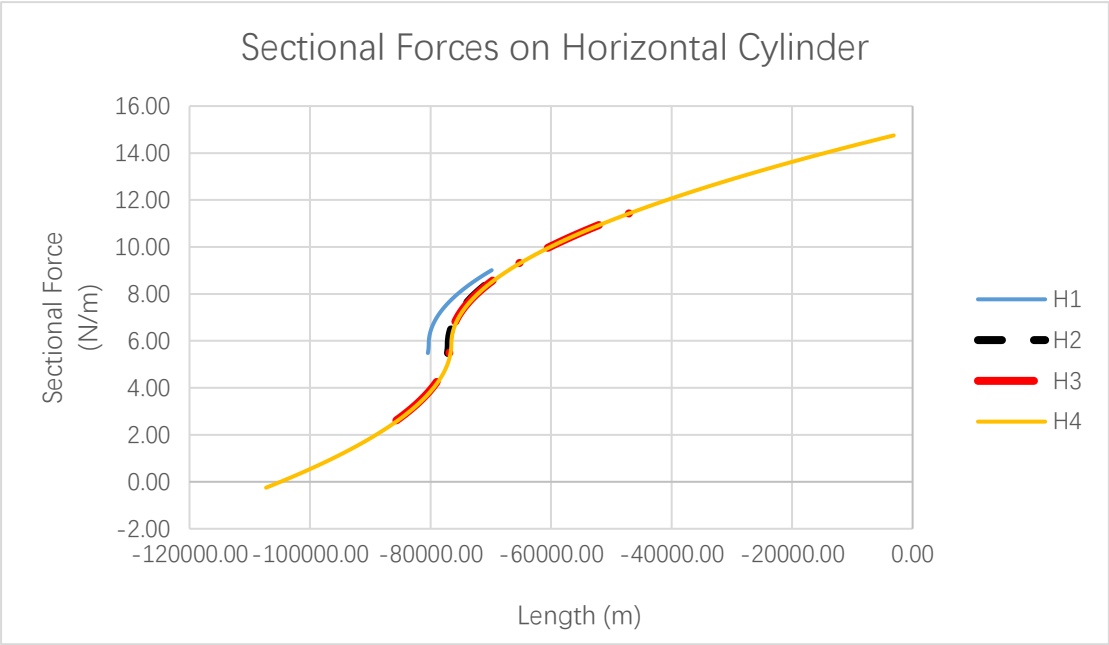

Figure 6-23 Sectional Forces on Horizontal Cylinder

Column	H5	H6	H7	H8
Sectional Forces (N/m)	-107301.31	-85674.10	-42107.77	-3127.92
Column	H9	H10	H11	H12
Sectional Forces (N/m)	-80448.83	-77111.11	-69817.06	-67314.06

Table 6-9 Sectional Forces on Horizontal Cylinder

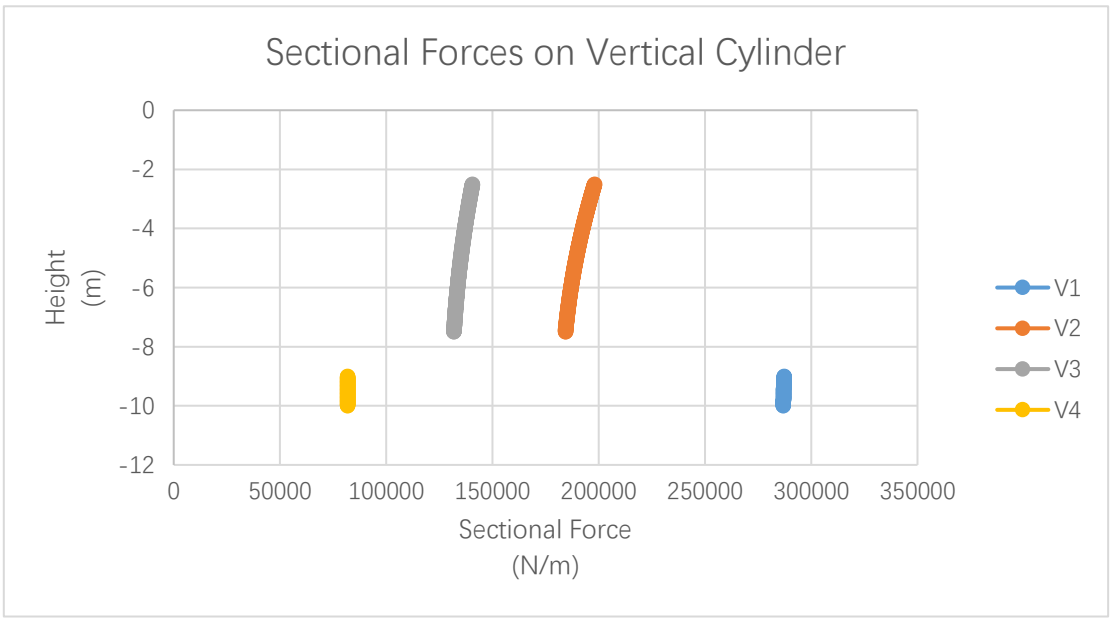

Figure 6-24 Sectional Forces on Vertical Cylinder

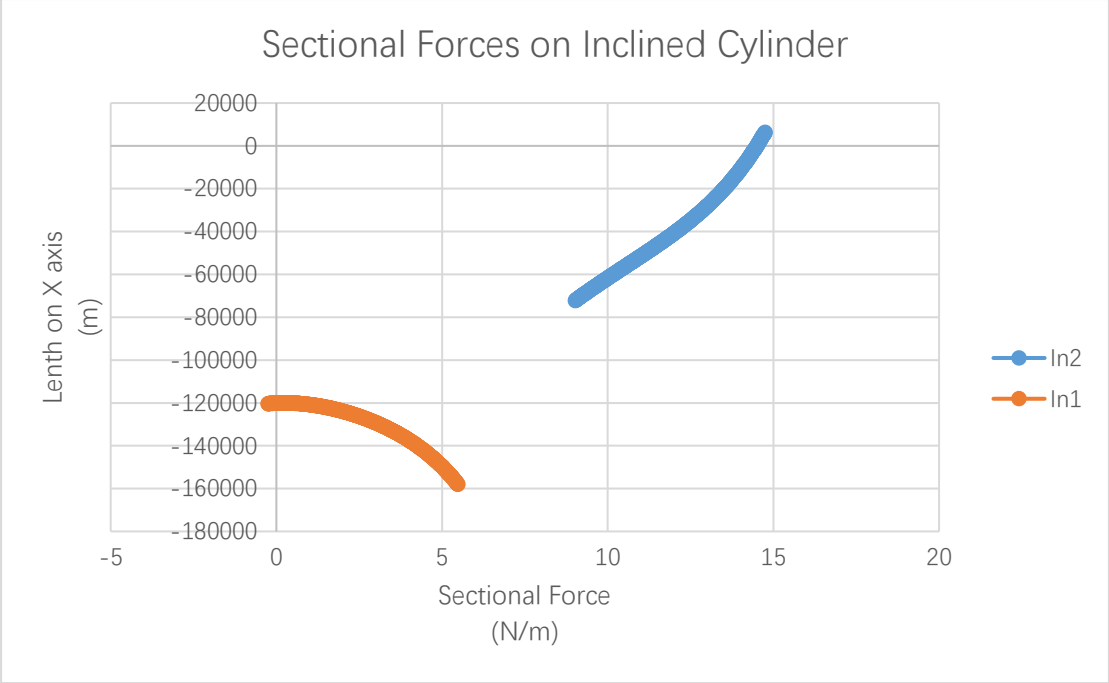

Figure 6-25 Sectional Forces on Inclined Cylinder

6.2.2. Wave Loads on the Disc

Need to pay attention here is that the time of the wave crest or trough movement to the disc is different from that to the cylinders. After running a programme to calculate the sectional force and pressure on the disc, we can get a distribution of sectional force like in Figure 6-26:

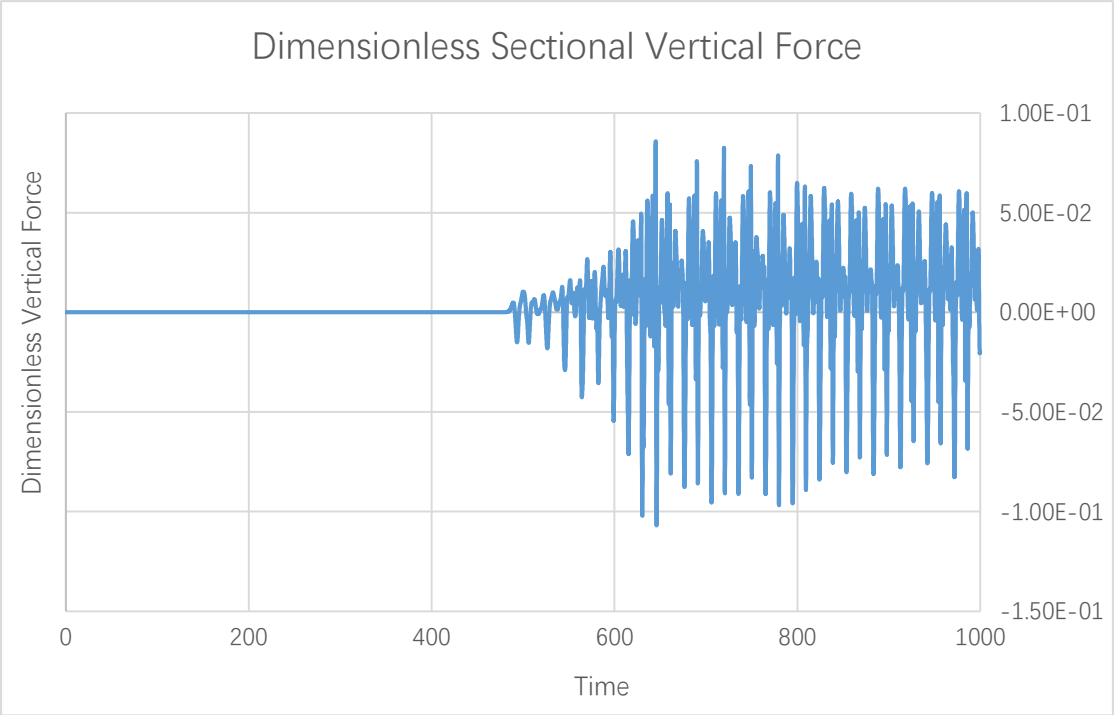

Figure 6-26 Dimensionless Sectional Vertical Force (Time Horizon from 0 to 1000)

Figure 6-26 demonstrates the variety of dimensionless sectional vertical force on the disc with the change of time in an environmental condition which is H=4m, S=3m, T=15s (belongs to Test Case 4 in Table 6-1). We can see there is almost 0 in dimensionless sectional force value in the beginning of time, then the value changes and oscillates, which gradually becomes stable until the time reaches about 800. Nextly, let us look at the relatively stable region of dimensionless sectional force. Here is the value of the time between 860 and 920:

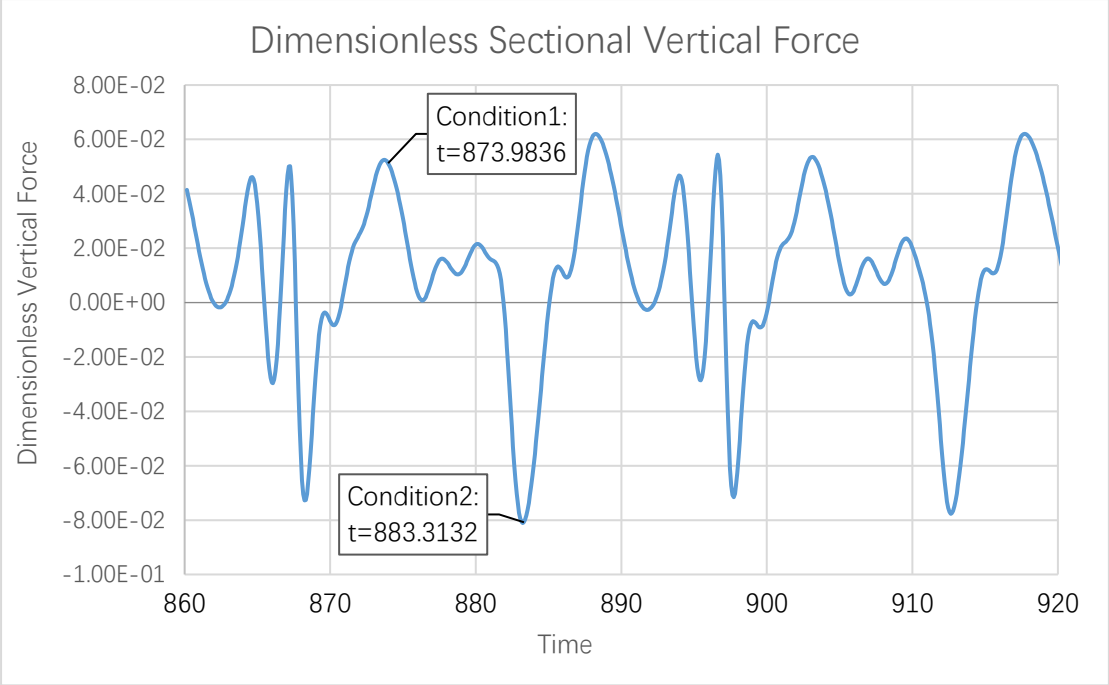

Figure 6-27 Dimensionless Sectional Vertical Force (Time Horizon from 860 to 920)

So we choose the time corresponding to the top value of the dimensionless sectional force to calculate the differential pressure on the disc from the wave crest movement (For instance, we choose t=874 to calculate the differential pressure on the disc in Condition 1). Similarly, we choose the time corresponding to the bottom value of the dimensionless sectional force to calculate the differential pressure on the disc from the wave trough movement (For instance, we choose t=883 to calculate the differential pressure on the disc in Condition 2).

Nextly, we can get the differential pressure in these certain time. For instance, Figure 6-28 demonstrates the differential pressure in the time of wave crest. Figure 6-29 shows the differential pressure in the time of wave trough. More detailed data about the calculation of differential pressure are shown in Chapter 6.2.2.1 and Chapter 0.

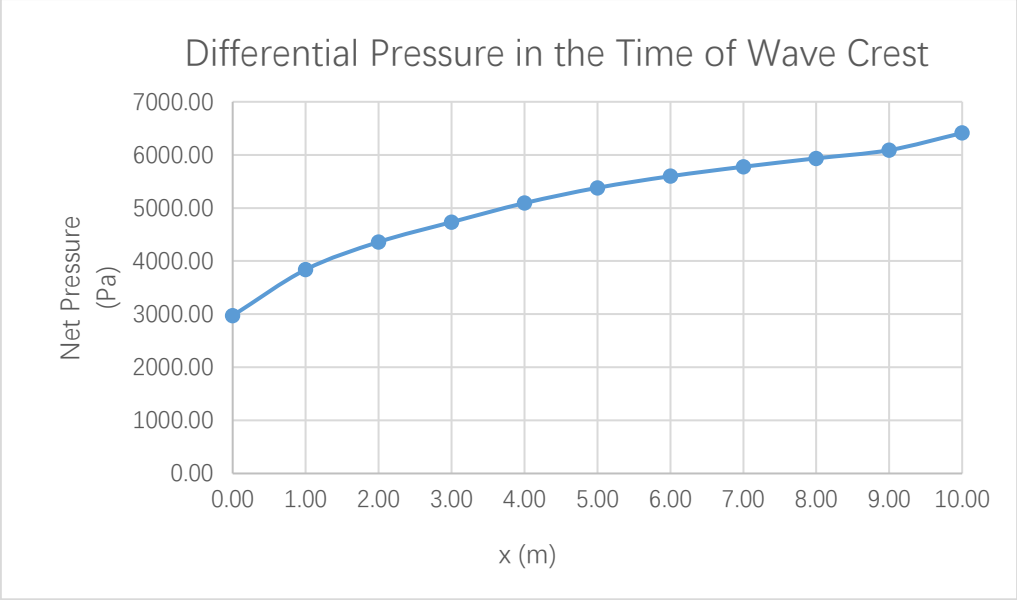

Figure 6-28 Differential Pressure in the Time of Wave Crest (H=4m, S=3m, T=15s, t=873.98s)

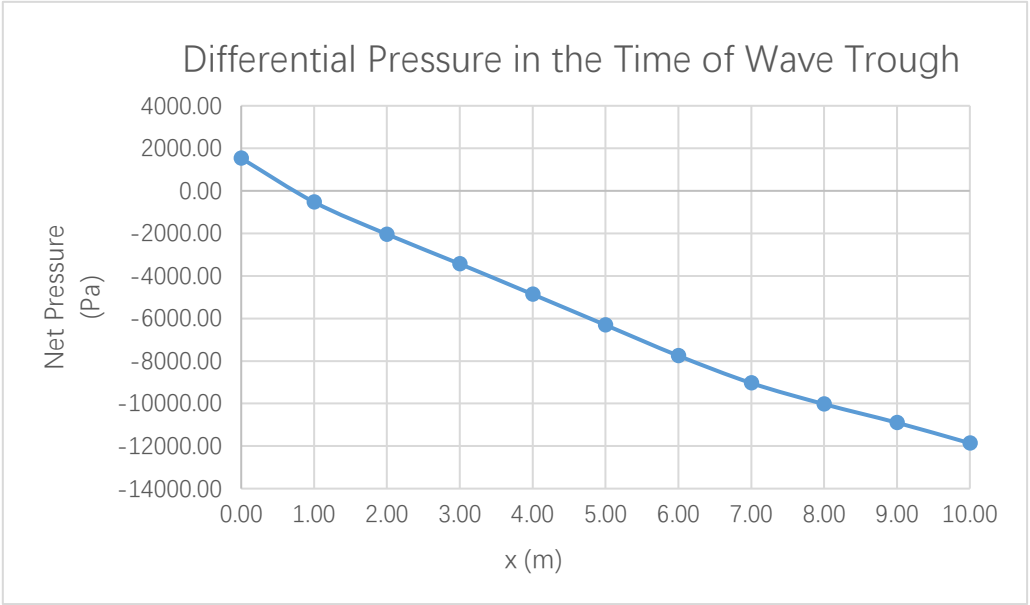

Figure 6-29 Differential Pressure in the Time of Wave Trough (H=4m, S=3m, T=15s, t=883.31s)

6.2.2.1. Differential Pressure on the Disc at Condition 1

The wave-induced two-dimensional force distribution on the submerged disc, calculated by The GN Equations, are shown in Table 6-10 for all test cases considered here.

X in Table 6-10 is measured from the leading edge of the disc like shown in Figure 6-30. In the part of the calculation of differential pressure on the disc, the disc is divided into 10 parts, which means there are 11 nodes on the disc,

every part is 1m width because of the diameter of the disc is 10m.

After conversion of the dimensionless data, the dimensional data of differential pressure on the disc are given directly here. The orange rows give the environmental conditions for the following values. The parameters below have been defined before in Chapter 6.1.

Figure 6-30 Schematic diagram of x in the disc (x in this table is measured from the leading edge of this disc)

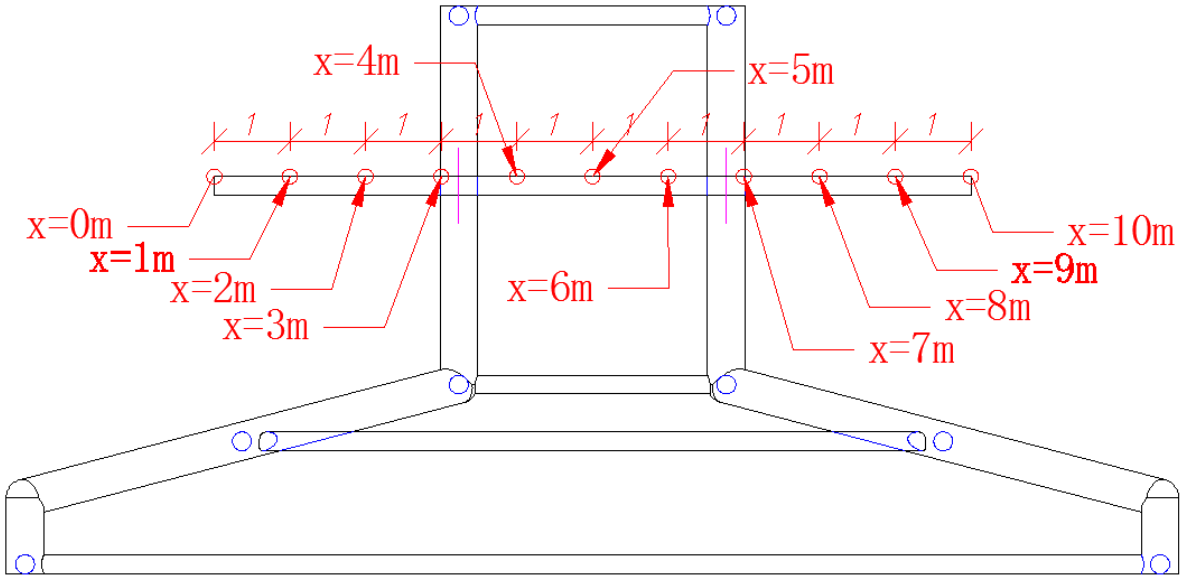

Table 6-10 Differential pressure on the disc in condition 1

H=3m, S=3m, T=10s, t=802.93s		H=3m, S=5m, T=10s, t=802.93s		H=3m, S=7m, T=10s, t=802.93s	
x (m)	P (Pa)	x (m)	P (Pa)	x (m)	P (Pa)
0.00	8210.03	0.00	1719.88	0.00	907.30
1.00	7587.94	1.00	2715.70	1.00	1953.00
2.00	7003.10	2.00	3305.03	2.00	2574.73
3.00	6443.43	3.00	3827.63	3.00	3065.70
4.00	5918.30	4.00	4387.99	4.00	3643.32
5.00	5512.83	5.00	4889.22	5.00	4234.11
6.00	5208.44	6.00	5305.62	6.00	4746.98
7.00	4935.12	7.00	5642.75	7.00	5116.13
8.00	4648.77	8.00	5882.03	8.00	5280.38
9.00	4320.89	9.00	5991.01	9.00	5231.23
10.00	4081.49	10.00	6064.51	10.00	5119.20
H=3m, S=3m, T=15s, t=967.95s		H=3m, S=5m, T=15s, t=967.95s		H=3m, S=7m, T=15s, t=967.95s	
x (m)	P (Pa)	x (m)	P (Pa)	x (m)	P (Pa)
0.00	5535.83	0.00	-173.77	0.00	-467.13

1.00	4694.41	1.00	240.64	1.00	59.36
2.00	4304.68	2.00	782.05	2.00	631.91
3.00	3940.28	3.00	1362.66	3.00	1183.95
4.00	3576.03	4.00	1939.17	4.00	1727.09
5.00	3349.48	5.00	2543.45	5.00	2300.83
6.00	3271.61	6.00	3186.79	6.00	2899.14
7.00	3288.15	7.00	3829.70	7.00	3441.32
8.00	3340.72	8.00	4406.32	8.00	3822.06
9.00	3404.28	9.00	4908.49	9.00	4049.57
10.00	3665.12	10.00	5561.28	10.00	4387.20
H=4m, S=3m, T=10s, t=901.97s		H=4m, S=5m, T=10s, t=860.99s		H=4m, S=7m, T=10s, t=860.99s	
x (m)	P (Pa)	x (m)	P (Pa)	x (m)	P (Pa)
0.00	7668.53	0.00	2675.75	0.00	447.72
1.00	7862.37	1.00	3444.77	1.00	1675.97
2.00	7530.92	2.00	3955.64	2.00	2400.76
3.00	7128.01	3.00	4442.49	3.00	3053.73
4.00	6765.43	4.00	4996.00	4.00	3883.53
5.00	6435.64	5.00	5542.50	5.00	4742.80
6.00	6140.21	6.00	6063.95	6.00	5522.85
7.00	5844.95	7.00	6570.68	7.00	6156.57
8.00	5528.63	8.00	7024.16	8.00	6556.43
9.00	5180.13	9.00	7347.93	9.00	6658.81
10.00	4886.95	10.00	7744.84	10.00	6665.63
H=4m, S=3m, T=15s, t=873.98s		H=4m, S=5m, T=15s, t=872.98s		H=4m, S=7m, T=15s, t=872.98s	
x (m)	P (Pa)	x (m)	P (Pa)	x (m)	P (Pa)
0.00	2972.09	0.00	-388.88	0.00	-1000.38
1.00	3839.10	1.00	519.63	1.00	9.21
2.00	4358.89	2.00	1339.00	2.00	838.75
3.00	4733.41	3.00	2223.49	3.00	1647.05
4.00	5092.12	4.00	3152.62	4.00	2516.67
5.00	5379.99	5.00	4089.92	5.00	3421.49
6.00	5598.11	6.00	5045.25	6.00	4326.16
7.00	5776.15	7.00	5999.19	7.00	5143.33
8.00	5935.03	8.00	6883.41	8.00	5749.13
9.00	6090.01	9.00	7632.32	9.00	6087.41
10.00	6411.43	10.00	8530.81	10.00	6441.98

6.2.2.2. Differential Pressure on the Disc at Condition 2

The wave-induced two-dimensional force distribution on the submerged disc, calculated by The GN Equations, are shown in Table 6-11 for all cases considered here.

X in Table 6-11 is measured from the leading edge of the disc like shown in Figure 6-30. The definition of x is the same as in Chapter 6.2.2.1.

After conversion of the dimensionless data, the dimensional data of differential pressure on the disc are given directly here. The orange rows give the environmental conditions for the following values. H is wave height, S is submergence depth of the disc, T is wave period, t is time used to calculate differential pressure. The parameters below have been defined before in Chapter 6.1.

Table 6-11 Differential pressure on the disc in condition 2 (x in this table is measured from the leading edge of this disc)

H=3m, S=3m, T=10s, t=797.93s		H=3m, S=5m, T=10s, t=796.93s		H=3m, S=7m, T=10s, t=796.93s	
x (m)	P (Pa)	x (m)	P (Pa)	x (m)	P (Pa)
0.00	-1333.15	0.00	-1961.48	0.00	-1874.71
1.00	-3184.81	1.00	-2529.41	1.00	-2227.94
2.00	-4655.94	2.00	-2794.11	2.00	-2260.53
3.00	-6092.04	3.00	-2973.79	3.00	-2224.72
4.00	-7558.52	4.00	-3094.52	4.00	-2170.74
5.00	-8998.91	5.00	-3115.94	5.00	-2087.58
6.00	-10517.48	6.00	-3079.79	6.00	-2018.59
7.00	-12146.99	7.00	-3144.65	7.00	-2021.53
8.00	-13408.80	8.00	-3144.14	8.00	-1847.42
9.00	-14983.27	9.00	-2469.73	9.00	-956.50
10.00	-18596.97	10.00	-2135.97	10.00	-388.47
H=3m, S=3m, T=15s, t=962.95s		H=3m, S=5m, T=15s, t=962.95s		H=3m, S=7m, T=15s, t=960.95s	
x (m)	P (Pa)	x (m)	P (Pa)	x (m)	P (Pa)
0.00	-255.48	0.00	256.18	0.00	-2690.71
1.00	-1966.30	1.00	-720.45	1.00	-2712.05
2.00	-3416.93	2.00	-1425.44	2.00	-2728.88
3.00	-4872.00	3.00	-2097.73	3.00	-2642.50
4.00	-6369.62	4.00	-2762.95	4.00	-2443.59
5.00	-7875.75	5.00	-3357.98	5.00	-2147.57

6.00	-9515.10	6.00	-3924.62	6.00	-1796.84
7.00	-11234.87	7.00	-4496.16	7.00	-1486.25
8.00	-12300.40	8.00	-4838.10	8.00	-1135.93
9.00	-13216.06	9.00	-4835.77	9.00	-318.64
10.00	-16117.08	10.00	-5435.49	10.00	407.61
H=4m, S=3m, T=10s, t=895.97s		H=4m, S=5m, T=10s, t=845.99s		H=4m, S=7m, T=10s, t=845.99s	
x (m)	P (Pa)	x (m)	P (Pa)	x (m)	P (Pa)
0.00	-314.80	0.00	-437.01	0.00	-599.11
1.00	-480.07	1.00	-1670.56	1.00	-1378.76
2.00	-399.74	2.00	-2440.98	2.00	-1712.31
3.00	-104.34	3.00	-3183.37	3.00	-1996.26
4.00	399.37	4.00	-3944.80	4.00	-2301.55
5.00	1076.93	5.00	-4634.34	5.00	-2562.12
6.00	1804.52	6.00	-5284.79	6.00	-2824.96
7.00	2043.25	7.00	-5953.43	7.00	-3114.83
8.00	1259.40	8.00	-6100.11	8.00	-2879.02
9.00	1918.45	9.00	-5412.72	9.00	-1674.27
10.00	4414.74	10.00	-6089.50	10.00	-1598.92
H=4m, S=3m, T=15s, t=883.98s		H=4m, S=5m, T=15s, t=867.99s		H=4m, S=7m, T=15s, t=867.99s	
x (m)	P (Pa)	x (m)	P (Pa)	x (m)	P (Pa)
0.00	1533.44	0.00	114.72	0.00	-137.48
1.00	-526.51	1.00	-1520.59	1.00	-1174.26
2.00	-2040.16	2.00	-2768.76	2.00	-1850.80
3.00	-3435.04	3.00	-3979.36	3.00	-2439.51
4.00	-4865.53	4.00	-5119.08	4.00	-2929.03
5.00	-6309.70	5.00	-6038.48	5.00	-3219.46
6.00	-7753.83	6.00	-6812.46	6.00	-3397.98
7.00	-9037.72	7.00	-7753.84	7.00	-3730.79
8.00	-10028.19	8.00	-8597.32	8.00	-3958.92
9.00	-10901.38	9.00	-8611.92	9.00	-3250.81
10.00	-11864.75	10.00	-9538.38	10.00	-3007.23

7. Analysis and Discussion

7.1. Condition 1

After running programme, we can get a set of data, and we can see the deformation of WEC in ANSYS Workbench. Here are parts of the examples:

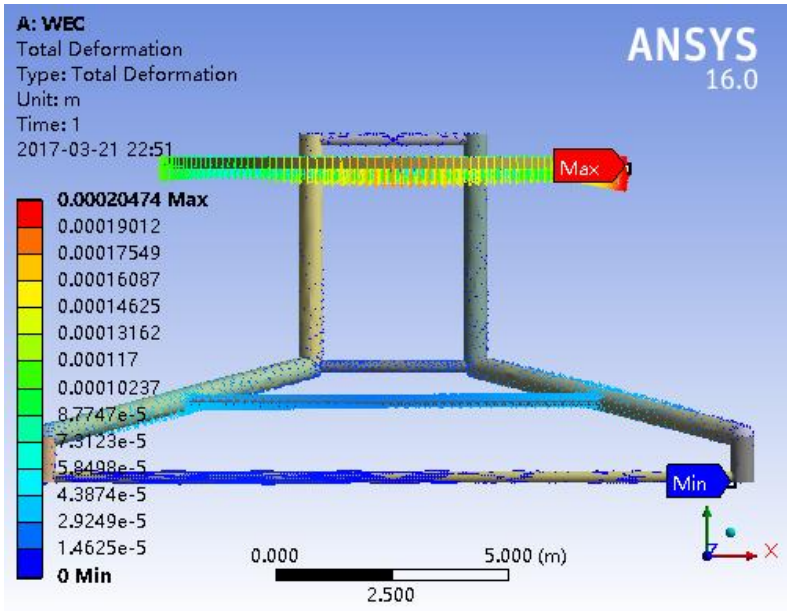

Figure 7-1 Deformation in true scale

Figure 7-1 shows the true scale deformation of the WEC when the wave crest at the top centre of the WEC in where the wave conditions are H=4m, S=3m, T=15s, t=837.98s, and the material is stainless steel. In the figure, we can see so many vectors appear in the WEC around. These vectors illustrate the direction of the deformation in their point. We can see there are different colours for the vectors, red means that the deformation of these points is relatively larger than other places. Then deformation is decreased in turn of red, orange, yellow, green, and blue. In addition, dark blue and grey mean that these points are basically not deformed. In addition, there are specific variables corresponding to the colour on the right side in Figure 7-1.

Figure 7-2 shows the Von-Mises stress in the WEC at the same conditions as in Figure 7-1. The relative large Von-Mises stress mainly concentrates on the part that the disc and cylinders contact each other. The maximum stress in the

WEC is 5.917x10^{6} Pa, which is much less than the yield strength of stainless steel (2.07x10^{8} Pa, see details in Table 5-1)

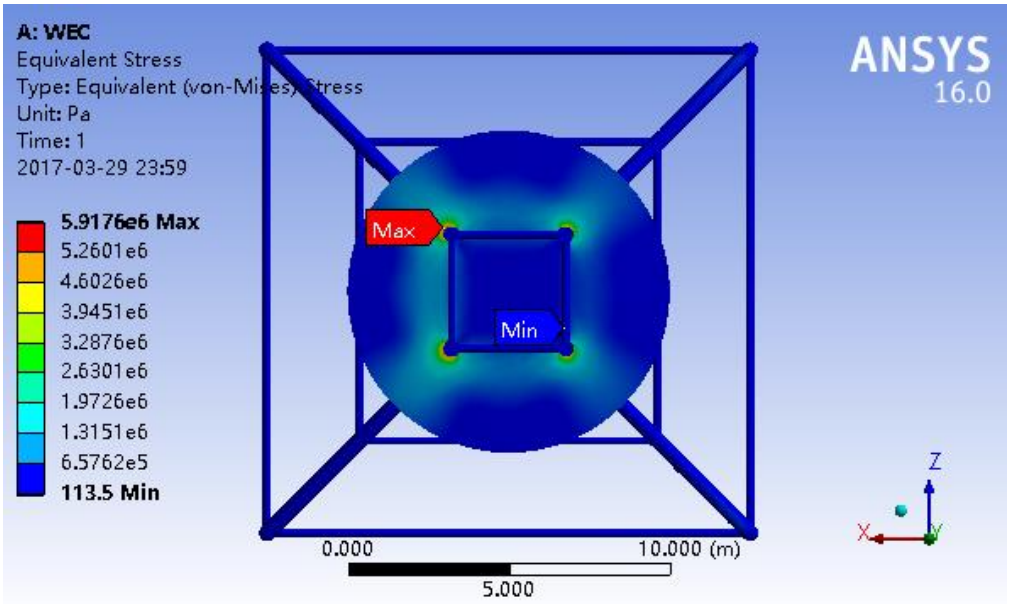

Figure 7-2 Von-Mises Stress in the WEC at Condition 1 (H=4m, S=3m, T=15s, t=883.98s)

In Figure 7-1, we can see most of the relative large deformation is on the disc. In order to know the distribution of deformation in the disc, we can get the distribution of deformation on the WEC's disc. Figure 7-3 shows the distribution of deformation of different materials, which has the same environmental conditions as in Figure 7-1.

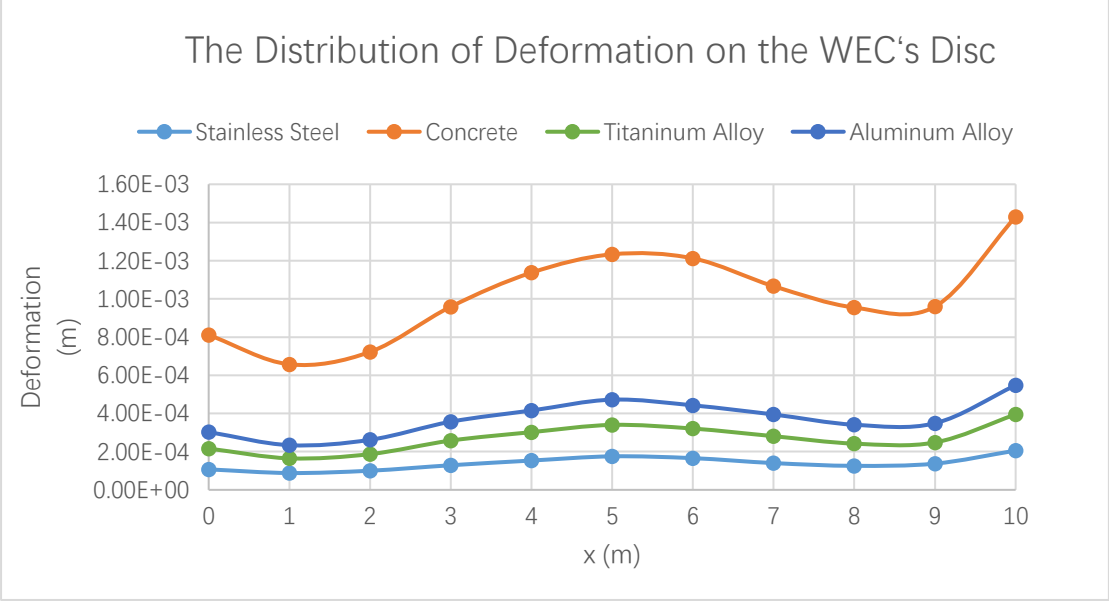

Figure 7-3 The Distribution of Deformation on the WEC's Disc (H=4m, S=3m, T=15s, t=873.98s)

we can know under the same conditions, the deformation of concrete is larger than aluminium alloy, larger than that of titanium alloy, and larger than that of stainless steel.

In this way, after analysing 48 sets of different environmental conditions and materials, the following figure is obtained:

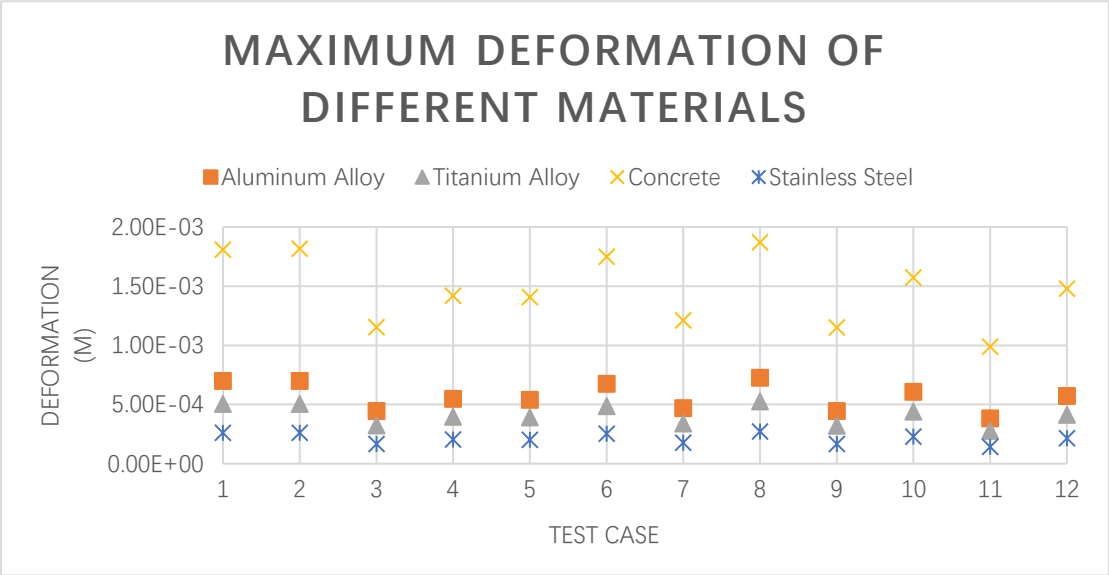

Figure 7-4 Maximum deformation of different materials

Test case 1~12 in Figure 7-4 are different environmental conditions which are shown in Table 6-1 (See Chapter 5.4.3 for more details).

From Table 6-1, we can divide 12 test cases into 3 part by the difference of submergence depth. Here we define that Group 1 is test case 1~4 whose S=3m. Group 2 is test case 5~8 whose S=5m. Group 3 is test case 9~12 whose S=7m. In addition, for example, in Part1, between test case 1 and test case 2, test case 3 and test case 4, the only variable parameter is wave period (T=10s to T=15s). Similarly, between test case 1 and test case 3, test case 2 and test case 4, the only variable parameter is wave height (H=3m to H=4m). Also, this law exists in Group 2 and Group 3 of the test cases.

By observing Figure 7-4 when the wave crest is at the top of the WEC, we can find the maximum deformation of the WEC is decreased generally (except test case 7 and test case 8) when wave period increase from 10s to 15s. On the other,

when the variable parameter is wave height, the maximum deformation of the WEC is increased more or less when wave height changes from 3m to 4m. Such as test case 1 and 3, test case 2 and test case 4, test case 5 and test case 7, test case 6 and test case 8, test case 9 and test case 11, test case 10 and test case 12. It is more clear when to change the sequences of test cases, which is shown in Figure 7-5. Additionally, there is no special law when compare Group 1, Group 2 and Group 3 in condition 1.

Apart from these, we can see under any environmental conditions the largest deformation appears in concrete, the second one is aluminium alloy, then the third one is titanium alloy, the minimum deformation appears in stainless steel.

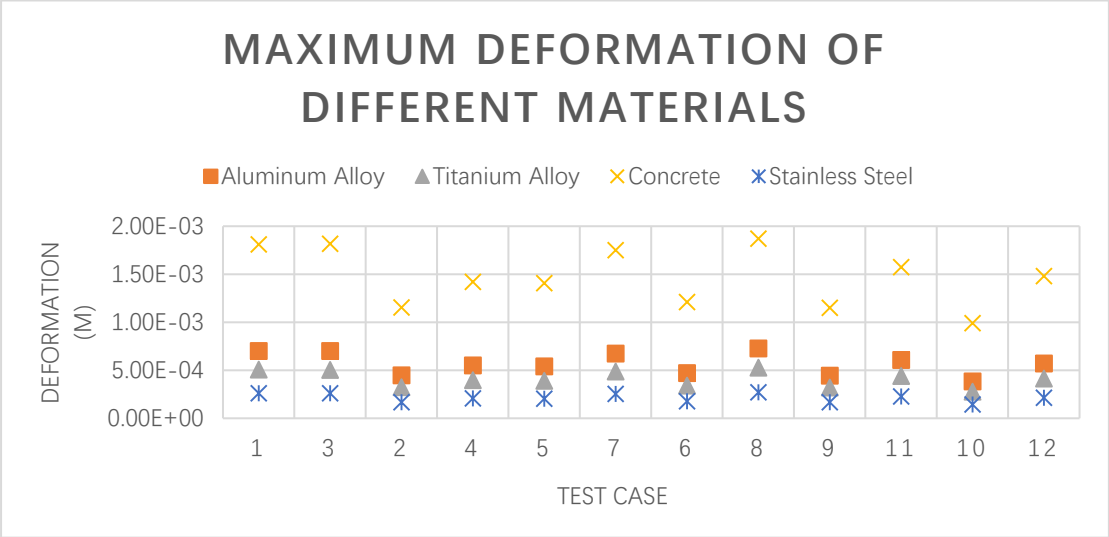

Figure 7-5 Maximum deformation of different materials in Condition 1 with different test cases sequences

7.2. Condition 2

In this case, the deformation graph which is similar to Figure 7-1, and will also be shown below.

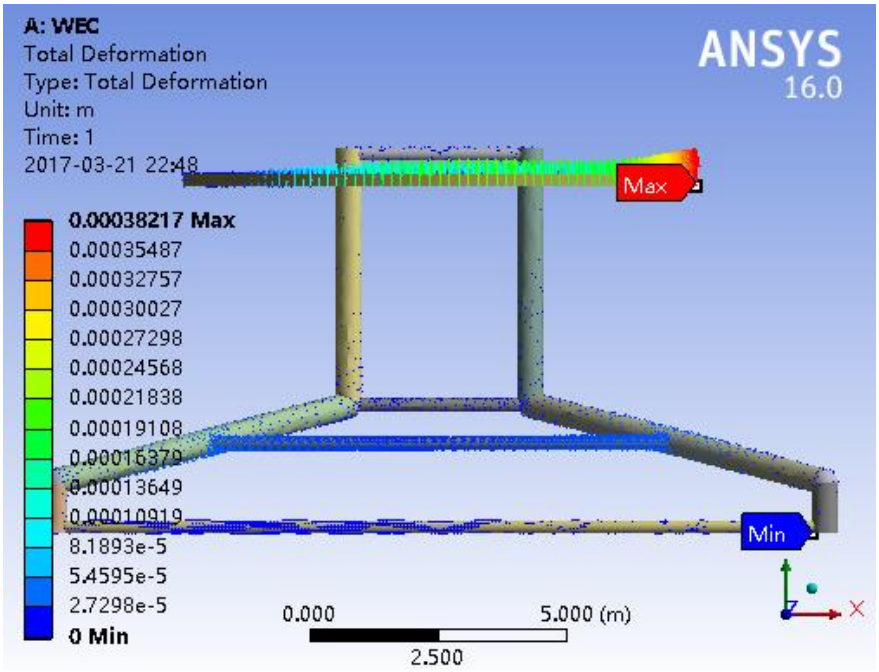

Figure 7-6 Deformation in true scale

Figure 7-6 shows the true scale deformation of the WEC when the wave trough at the top centre of the WEC in where the wave conditions are H=4m, S=3m, T=15s, t=883.98s, and the material is stainless steel. In addition, the properties of vectors are the same as in Chapter 7.1.

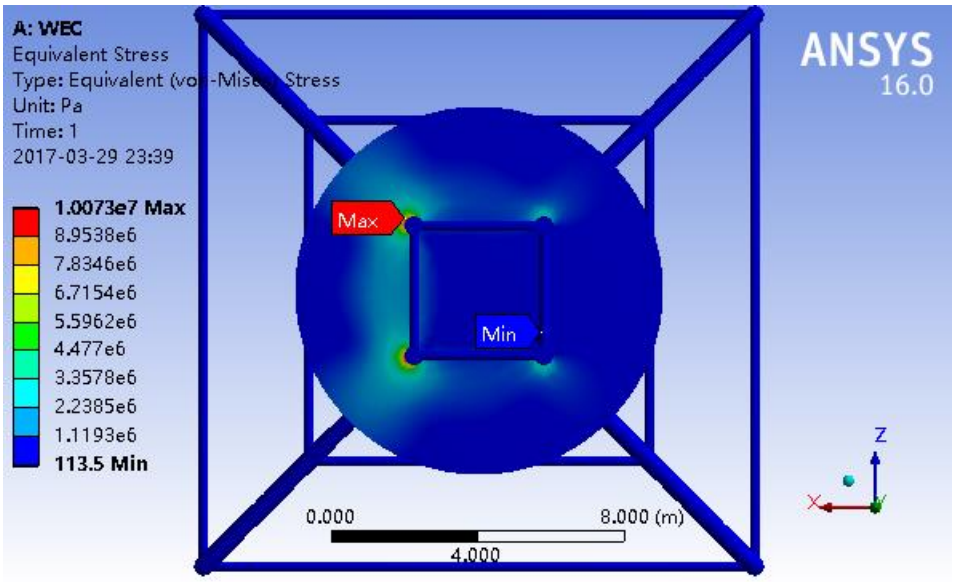

Figure 7-7 Von-Mises Stress in the WEC at Condition 2 (H=4m, S=3m, T=15s, t=883.98s)

Figure 7-7 shows the Von-Mises stress in the WEC at the same conditions as in Figure 7-6. The relative large Von-Mises stress mainly concentrates on the part that the disc and cylinders contact each other. The maximum stress in the WEC is 1.0073×10^{7} Pa, which is much less than the yield strength of stainless steel (2.07×10^{8} Pa, see details in Table 5-1)

In Figure 7-6, we can see most of the relative large deformation is on the disc, which is similar to condition 1. In order to know the distribution of deformation in the disc, we can get the distribution of deformation on the WEC's disc in ANSYS Workbench, like shown in Figure 7-8.

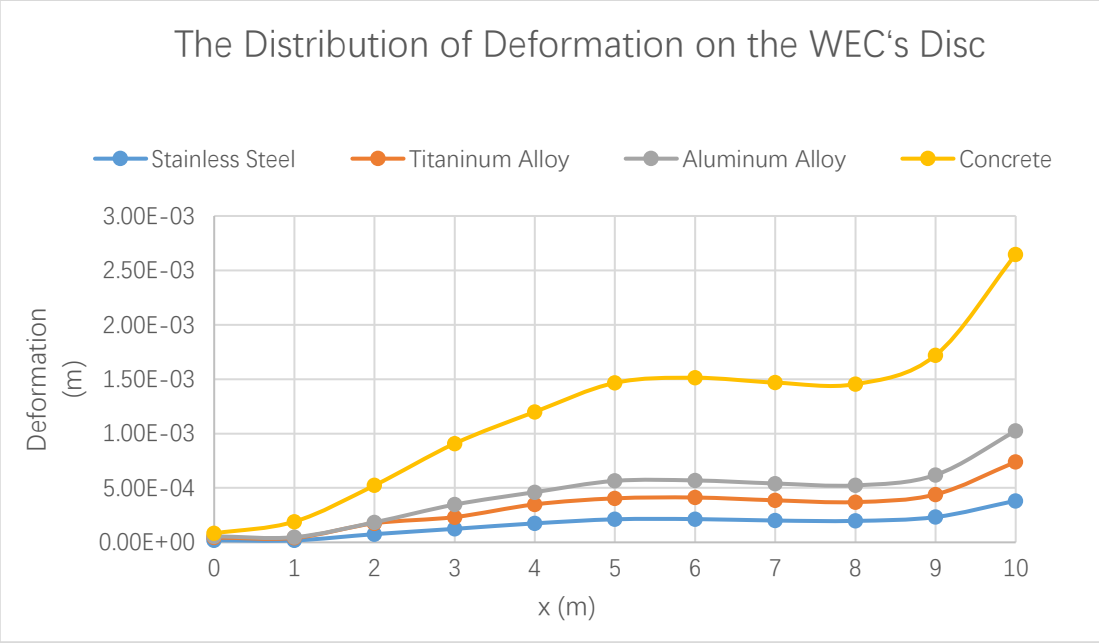

Figure 7-8 The Distribution of Deformation on the WEC's Disc (H=4m, S=3m, T=15s, t=883.98s)

Figure 7-8 shows the distribution of deformation of different materials, which has the same environmental conditions as in Figure 7-6. Also, we can know under the same conditions, the deformation of concrete is larger than aluminium alloy, larger than that of titanium alloy, and larger than that of stainless steel.

Similarly, as in Chapter 7, the following figure is obtained after analysing 48 different data. And the analysis of the test cases is the same as in Chapter 7.

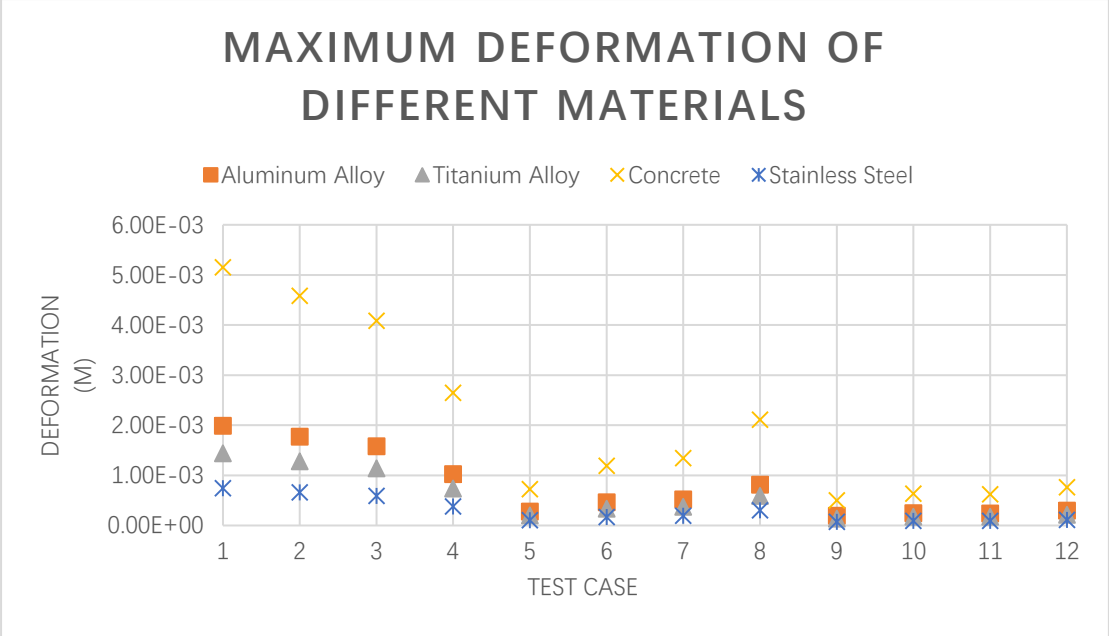

Figure 7-9 Maximum deformation of different materials

Test case 1~12 in Figure 7-9 are different environmental conditions which are shown in Table 6-1 (See Chapter 5.4.3 for more details).

The variety of maximum deformation of WEC becomes more significantly when submergence depth decreases in where the wave trough at the top centre of WEC. In condition 2, we define test case 1~4 as Group 4, test case 5~8 as Group 5, test case 9~12 as Group 6 hereafter.

We find that the maximum deformation of WEC is decreasing obviously as the decreasing of the submergence depth of disc. However, the change of wave height and wave period has not some general laws in condition 2. But when observe separately, the maximum deformation of the WEC is decreasing in Group 4 and Group 6 when wave height is increasing or wave period is reducing. Group 5 has the different situation, the maximum deformation of the WEC is increasing in Group 4 and Group 6 when wave height is decreasing or wave period is increasing.

7.3. Discussion

Let us focus on the deformation in a specific case. For instance, in Figure 7-1 and Figure 7-6, we can see the true scale deformation in the WEC (The environmental conditions in Figure 7-1 and Figure 7-6 belong to test case 4 in Table 6-1). Actually, an obvious deformation is hard to be directly found in true scale. Nextly, the main deformation is concentrated on the disc rather than on the cylinders. Although there are a few deformations of the columns, the vectors in columns are in blue and grey (i.e. the deformations of the columns are too small and close to nought). Additionally, the relative large deformation is concentrated on the edge of the disc. Although there are some deformations on the device, the deformation is within an acceptable range.

Then we compare the properties of materials in the same conditions according to Figure 7-3 and Figure 7-8. For example, in Figure 7-3, we can see concrete have the largest deformation among 4 materials, which is much larger than the deformation of other materials. Furthermore, actually, in all cases and test cases, concrete have the absolute largest deformation among the 4 materials in the same conditions. That is because concrete is too prone to be tension failure (Balaguru, Naaman and Weiss 2002). On the other hand, the deformation of aluminium alloy is almost twice larger than that of titanium alloy, and about 3 times than that of stainless steel.

By comparing Figure 7-4 and Figure 7-9, we can know the maximum deformation on the WEC changes significantly with the change of submergence depth of the disc in condition 2. However, the maximum deformation on the WEC changes slightly with the change of submergence depth of the disc in condition 1. So wave movement has a significantly larger impact than other conditions. In addition, by comparing other environmental conditions in the same wave movement, we can find that the change of wave height has a relative obvious impact on the deformation of the WEC. The change of wave period has a relatively

slight impact on the deformation of the WEC.

In view of the deformation of concrete is too large, we do not consider using it. Secondly, the WEC is immersed in seawater, so its material needs to have a good corrosion resistance. And the rest of the materials have good corrosion resistance, so we keep aluminium alloy, titanium alloy, and stainless steel finally.

Additionally, the remaining materials have good corrosion resistance. Although the 3 materials have so many different types on the market, in general, the corrosion resistance of titanium alloy is similar to that of aluminium alloy better than that of stainless steel (Hornbacher 2017). Considering the price of the three materials, stainless steel is cheaper than aluminium alloy, aluminium alloy is cheaper than titanium alloy (Metal Costs 2017).

8. Conclusion

In this article, the goal is to structurally assess WEC under extreme wave conditions. The process of analysis has been shown in Figure 5-10. We choose ANSYS Workbench to be used to analyse the structure of the WEC. Four kinds of materials, which is concrete, aluminium alloy, titanium alloy, stainless steel, respectively, are used in WEC have been tested in different environmental conditions in ANSYS Workbench.

We conclude that the maximum deformation of the WEC has significant influence by the submergence depth of disc when wave trough at the top centre of the WEC. The deformation on the disc when the submergence depth of disc is shallow is larger than the deformation on the disc when the submergence depth of disc is deep. But it is different in condition 1, when the wave crest at the top centre of the WEC, the deformation on the disc is relatively stable, no matter at which submergence depth. We can say the movement of wave has the most impact of the maximum deformation on the WEC, the submergence depth of disc has the second impact of the maximum deformation on the WEC, the wave height has the relatively small impact than the submergence depth of disc, the wave period has the relatively minimum impact to the deformation of the WEC among the four conditions. Additionally, the maximum deformation of the WEC always presents at the edge of the disc.

Concrete has the largest deformation, stainless steel has the smallest deformation among the 4 materials. However, it is recommended that an economic analysis should be performed to determine the appropriate material of the disc.

9. Bibliography

Airy, George Biddell. 1841. “Tides and Waves.” *Encyclopedia metropolitana.*

Baidupedia. 2017. *主 应 力 .* Accessed 01 25, 2017. http://baike.baidu.com/view/1583998.htm.

Balaguru, Perumalsamy N, Antoine E Naaman, and W Weiss. 2002. *Concrete : material science to application. A tribute to Surendra P. Shah.* Farmington Hills, Mich. : American Concrete Institute.

Callaghan, J, and R Boud. 2006. “Future marine energy—results of the marine energy challenge: cost competitiveness and growth of wave and tidal stream energy.” *Technical Report, The Carbon Trust.*

Clément, Alain, Pat McCullen, António Falcão, Antonio Fiorentino, Fred Gardner, Karin Hammarlund, George Lemonis, et al. 2002. “Wave energy in Europe: current status and.” *Renewable and Sustainable Energy Reviews*, 405-431.

Corrosion Doctors. 2017. “Titanium Corrosion.” *Corrosion Doctors.* Accessed 03 13, 2017. http://corrosion-doctors.org/MatSelect/corrtitanium.htm.

Drew, B, A R Plummer, and M N Sahinkaya. 2009. “A review of wave energy converter technology.” *Proceedings of the Institution of Mechanical Engineers, Part A: Journal of Power and Energy* 887-902.

EMEC. 2016. *Wave Devices.* Accessed 10 31, 2016. http://www.emec.org.uk/marine-energy/wave-devices/.

EPA. 2012. *Inventory of U.S. Greenhouse Gas Emissions and Sinks: 1990–1998.* Washington DC: US EPA.

Ertekin, C. R., and D. Xia. 2014. “Hydroelastic response of a floating runway to cnoidal waves.” *Physics of Fluids*, 1-16.

Falcão, A. F. de O. 2010. “Wave energy utilization: A review of the technologies.” *Renewable and Sustainable Energy Reviews*, 899-918.

GEA. 2012. *Global Energy Assessment.* Cambridge University Press, Cambridge UK and New York, NY, USA and the International Institute for Applied Systems

Analysis: Schlossplatz 1, A-2361 Laxenburg, Austria.

Goldemberg, J. 2000. *World Energy Assessment - Energy and the Challenge of Sustainability.* New York (USA).

Green, E. A., and M. P. Naghdi. 1977. "Water waves in a nonhomogeneous incompressible fluid." *ASME J. Appl. Mech*, 523-528.

—. 1976. "Directed fluid sheets." *Mathematical, Physical and Engineering Sciences*, 447-473.

Hayatdavoodi, Masoud, and R. Cengiz Ertekin. 2015. "Wave forces on a submerged horizontal plate-Part I: Theory and modelling." *Journal of Fluids and Structures*, 566-579.

—. 2015. "Wave forces on a submerged horizontal plate–Part II: Solitary and cnoidal waves." *Journal of Fluids and Structures*, 580-596.

Herzog, SJ. 1999. "Wind Energy: Power and Policy." *Appraisal Journal.*

Hodgson, P. E. 2008. "Nuclear Power and Energy Crisis." *Modern Age* 238.

Hope, Chris, Paul Gilding, and Jimena Alvarez. 2016. "Quantifying the implicit climate subsidy received by leading fossil fuel companies — Working Paper No. 02/2015." Cambridge: UK: Cambridge Judge Business School, University of Cambridge, 27 06.

Hornbacher, Adam. 2017. *Steel versus Aluminum Weight, Strength, Cost, Malleability Comparison.* Accessed 03 13, 2017. http://www.wenzelmetalspinning.com/steel-vs-aluminum.html.

López, I, J Andreu, S Ceballos, I Martínez de Alegría, and I Kortabarria. 2013. "Review of wave energy technologies and the necessary power-equipment." *Renewable Sustainable Energy*, 413-434.

Morison, J R, M. P. O'Brien, J W Johnson, and S A Schaaf. 1950. "The force exerted by surface waves on piles." *Journal of Petroleum Technology*, May: 149-154.

Naghdi, M. P., and L. Vongsarnpigoon. 1986. "The Downstream Flow beyond an

Obstacle." *Journal of Fluid Mechanics*, 223-36.

Naghdi, M. P., and M. B. Rubin. 1981. "On Inviscid Flow in a Waterfall." *Journal of Fluid Mechanics*, 375-387.

Ocean Power Technologies. 2016. *Ocean Power Technologies PowerBuoy.* 31 10. www.oceanpowertechnologies.com/powerbuoy/.

Patel, H M, and A J Witz. 2013. *Compliant offshore structures[M].* Butterworth-Heinemann.

Pelc, Robin, and Rod M. Fujita. 2002. "Renewable energy from the ocean." *Mar. Policy*, 471-479.

Reeve, Dominic, Chadwick Andrew, and Fleming Chris. 2012. *Coastal Engineering: processed, theory and design practice.* USA and Canada: Spon Press.

Roymech. 2017. *Metal Costs.* Accessed 03 13, 2017. http://www.roymech.co.uk/Useful_Tables/Matter/Costs.html.

Saeed, Moaveni. 1999. *Finite Element Analysis: Theory and Application with ANSYS.* Upper Sadle River, New Jesery: Prentice-Hall.

Sarpkaya, T. 2010. *Wave forces on offshore structures[M].* Cambridge: Cambridge university press.

Specialty Steel Industry of North America. 2017. "ssina.com." *ssina.com.* Accessed 03 13, 2017. www.ssina.com/download_a_file/corrosionfinal.pdf.

Turgut, Sarpkaya, and Isaacson Michael. 1981. *Mechanics of Wave Forces on Offshore Structures.* New York: Van Nostrand Reinhold Company.

Ugural, A. C. 1991. *Mechanics of Materials.* New York; London: McGraw-Hill.

University of Cambridge Judge Business School. 2016. *Measuring fossil fuel 'hidden' costs.* Accessed 11 13, 2016. http://insight.jbs.cam.ac.uk/2015/measuring-fossil-fuel-hidden-costs/.

Urgural, Ansel C., and Saul K. Fenster. 2012. *Advanced Mechanics of Materials and Applied Elasticity: Analysis of Stress.* New York; London: Prentice Hall.

Venugopal, Vengatesan, and Reddy Nemalidinne. 2015. "Wave resource

assessment for Scottish waters using a large scale." *Renewable Energy 76*, 503-525.

WavePlane Production. 2016. *WavePlane.* Accessed 10 31, 2016. http://www.waveplane.com/index.html.

Wikipedia. 2017. *Cartesian coordinate system.* 09 Mar. Accessed Mar 21, 2017. https://en.wikipedia.org/wiki/Cartesian_coordinate_system.

—. 2016. *Fossil Fuel.* Accessed 11 13, 2016. https://en.wikipedia.org/wiki/Fossil_fuel.

—. 2016. *Pelamis Wave Energy Converter.* Accessed 10 31, 2016. https://en.wikipedia.org/wiki/Pelamis_Wave_Energy_Converter.

—. 2017. *Right-hand rule.* 27 Feb. Accessed Mar 21, 2017. https://en.wikipedia.org/wiki/Right-hand_rule.

—. 2017. *Stress (mechanics).* 16 1. Accessed 01 24, 2017. https://en.wikipedia.org/wiki/Stress_(mechanics).

World Energy Council. 2010. *2010 Survey of Energy Resources.* London: World Energy Council.

—. 2013. *World Energy Resources 2013 Survey.* London: World Energy Council.

Xia, D., R. C. Ertekin, and J. W. Kim. 2008. "Fluid–structure interaction between a two-dimensional mat-type VLFS and solitary waves by the Green–Naghdi theory." *Journal of Fluids and Structures*, 4 ed.: 527-540. http://dx.doi.org/10.1016/j.jfluidstructs.2007.10.009.

10. Appendices

10.1. Process in Running the GN Equation Program

This program includes two parts, a GNSP.exe file and a Cinput.INP file.

Cinput.INP can open with notebook, we can see:

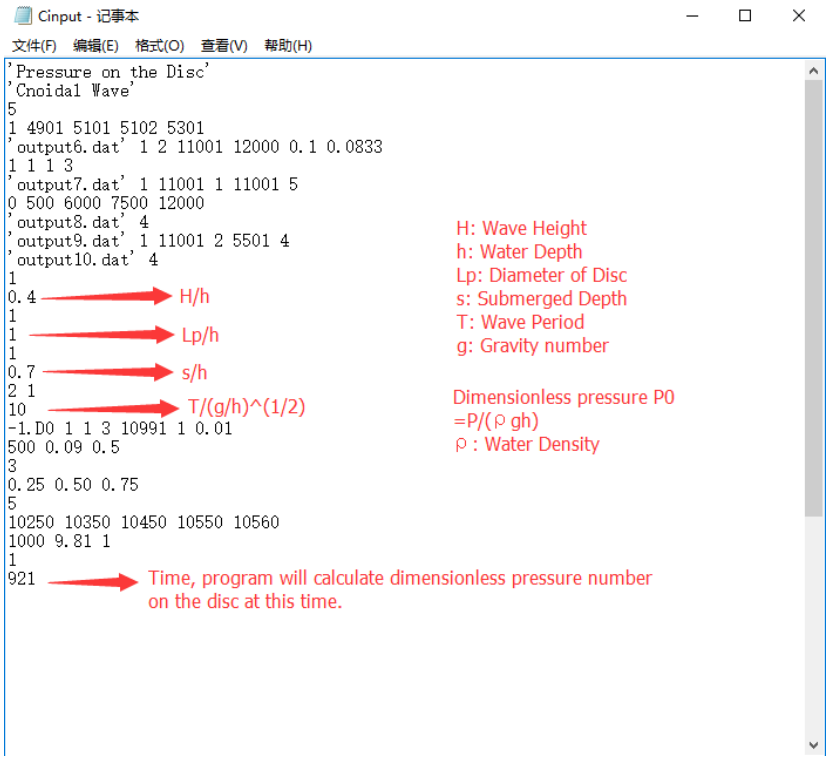

Figure 10-1 Cinput.INP file

After inputting the corresponding data in Cinput.INP, we run GNSP.exe. We will see an interface like:

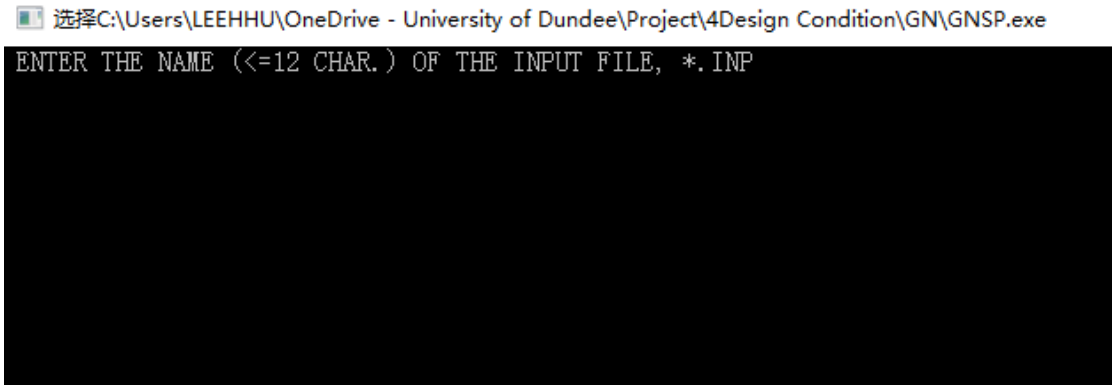

Figure 10-2 The interface of GNSP.exe

Then type "Cinput.INP" and press Enter. After a few minutes, the program will give you 3 useful files, VFORCEND.dat (The data of vertical force per unit

length), HFORCEND.dat (The data of horizontal force per unit length), and PressDist.dat (The data of differential pressure). Then use Notebook to open them and record the data.

10.2. Preliminary Computational Steps

10.2.1. Import 3D Model into ANSYS Workbench

Step1:

Create a Section of analysis. Save file.

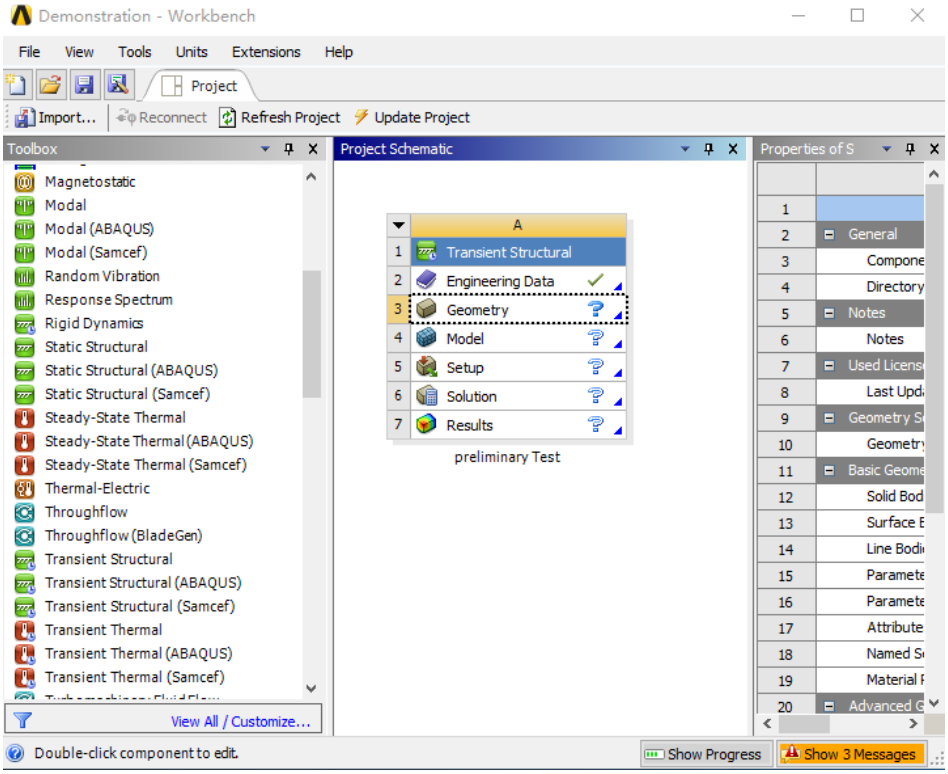

Figure 10-3 Create a Section of Analysis

Step2:

Double-click Geometry (A3), open DensignModeler (DM). Click File-Import External Geometry File, then select 3D model file import into DM.

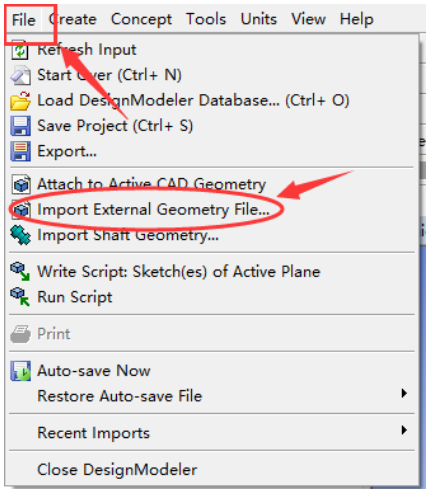

Figure 10-4 Select Import External Geometry File...

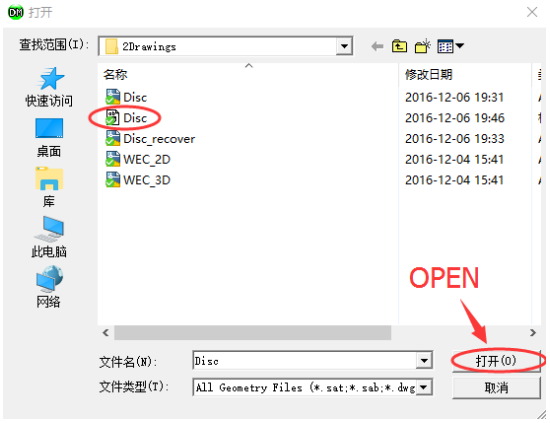

Figure 10-5 Open File

Step3:

Select “Import1” in Tree Outline. In Detail View window, change Base Plane to ZXPlane.

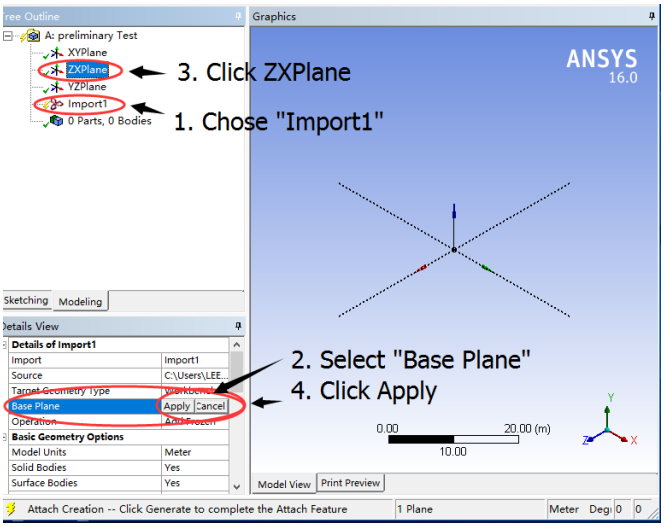

Figure 10-6 Import file

Step4:

Right-click “Import1”, select “generate” to generate a model in DM.

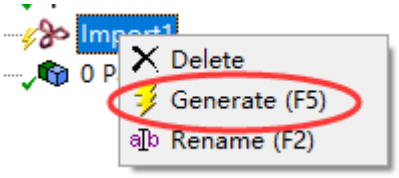

Figure 10-7 Select "Generate"

Step5:

In top menu, click Tool-Unfreeze. Select model in Graphics window, then click “Apply” in Details View window.

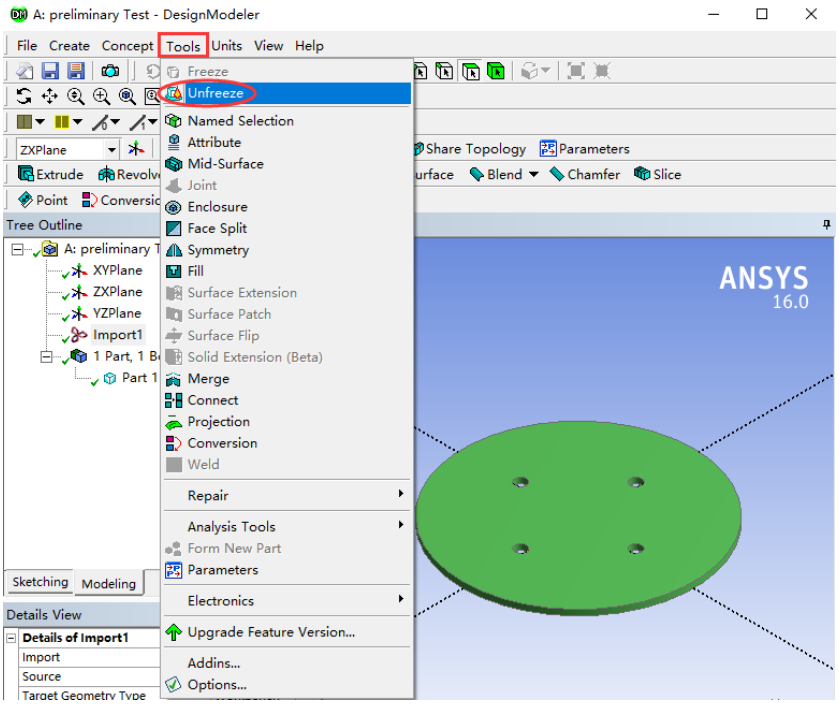

Figure 10-8 Select “Unfreeze”

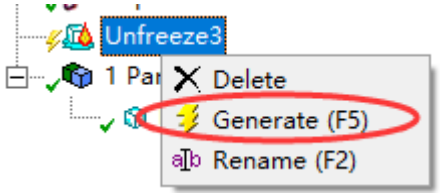

Figure 10-9 Select "Generate"

Step6:

Close DM, back to Workbench. Save file.

10.2.2. Mesh Generation

Step1:

Double-click Model (A4) in ANSYS Workbench. Open Mechanical.

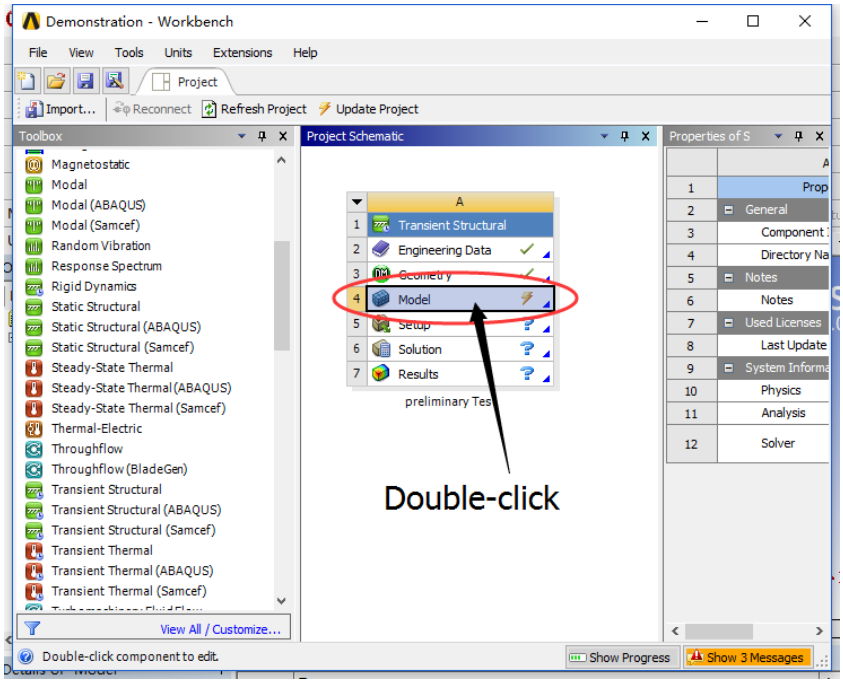

Figure 10-10 Select "Model"

Step2:

Right-click “Mech” in Outline, select Insert-Method.

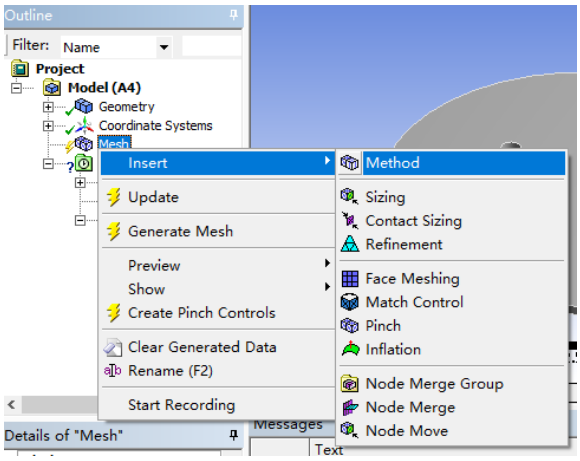

Figure 10-11 Insert mesh method

Step3:

Click “Geometry” in Details window, then select model, click Apply.

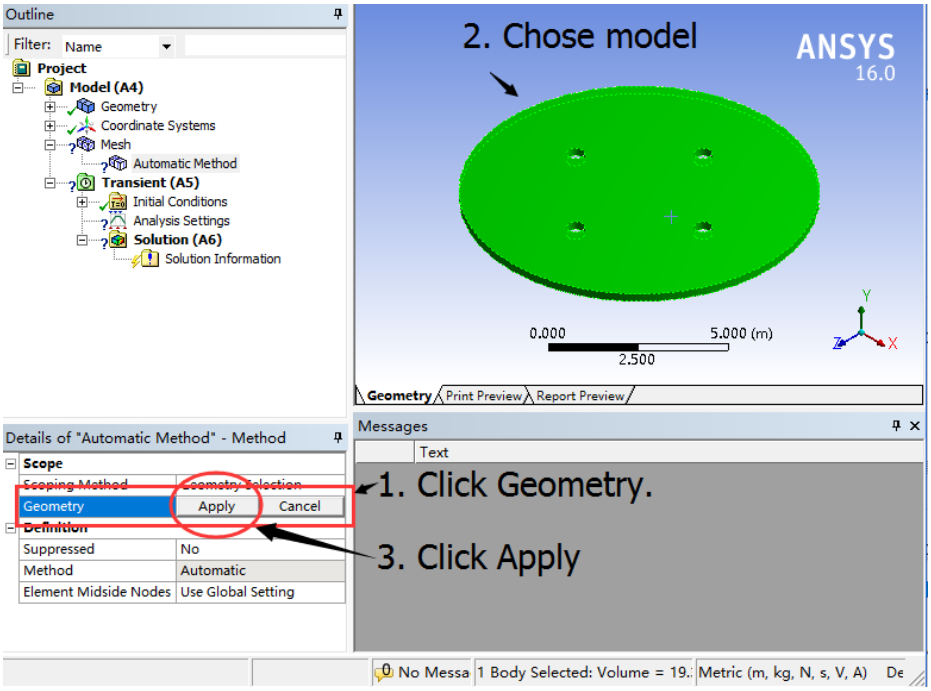

Figure 10-12 Select model

Step4:

Select "Method"-"Multizone". Change "Free Mesh Type" to "Hexa Dominant".

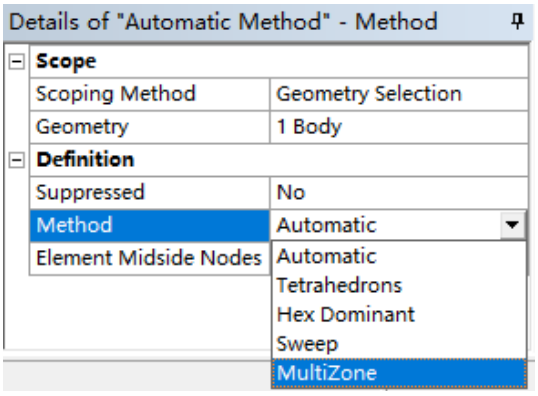

Figure 10-14 Select detailed method

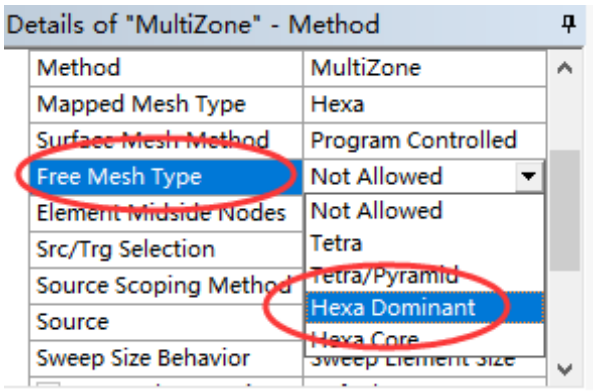

Figure 10-14 Select Free Mesh Type

Step5:

Choose “Mech”, change “Sizing”-“Relevance Center” to Fine in Details window. Change “Sizing”-“Span Angle Center” to Fine.

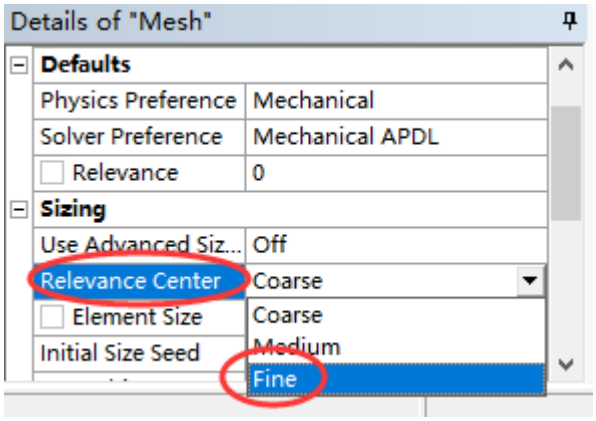

Figure 10-16 Select Relevance Center

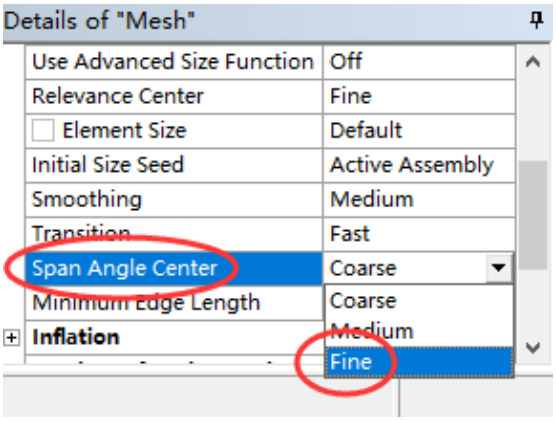

Figure 10-16 Select Span Angle Center

Step6:

Right-click “Mesh” in Outline. Select “Generate Mesh”. Then save file.

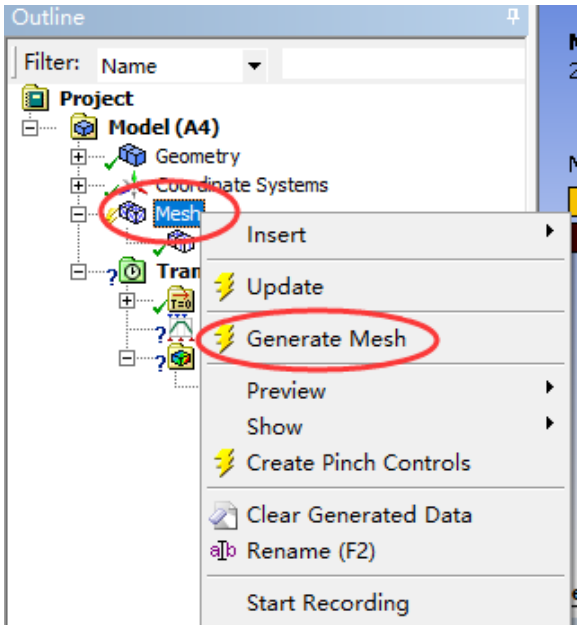

Figure 10-17 Generate mesh

10.2.3. Loads Input

Step1:

Select “Transient (A5)” in Outline in Mechanical. Click “Loads”-“Pressure” in the toolbar.

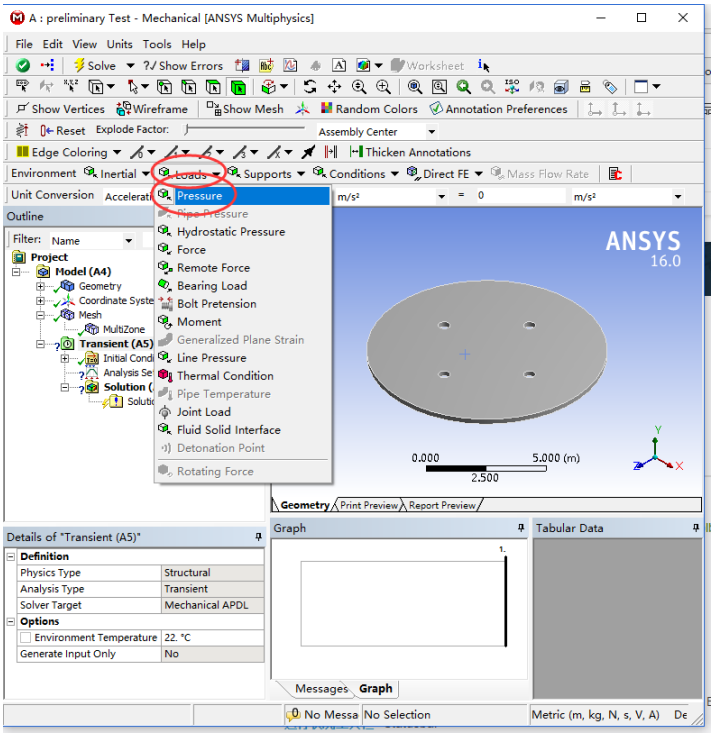

Figure 10-18 Select Loads type

Step2:

Select the pressure surface, click “Apply”.

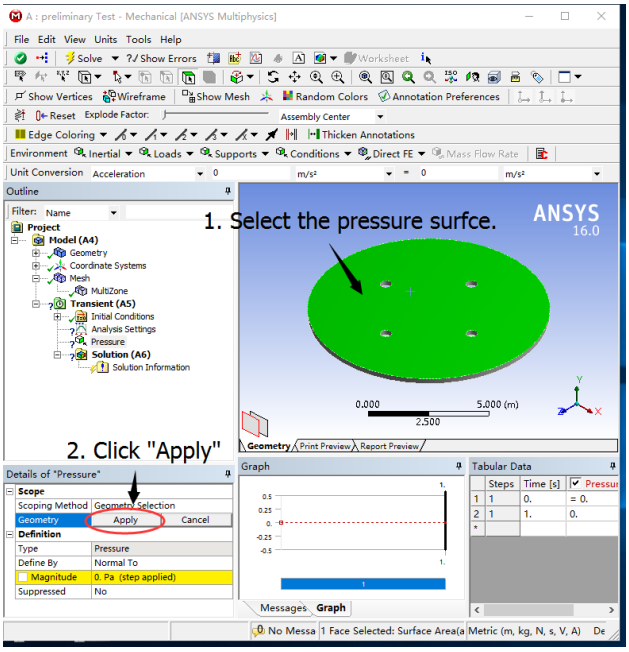

Figure 10-19 Select the pressure surface

Step2:

Right-click “Coordinate Systems” in Outline, select “insert”- “Coordinate Systems”.

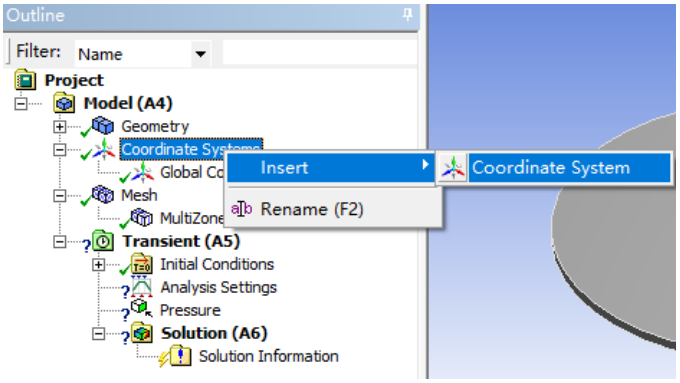

Figure 10-20 Alter Coordinate System

Step3:

Select “Define by” in Details window-“Origin”. Select “Global Coordinates”. Change the origin X to -5m, origin Y to 0.25m, origin Z to 0m.

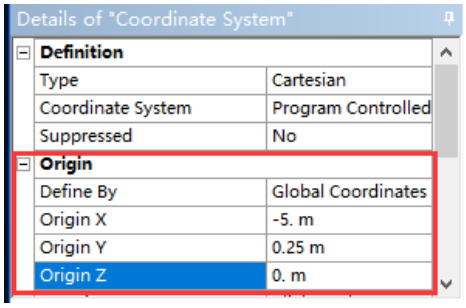

Figure 10-21 Change the coordinate origin

Step4:

Change the form of “Magnitude” to Tabular in Details window-“Definition”. Change “Definition”-“Independent Variable” to X.

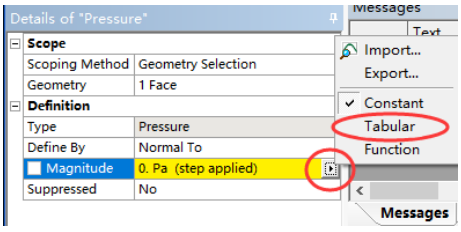

Figure 10-23 Change the form of inputting Magnitude

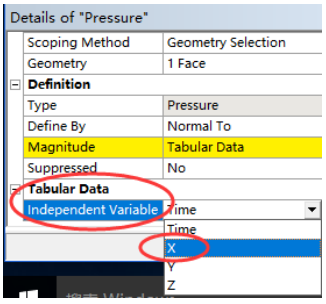

Figure 10-23 Change

Step5:

Paste pressure data in Tabular Data window.

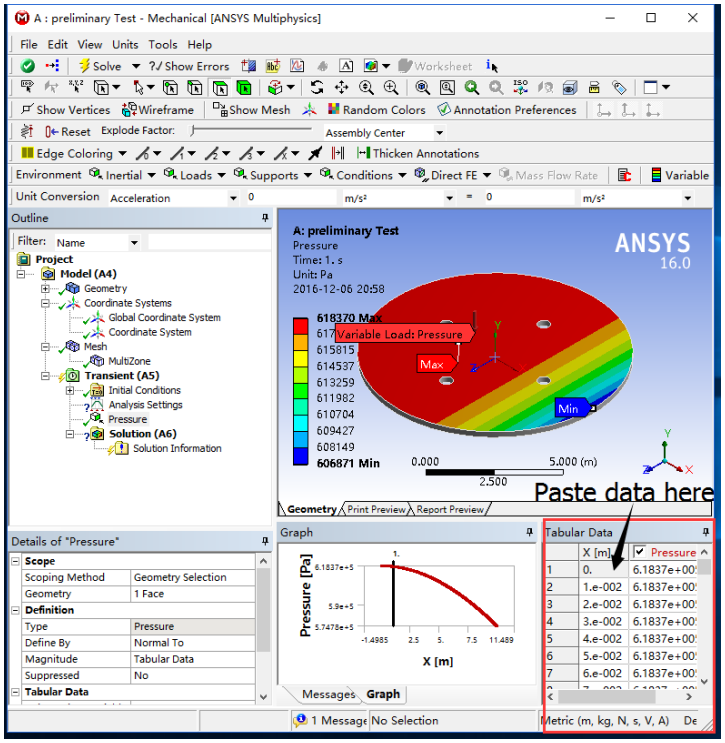

Figure 10-24 Input data

Step6:

Select "Transient (A5)"-"Analysis Settings" in Outline window, input 1s into "Initial Time Step", "Minimum Time Step", and "Maximum Time Step" in Details window. Save file.

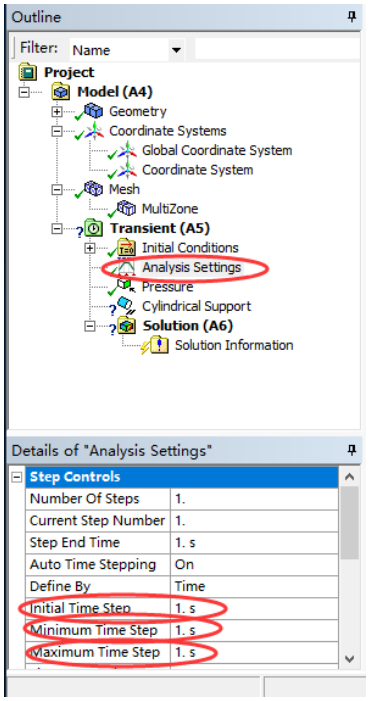

Figure 10-25 Change Analysis Settings

10.2.4. Give Supports

Step1:

Select “Transient (A5)” in Outline. Select “Supports”-“cylindrical Support” in Toolbar.

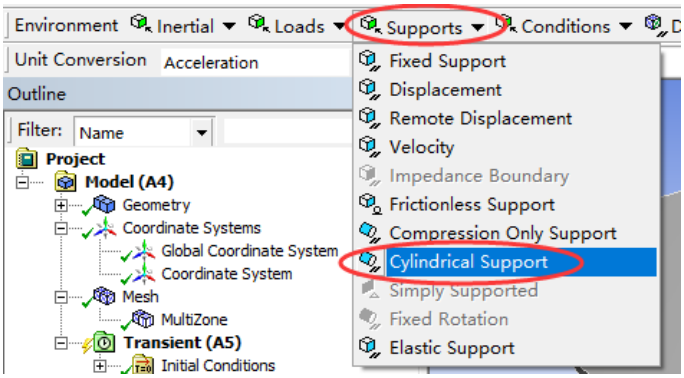

Figure 10-26 Select Supports

Step2:

Select “Cylindrical Support” in Outline window, select “Geometry” in Detail window. Select all cylindrical surfaces, then click “Apply”. Save file.

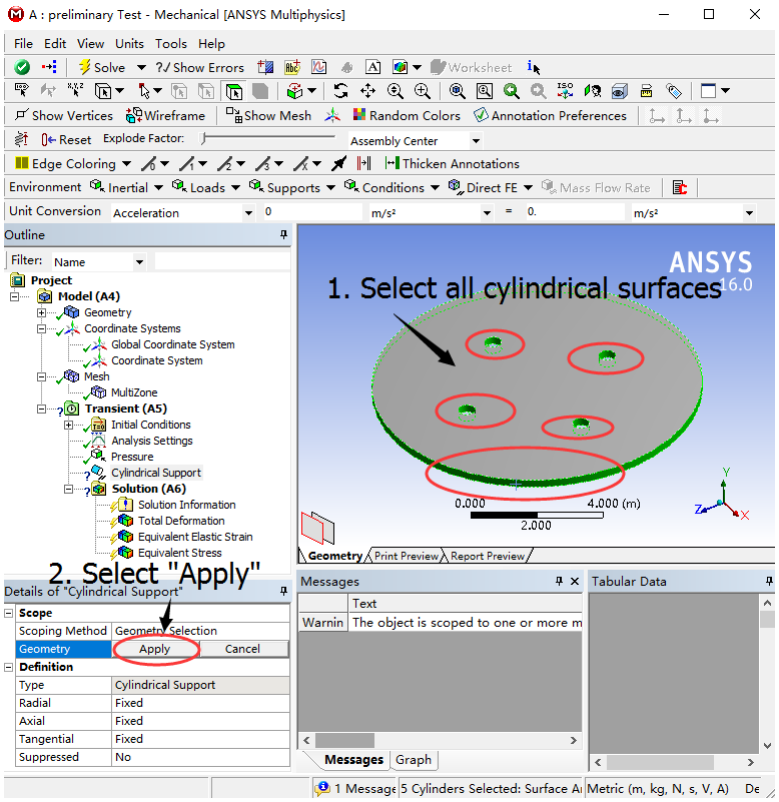

Figure 10-27 Select all cylindrical surfaces

10.2.5. Analysis

Step1:

Select “Solution (A6)” in Outline window. Select “Deformation”-“Total”, “Strain”-“Equivalent (von-Mises)”, and “Stress”-“Equivalent (von-Mises)” in the toolbar.

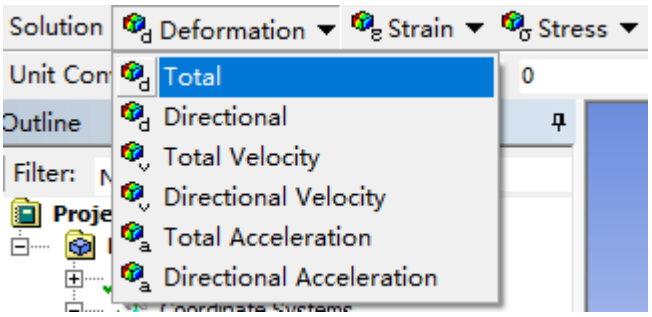

Figure 10-28 Select the form of deformation

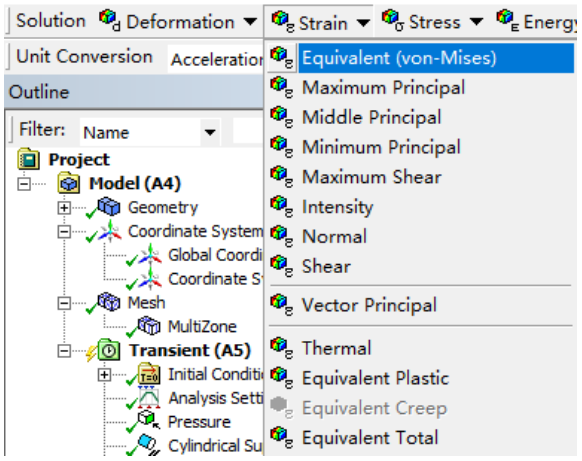

Figure 10-29 Select the form of Strain

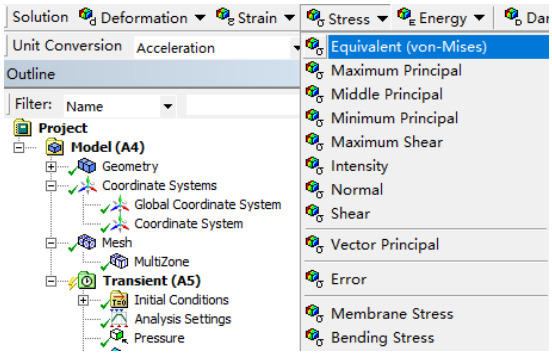

Figure 10-30 Select the form of Stress

Step2:

Right-click “Solution (A6)” in Outline window. Select “Solve” to analyse results. Save file.

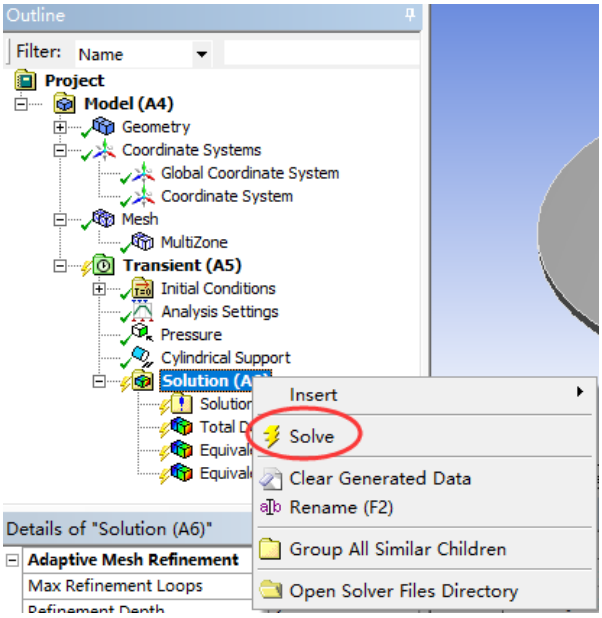

Figure 10-31 Select "Solve" to analyse results

10.3. MATLAB Code

The code that is the time of the wave crest or trough movement to the top centre of WEC is shown in Chapter 10.3.1. Besides, in this project, there are 3 different situations of the columns, which are vertical, horizontal, and inclined, showed in Chapter 10.3.4, 10.3.2, and 10.3.3 respectively.

10.3.1. The Time of the Wave Movement

```
%% CODE DESCRIPTION
% Project: Structural Analysis of a Wave Energy Device
% Author: Shuijin Li
% 13/02/2017

clear all;
close all;
clc

%% INPUT

T=input ('Please input wave period T=');        % Wave Period, s
d=10;                                           % Water Depth, m
g=9.81;                          % Gravitational Acceleration, m/s^2
Lx=zeros(1000,1);
Lx(1)=g*T^2/(2*pi);                             % Wave Length, m
for i=2:1000                                    % This loop aims at calculating
the exact wave length
    Lx(i)=g*T^2*tanh(2*pi*d/Lx(i-1))/(2*pi);
    if (abs(Lx(i)-Lx(i-1))/Lx(i))<0.0001
        L=Lx(i);
        break;
```

```
    end
end

x=5.4822;       % The distance from the origin of the coordinate to the
top centre of the WEC
C=L/T;          % Velocity of wave
t=x/C;          % The time the wave moves from the coordinate origin to
the top centre of the WEC

%% RESULTS

t1=t+3*T/4; %The time of the wave crest movement to the top centre of
WEC
t2=t+T/4; % The time of the wave trough movement to the top centre of
WEC

%% SAVE DATA
save t;

%% END
```

10.3.2. Horizontal Cylinder

```
%% CODE DESCRIPTION
% Project: Structural Analysis of a Wave Energy Device
% Author: Shuijin Li
% 24/02/2017

%% PART1 HORIZONTAL

clear all;
close all;
clc

%% INPUT
% The data in this section should be based on the project

T = input('Please input wave period T=');             % Seconds, Wave
Period
H = input('Please input wave height H=');             % Meter, Wave
Hight
h = 10;           % Meter, Water Depth
g = 9.81;         % m/s^2, Gravitational acceleration
rou = 1025;       % kg/m^3, Seawater Density
tpeak = 0.593499591649859+T/4     % One of the Time in Crest

D = 0.25;           % Meter, Cylinder Diameter

Ca = 1;             % Added-mass coefficient, Given.
Cd = 1.2;           % Drag-form coefficient, Given.


%% PRELIMINARY CALCULATIONS
% L=(g*T*T)/(2*pi);     % Meter, Wavelength, Deep water approximation.
L=T*sqrt(g*h);          % Meter, Wavelength, Shallow water
approximation.
k=(2*pi)/L;             % Wave number
w=(2*pi)/T;             % Wave angular frequency
```

```
%% DATA
P = [5.4822 5.4822 2.6161 -0.25 -0.25 2.6161 11.8839 14.75 5.4822 5.4822
9.0178 9.0178;...
    9.0178 9.0178 11.8839 14.75 -0.25 2.6161 11.8839 14.75 5.4822 5.4822
9.0178 9.0178;...
    -2.625 -7.5 -8.2486 -9.875 -9.875 -8.2486 -8.2486 -9.875 -2.625 -7.5
-2.625 -7.5];
        % Coordinate
R = {'D4','H4','L4','P4','T4','X4','T9','X9','T14','X14','T19','X19'};
        % Excel column

%% INITIALIZATION
for l=1:12
x1=P(1,l);
x2=P(2,l);
z=P(3,l);

dx = 0.01;                          % meter, Horizontal Space Intervals
x = x1:dx:x2;                       % Horizontal Axis Vector, from the
origin to the Bottom of the Cylinder

theta0 = (k*x)-(w*tpeak);           % Calculating the Phase Angle Vector

u = zeros(length(x),1);             % Velocity matrix
udot = zeros(length(x),1);          % Acceleration matrix

dfI = zeros(length(x),1);           % Sectional inertia force
dfD = zeros(length(x),1);           % Sectional drag force
dfT = zeros(length(x),1);           % Sectional total force

%% CALCULATIONS
for i=1:length(x)

    % Calculating horizontal velocity and acceleration at each height
    u(i) =
(((H*g*k)/(2*w))*((cosh(k*(z+h)))/(cosh(k*h))))*(cos(theta0(i)));

udot(i)=(((H*g*k)/(2))*((cosh(k*(z+h)))/(cosh(k*h))))*(sin(theta0(i)));

    % Calculating the sectional forces
    dfI(i) = ((1+Ca)*rou*pi*(D/2)*(D/2)).*udot(i);
    dfD(i) = (0.5*rou*D*Cd).*u(i).*(abs(u(i)));
    dfT(i) = dfI(i)+dfD(i);

end

%% SAVE FILES
eval(['save H',num2str(l)]);
        % Save data
s=strcat(['H',' ',num2str(H),',',num2str(T)]);          % Change column
name in Excel automatically
xlswrite('C:\Users\LEEHHU\OneDrive - University of
Dundee\Project\4Design Condition\Data\Trough.xlsx'...
    ,dfT,s,R{l});
                % Write specific data into Excel
end
```

10.3.3. Inclined Cylinder

```
%% PART2 INCLINED

clear all;
close all;
clc

%% INPUT
% The data in this section should be based on the project

T = input('Please input wave period T=');       % Seconds, Wave Period
H = input('Please input wave height H=');       % Meter, Wave Hight
h = 10;           % Meter, Water Depth
g = 9.81;         % m/s^2, Gravitational acceleration
rou = 1025;     % kg/m^3, Seawater Density
tpeak = 0.593499591649859+T/4;    % One of the Time in Crest

D = 0.25;           % Meter, Cylinder Diameter

Ca = 1;             % Added-mass coefficient, Given.
Cd = 1.2;           % Drag-form coefficient, Given.

%% PRELIMINARY CALCULATIONS
% L=(g*T*T)/(2*pi);     % Meter, Wavelength, Deep water approximation.
L=T*sqrt(g*h);          % Meter, Wavelength, Shallow water
approximation.
k=(2*pi)/L;             % Wave number
w=(2*pi)/T;             % Wave angular frequency

%% DATA
P = [-0.25 9.0178; 5.4822 14.75; -9 -7.5; -7.5 -9]; % Coordinate
R = {'T4','X4'};        % Excel Column

%% INITIALIZATION
for l=1:2
x1=P(1,l);
x2=P(2,l);
z1=P(3,l);
z2=P(4,l);

dx = 0.01;               % meter, Horizontal Space Intervals
x = x1:dx:x2;            % Horizontal Axis Vector, from the origin to
the Bottom of the Cylinder

theta0 = (k*x)-(w*tpeak);        % Calculating the Phase Angle Vector
theta1 = atan((x2-x1)/(z2-z1));  % The Angle of Inclined Cylinder of X
Axis

u = zeros(length(x),1);          % Velocity matrix
udot = zeros(length(x),1);       % Acceleration matrix

dfI = zeros(length(x),1);        % Sectional inertia force
dfD = zeros(length(x),1);        % Sectional drag force
dfT = zeros(length(x),1);        % Sectional total force

%% CALCULATIONS
for i=1:length(x)
```

```
    % Calculating horizontal velocity and acceleration at each height
    u(i) = (((H*g*k)/(2*w))*((cosh(k*((x(i)-
x(1))*tan(theta1)+h)))/(cosh(k*h))))*(cos(theta0(i)));
    udot(i)=(((H*g*k)/(2))*((cosh(k*((x(i)-
x(1))*tan(theta1)+h)))/(cosh(k*h))))*(sin(theta0(i)));

    % Calculating the sectional forces
    dfI(i) = ((1+Ca)*rou*pi*(D/2)*(D/2)).*udot(i);
    dfD(i) = (0.5*rou*D*Cd).*u(i).*(abs(u(i)));
    dfT(i) = dfI(i)+dfD(i);

end

%% SAVE FILES
eval(['save In',num2str(l)]);                                    % Save data
s=strcat(['V',' ',num2str(H),',',num2str(T)]); % Change column name in
Excel automatically
xlswrite('C:\Users\LEEHHU\OneDrive - University of
Dundee\Project\4Design Condition\Data\Trough.xlsx'...
    ,dfT,s,R{l});
           % Write data into Excel
end
```

10.3.4. Vertical Cylinder

```
%% PART3 VERTICAL
clear all;
close all;
clc

%% INPUTS
% The data in this section should be based on the project

T = input('Please input wave period T=');  % Seconds, Wave Period
H = input('Please input wave height H=');  % Meter, Wave Hight
h=10;     %meter, Water depth
g=9.81;   %m/s^2, Gravitational acceleration
rho=1025;         %kg/m^3,Density
tpeak = fprintf('tpeak = %.2f\n',0.593499591649859+T/4);  % One of the
Time in Crest
tend=2*T;         %Duration of calculations

D=0.25;           %meter, cylinder diameter

Ca=1;             %Added-mass coefficient, Given.
Cd=1.2;           %Drag-form coefficient, Given.

%% DATA
P = [-9 -2.5 -2.5 -9; -10 -7.5 -7.5 -10; -0.25 5.48 9.02 14.75]; %
Coordinate
R = {'D4','H4','L4','P4'};               % Column in Excel

%% PRELIMINARY CALCULATIONS
% L=(g*T*T)/(2*pi);   %meter, Wavelength, Deep water approximation.
L=T*sqrt(g*h);   %meter, Wavelength, Shallow water approximation.
k=(2*pi)/L;         %Wave number
w=(2*pi)/T;         %Wave angular frequency
```

```
%% INITIALIZATION
for l=1:4
z1=P(1,l);
z2=P(2,l);
x=P(3,l);

dz=-0.01;            %meter, vertical space intervals
dt=0.01;             %s, time intervals

z=z1:dz:z2;        %vertical axis vector, from the SWL to the bottom of
the cylinder
t=0:dt:tend;        %time vector
theta=(k*x)-(w*t);  %Calculating the phase angle vector

u=zeros(length(t),length(z));          %Velocity matrix
udot=zeros(length(t),length(z));       %Acceleration matrix
dfI=zeros(length(t),length(z));        %Sectional inertia force
dfD=zeros(length(t),length(z));        %Sectional drag force
dfT=zeros(length(t),length(z));        %Sectional total force
dfT0=zeros(length(z),1);               %Sectional total force in a
certain time

%% CALCULATIONS
for i=1:length(t)       % Calculating horizontal velocity and
acceleration at each time

u(i,:)=(((H*g*k)/(2*w))*((cosh(k*(z(:)+h)))/(cosh(k*h))))*(cos(theta(i))
);

udot(i,:)=(((H*g*k)/(2))*((cosh(k*(z(:)+h)))/(cosh(k*h))))*(sin(theta(i)
));

    % Calculating the sectional forces
    dfI(i,:)=((1+Ca)*rho*pi*(D/2)*(D/2)).*udot(i,:);
    dfD(i,:)=(0.5*rho*D*Cd).*u(i,:).*(abs(u(i,:)));
    dfT(i,:)=dfI(i,:)+dfD(i,:);

end

row=tpeak/dt;
dfT0(:,1)=dfT(row,:);

%% SAVE
eval(['save V',num2str(l)]);                    % Save data
s=strcat(['V',' ',num2str(H),',',num2str(T)]);  % Change column name in
Excel automatically
xlswrite('C:\Users\LEEHHU\OneDrive - University of
Dundee\Project\4Design Condition\Data\Trough.xlsx'...
    ,dfT0,s,R{l});                      % Write data into Excel
end

%% END OF THE CODE. NO LINE AFTER THIS
```